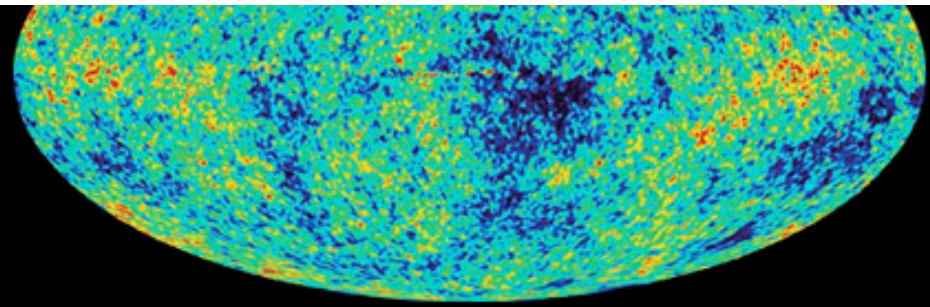




CMB and High Energy Physics

from Early Universe to clusters
of galaxies and Large Scale Structure

La Palma, July 16-24, 2012



Primordial Gravitational waves and the polarization of the CMB

José Alberto Rubiño Martín
(IAC, Tenerife)



Outline

Lecture 1.

- Theory of CMB polarization.
 - E and B modes.
 - Primordial Gravitational waves.
- Observational status: CMB polarization measurements. E-mode detections and B-mode constraints.

Lecture 2.

- Foregrounds of the CMB.
- The future (CMB polarization experiments).
 - The Planck satellite.
 - QUIJOTE CMB experiment.
 - Core satellite.

Lecture 2. Bibliography

Books:

- ❖ **Radiative Processes in Astrophysics.** Rybicki & Lightman (John Wiley & Sons 1979).
- ❖ **High Energy Astrophysics.** Longair (CUP 1993. Third Edition 2011)
- ❖ **Tools of Radioastronomy.** Rohlfs & Wilson (Springer 2000).
- ❖ **Physics of the interstellar medium.** Draine (Princeton Series 2011).
- ❖ **The Cosmic Microwave Background: from quantum fluctuations to the present Universe.** Eds. Rubiño-Martin, Rebolo, Mediavilla (Cambridge Univ. Press 2010).

Online course

- ❖ <https://www.cv.nrao.edu/course/ast534/ERA.shtml>

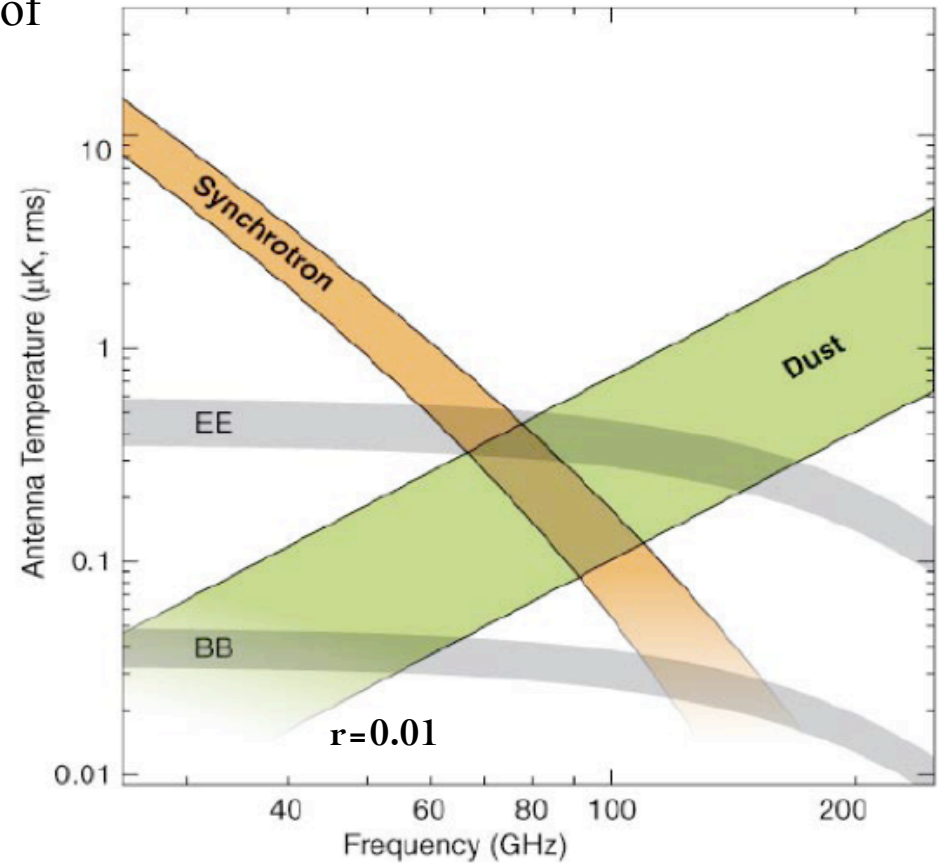
Papers

- ❖ Blumenthal & Gould (1993), Rev. Mod. Phys. 42, 237.
- ❖ Planck Collaboration XIII-XX, 2011, A&A 536.

Observability of B-modes

★ Critical Issues

- **Signals are extremely small** \Rightarrow large number of receivers with large bandwidths are required.
- Accurate **control of systematics** (cross-pol, spillover,...) is mandatory.
- **Foregrounds**. B-mode signal is subdominant over Galactic foregrounds
 - **Free-free**, low-freq, not polarized
 - **Synchrotron**, low-freq, pol $\sim 10\%$
 - **Thermal dust**, high-freq, pol $\sim 10\%$
 - **Anomalous emission**, 20-60 GHz, pol $\sim 3\%$?
 - **Point sources**, low-freq, pol $\sim 5\%$



CMB foregrounds in the microwave sky

- ❖ **Synchrotron emission** (relativ e, associated to SNs,..) ($\nu < 10$ GHz)

$$T_\nu \propto \nu^{-\beta_s}, \quad \beta_s \approx 2.76 \pm 0.11$$

- ❖ **Free-free emission** (interactions thermal e⁻/p⁺ in ISM)

$$T_\nu \propto \nu^{-\beta_b}, \quad \beta_b \approx 2.15$$

- ❖ **Dust emission** (vibrational emission in far IR) ($\nu > 100$ GHz)

$$I(\nu) \propto \nu^2 [B_\nu(20.4 K)].$$

- ❖ **Point sources** (radio-galaxies, IR galaxies, etc.) (Small scales).

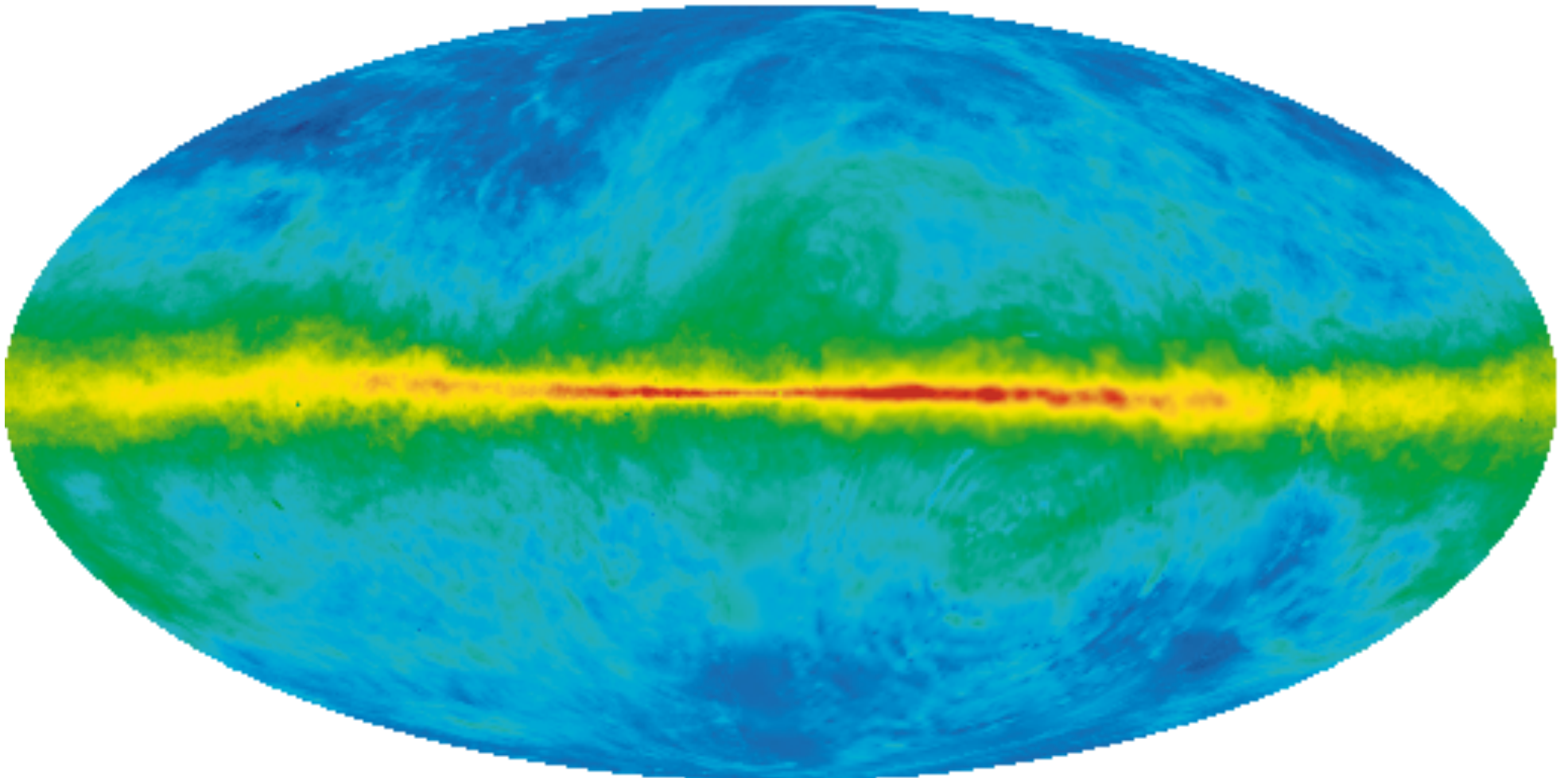
ISM (Inter-Stellar Medium). Basic concepts

| Regions | Density [cm ⁻³] | Temp [K] | Observable |
|----------------------------------|----------------------------------|----------------------------------|---|
| Cold atomic (HI) | 1-100 | 50-150 | 21cm line. Occupies 2-3% galactic volume, but contains 50% of the mass. |
| Cold molecular (H ₂) | 10 ³ -10 ⁴ | 10-30 | CO line. Stellar formation takes place here. |
| Intercloud gas | 0.3 | 6000 | 21cm (20% HI). Occupies 50% in volume |
| HII regions | >10 ² | 8000 | Free-free emission. Recombination lines. |
| Coronal gas | <10 ⁻² | 10 ⁵ -10 ⁶ | In soft X-rays (0.1-2 keV). Produced in SN explosions. |

Other components of the ISM

- **Dust.** Provides about 1% of the mass of the ISM.
- **Magnetic field.** B ~2-3 μG.
- **Cosmic rays** [84% p; 14% He; 1% e⁻ y e⁺; 1% others]. Energy spectrum from 10⁶ to 10²⁰ eV. Energy density 1eV/cm³.

Our Galaxy in neutral hydrogen (21cm)



(Hartmann et al. 1997, complemented with data from Dickey & Lockman 1990).

Photo-ionized regions (HII)

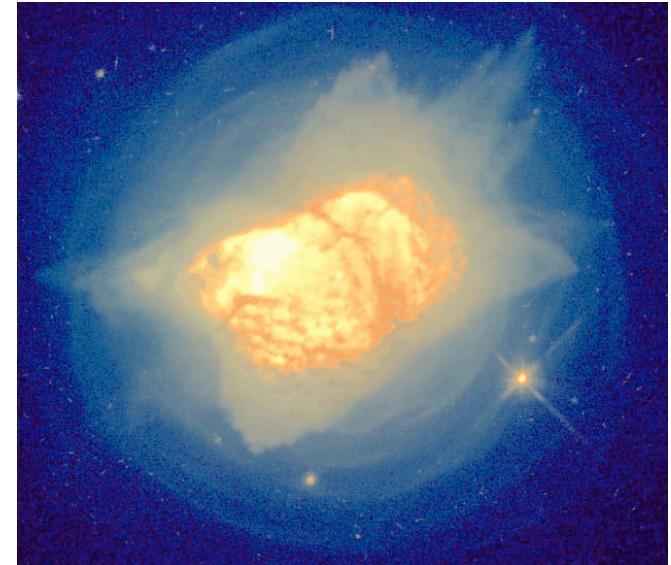
Orion Nebula

Optical: dust

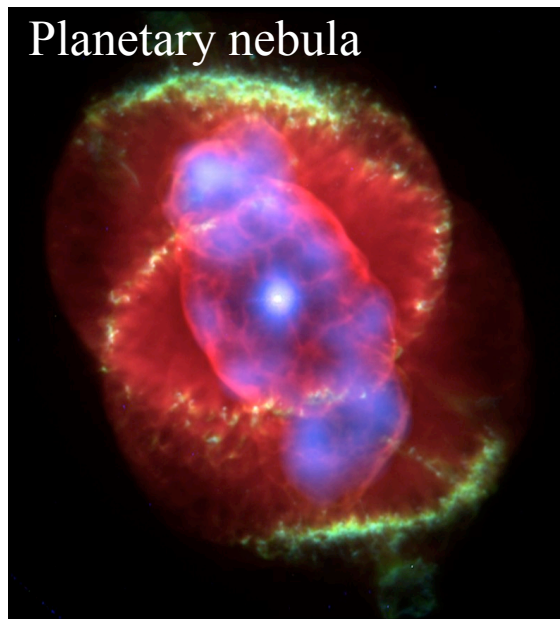
IR: stars

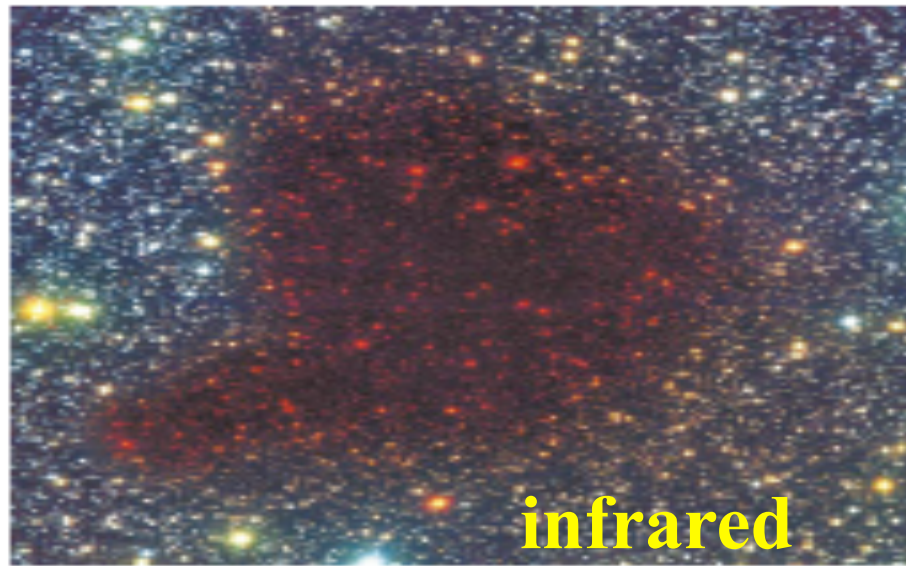


NGC 7027 (HST)



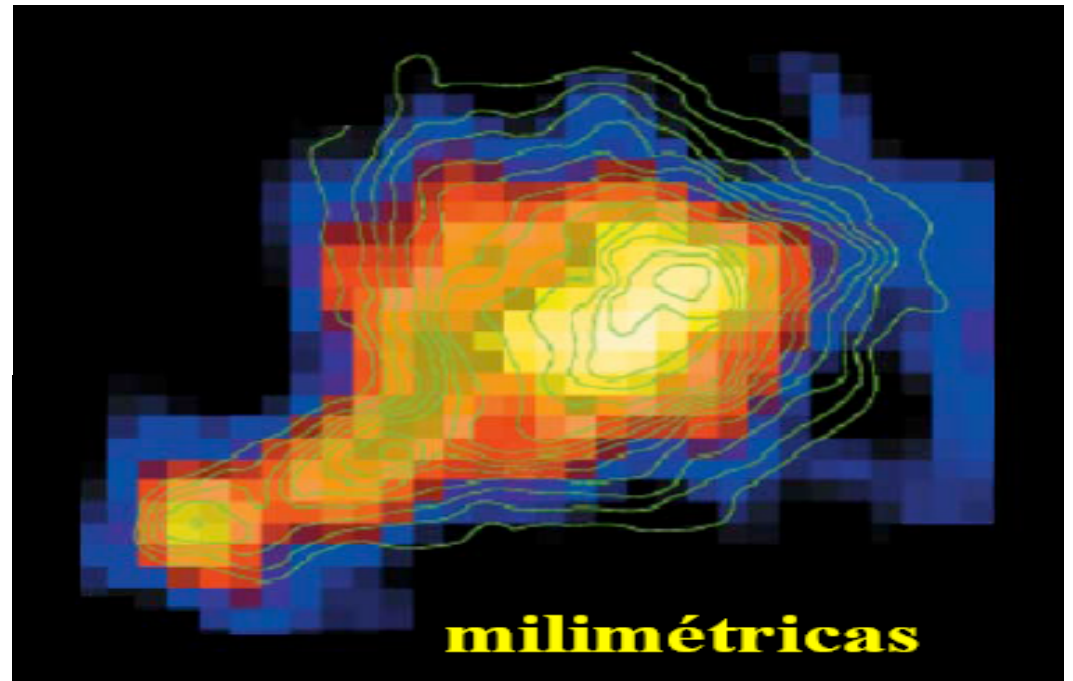
Planetary nebula



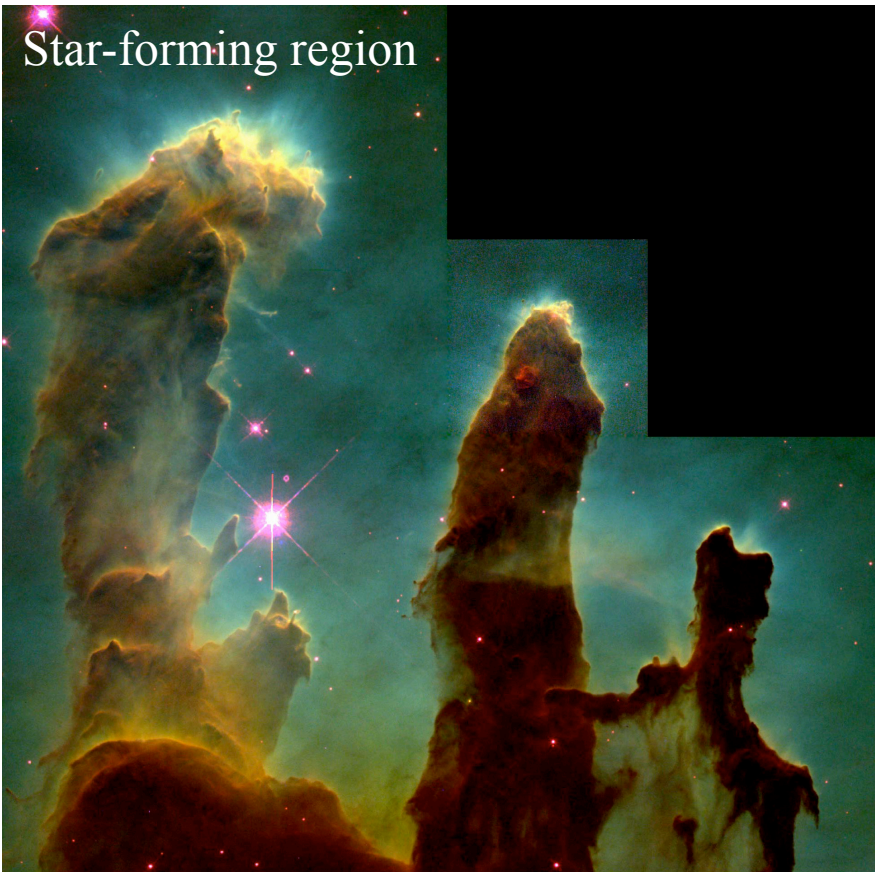


Alves et al. (2001, Nature 409,
159)

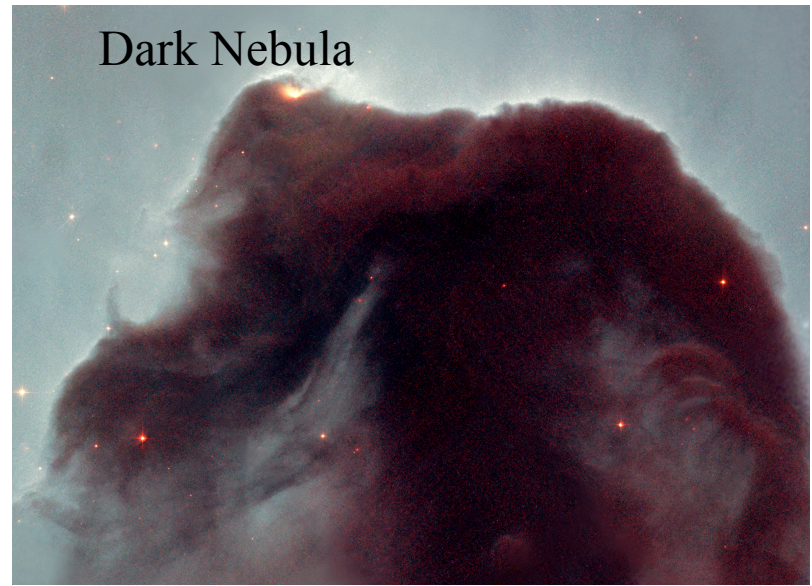
Dark cloud
observed in mm
wavelengths



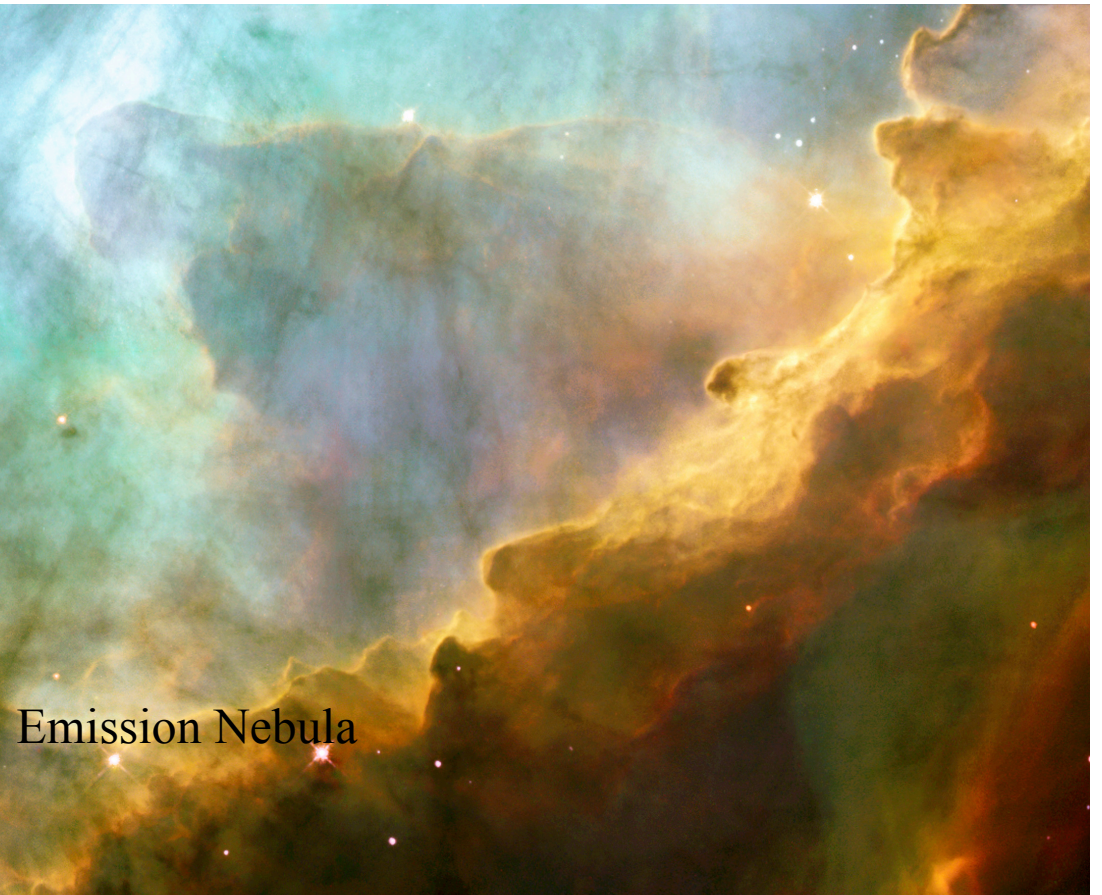
Star-forming region



Dark Nebula



Molecular clouds





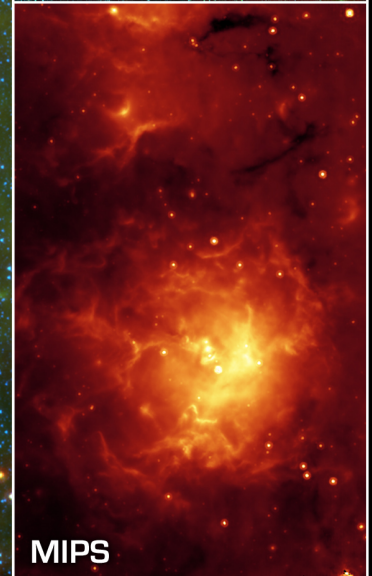
Visible (NOAO)



Infrared IRAC + MIPS



IRAC



MIPS

Trifid Nebula/Messier 20

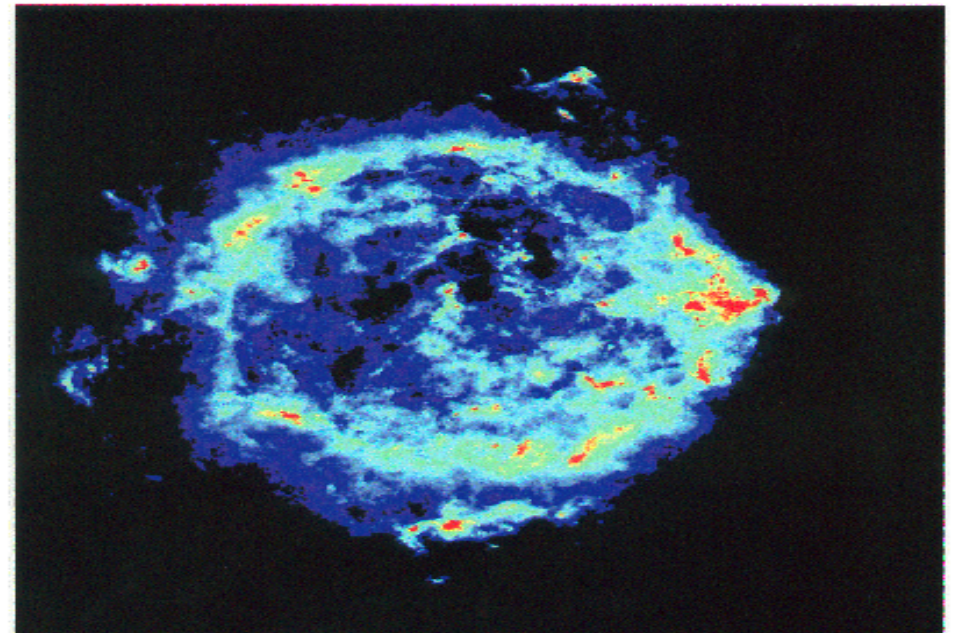
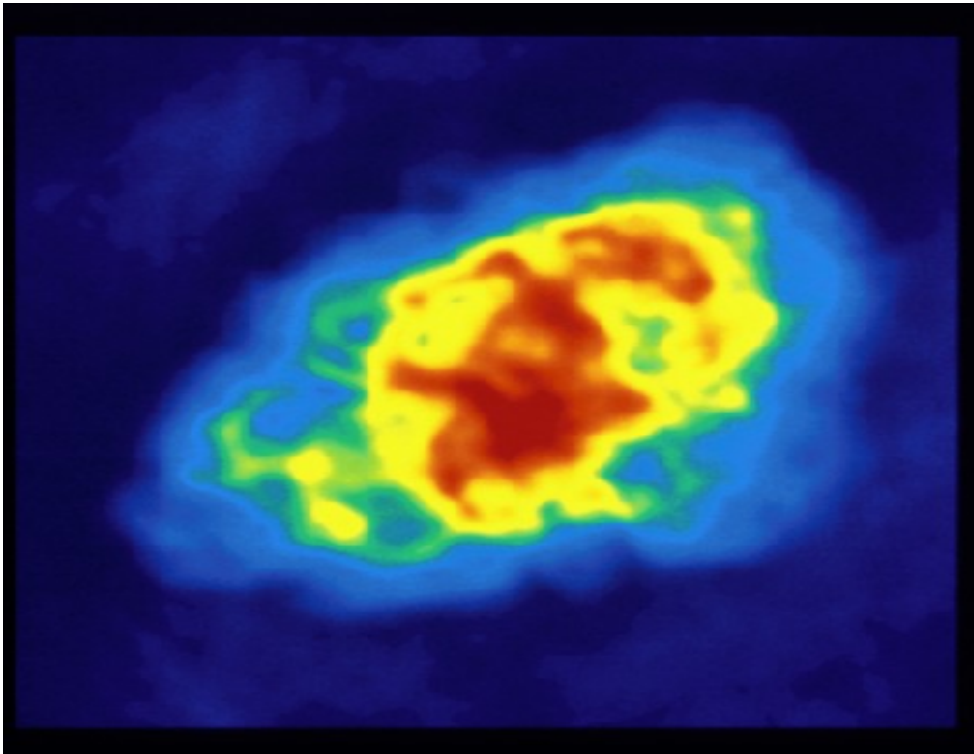
NASA / JPL-Caltech / J. Rho (SSC/Caltech)

Spitzer Space Telescope • IRAC + MIPS

ssc2005-02a



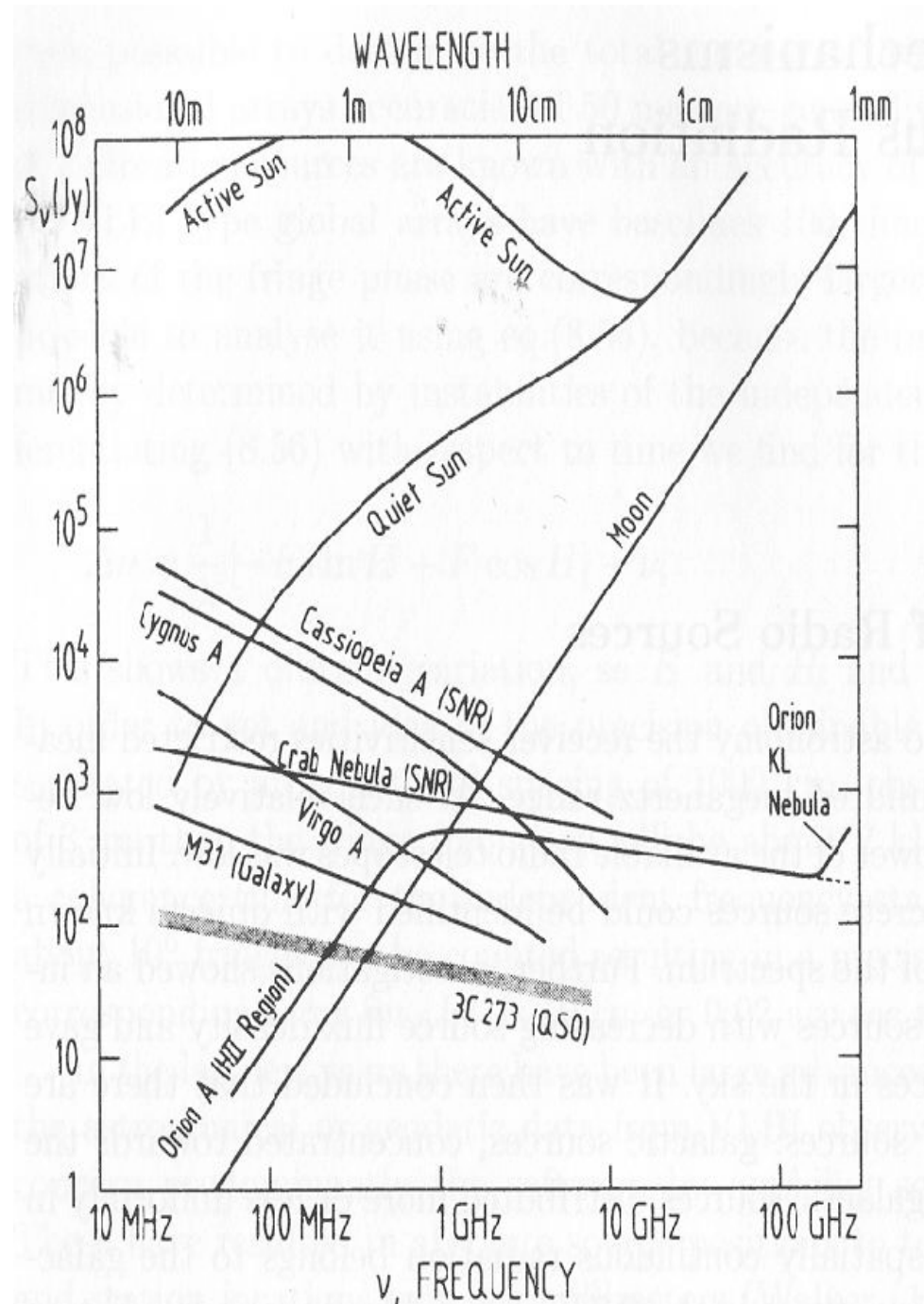
Supernova remnants



Radiocontinuum emission

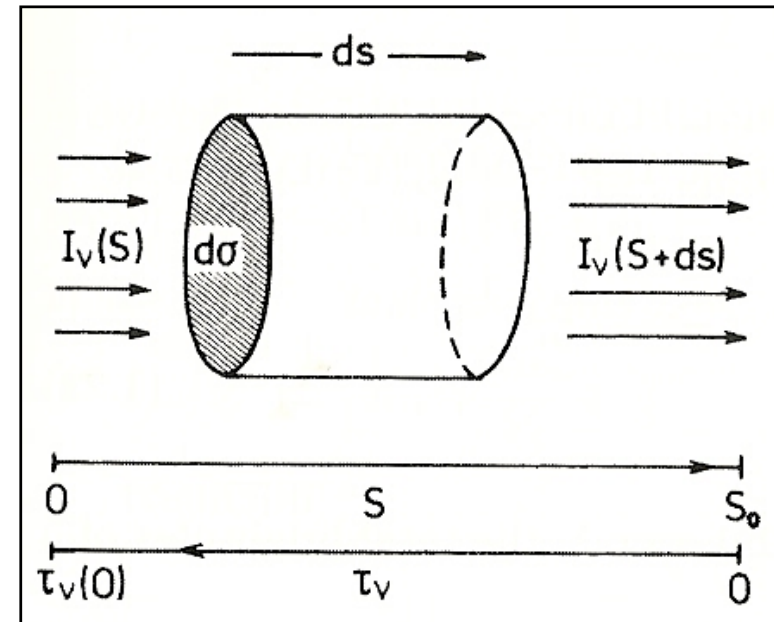
Physical processes of radio-continuum emission from our Galaxy.

- ❖ **Black body emission.** Examples: planets, Moon, Sun.
- ❖ **Pseudo-thermal dust emission.**
- ❖ **Thermal emission from a ionised gas.** Free-free (bremsstrahlung).
 - ❖ Photo-ionised regions (HII, PNe). Stellar winds.
- ❖ **Non-thermal emission. Synchrotron.**
 - ❖ SN remnants. Pulsars.
- ❖ **Anomalous microwave emission.** A new process in the Galaxy?



Radiative transfer fundamentals

$$\frac{dI_\nu}{ds} = -\kappa_\nu I_\nu + \epsilon_\nu$$



Formal solution:

$$I_\nu(\tau_\nu) = I_\nu(0)e^{-\tau_\nu} + B_\nu(T_{ex})(1 - e^{-\tau_\nu})$$

$$\tau_\nu(s) = - \int_{s_0}^s \kappa_\nu(s) ds \equiv \text{optical depth}$$

Thermal dust emission

- This is the most important physical process of continuum emission in IR and mm wavelenths in star forming regions.
- Dust constitutes 1% of the mass (compared to the gas).
- Typical dust particle sizes $\sim 0.01-1 \mu\text{m}$
- The continuum spectrum is a modified black-body

$$I_{\nu} = B_{\nu}(T_{dust}) \left(1 - e^{-\tau_{\nu}}\right)$$

- In the sub-mm domain, emission is optically thin, and thus

$$I_{\nu} = \tau_{\nu} B_{\nu}(T_{dust})$$

$$\tau_{\nu} = \tau_0 \left(\frac{\nu}{\nu_0}\right)^{\beta}$$

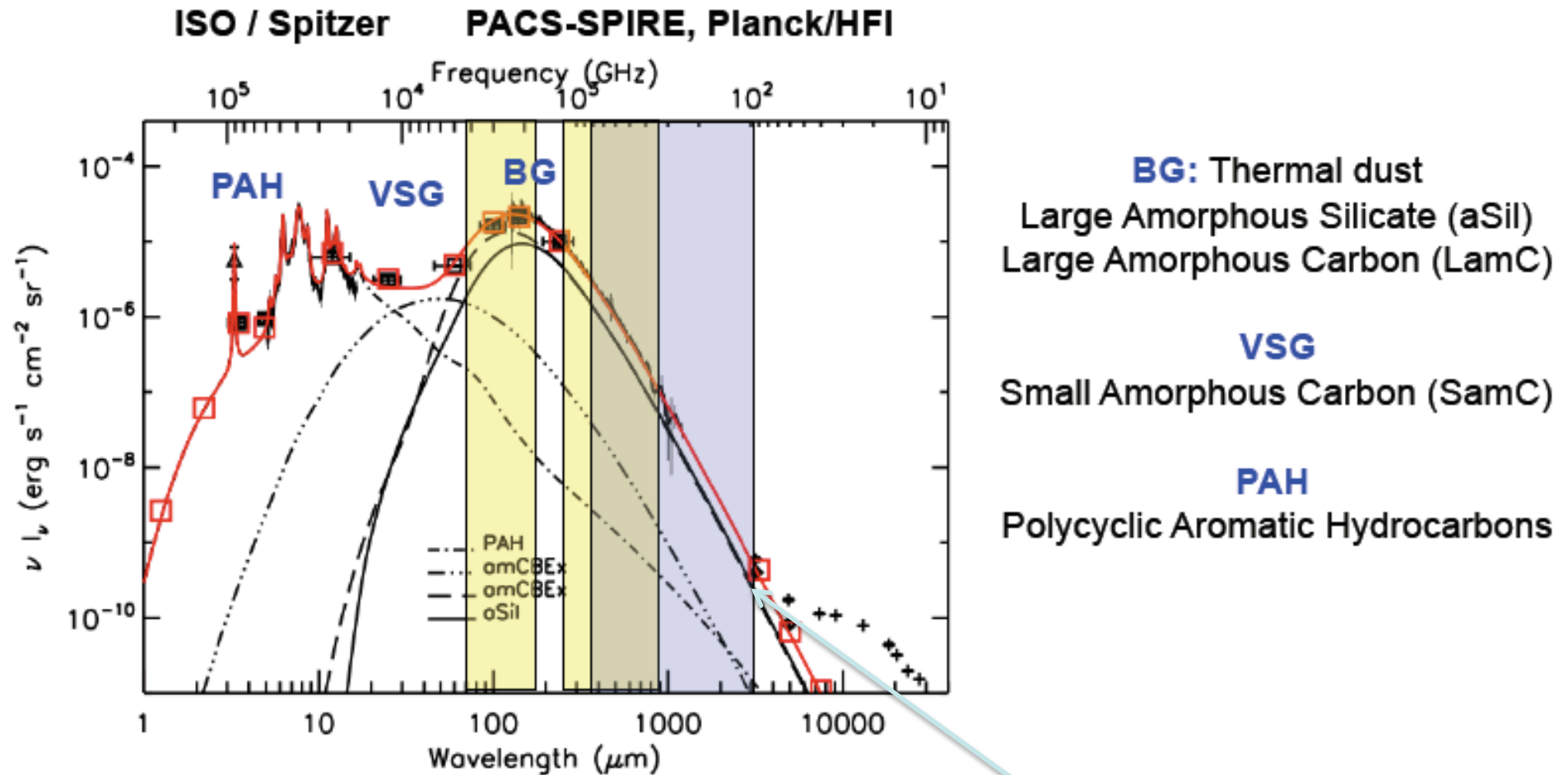
$$\tau_0 = \sigma_{\nu_0} N_H$$

- $\beta=1.5-2.0$. Spatial variations indicate changes in the grain composition, grain sizes and shapes, porosity, etc.



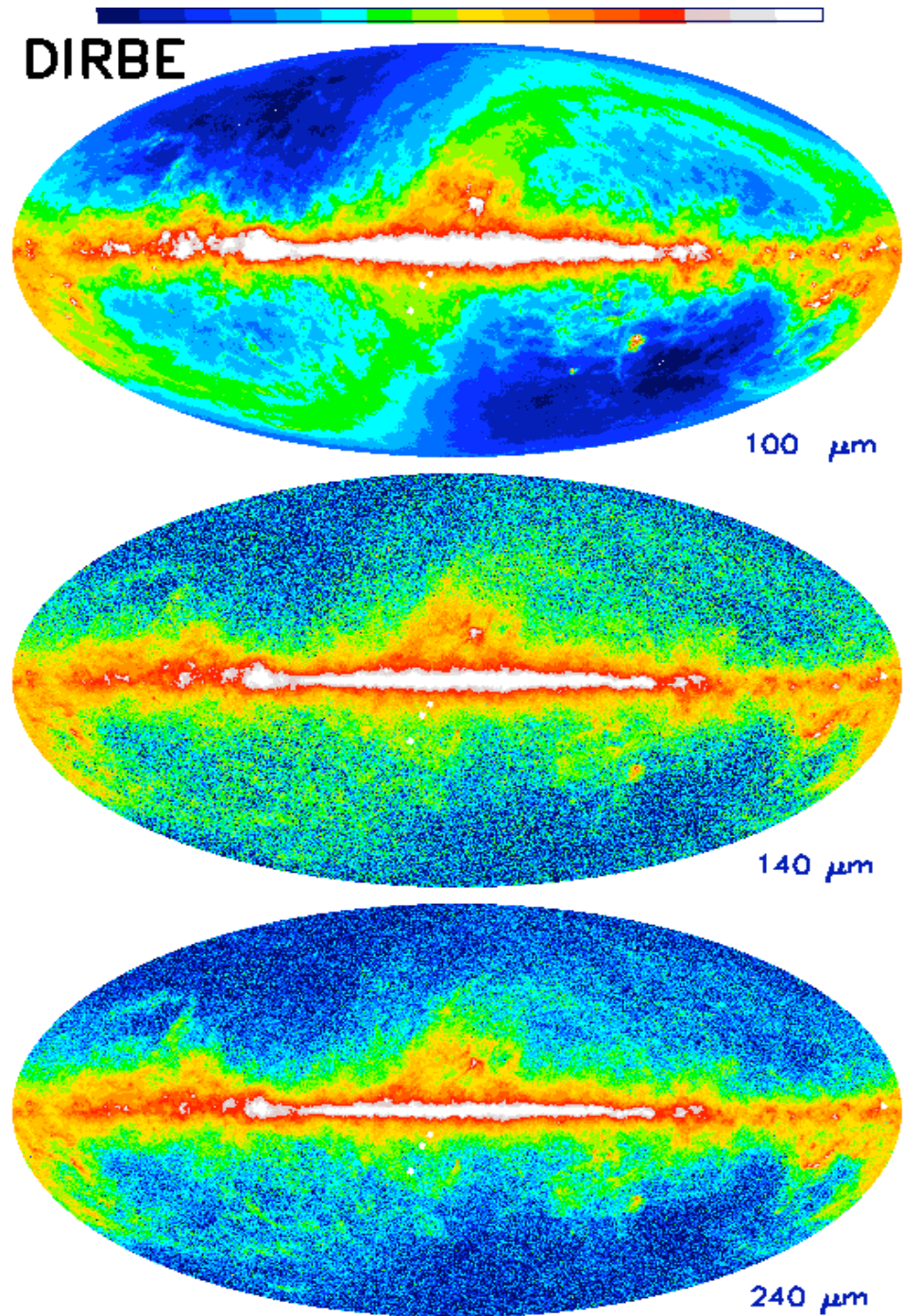
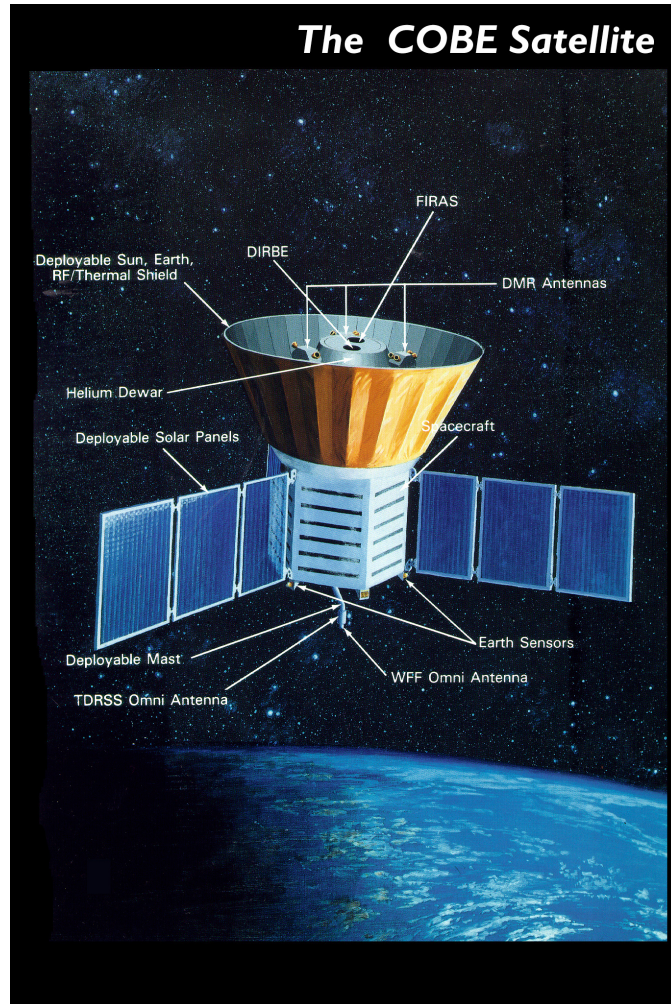
Dust emission from our Galaxy

Emission spectrum of interstellar dust



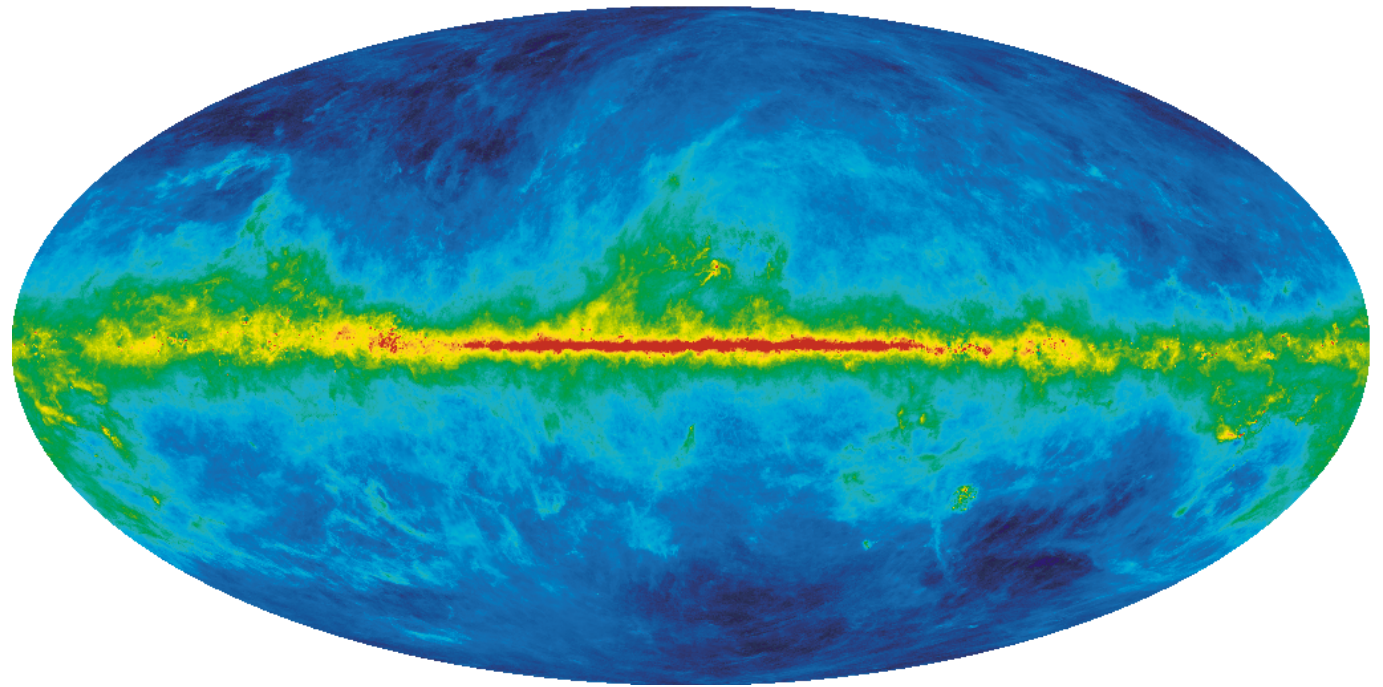
$$I_\nu = \tau_\nu B_\nu(T_{dust})$$

Thermal dust emission



<http://lambda.gsfc.nasa.gov/product/cobe/>

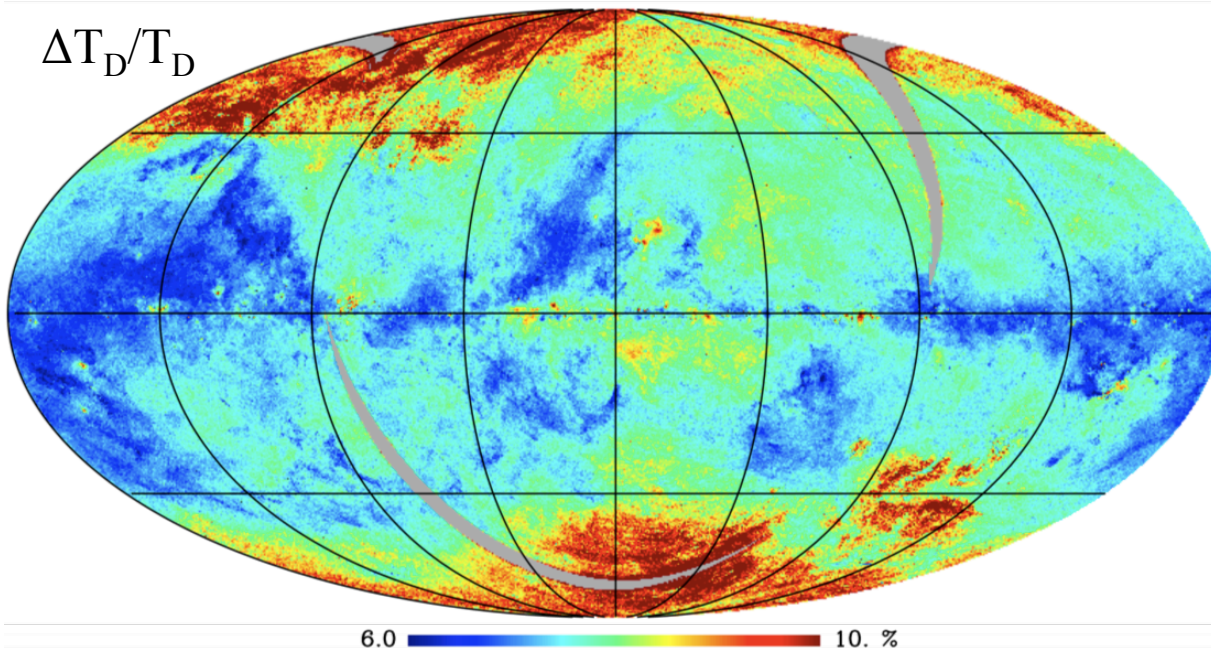
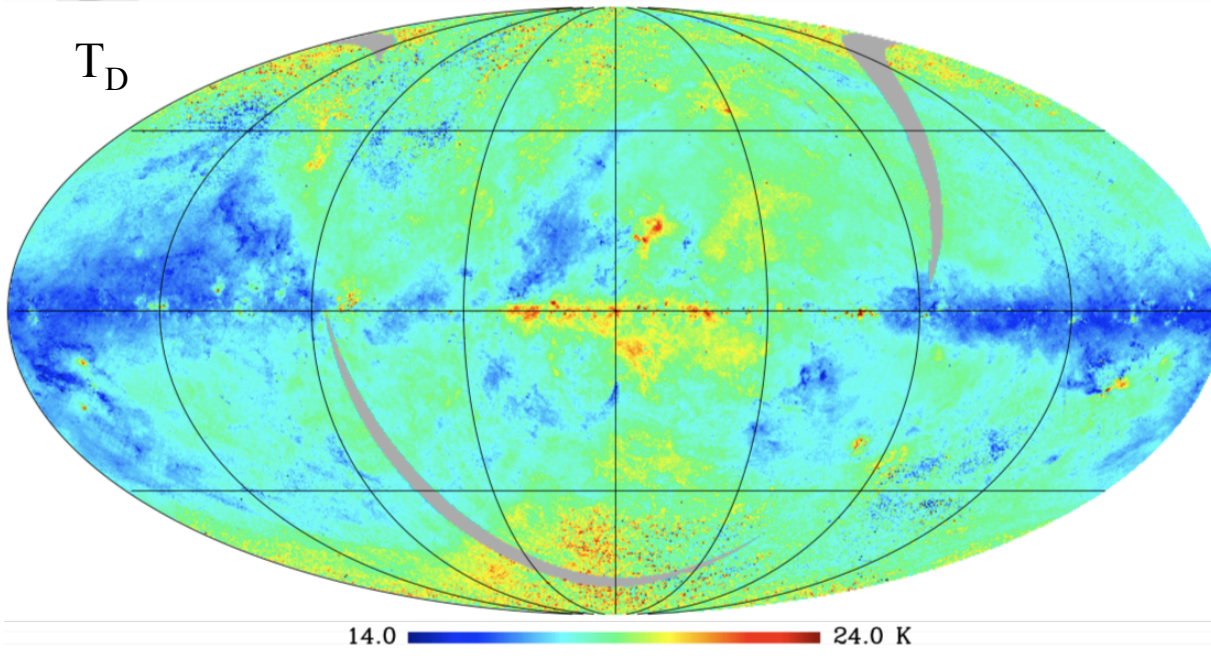
Thermal dust emission: IRAS 100 μ m



Schlegel, Finkbeiner & Davis (1998). Combinationn of 100 μ m [IRAS/ISSA](#) and calibrated using [DIRBE](#).



Planck Early Results: Dust properties



Temperature (T_{dust}) computed from IRAS 100 μm , HFI 857 GHz, HFI 545 GHz, using $\beta=1.8$ (median value derived from T- β fit)

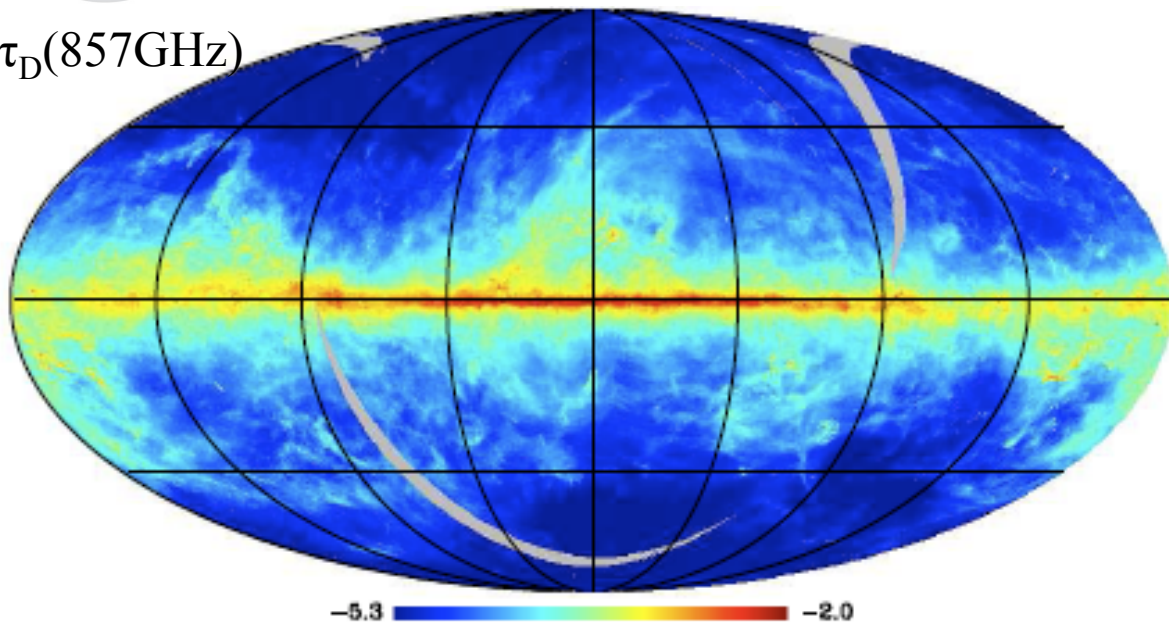
- $12 \text{ K} < T_{\text{dust}} < 50 \text{ K}$. Dust temp. clearly traces the intensity of the radiation field:**
- External galaxy is colder than inner Galaxy (was already known from COBE data)
 - Molecular clouds are colder than surrounding
 - Warm regions are star forming regions, HII regions, etc ..

Uncertainty on dust temperature from χ^2 minimization using relative and absolute error. $\Delta T_D / T_D < 10\%$ except at high latitudes (low brightness)



Planck Early Results: Dust properties

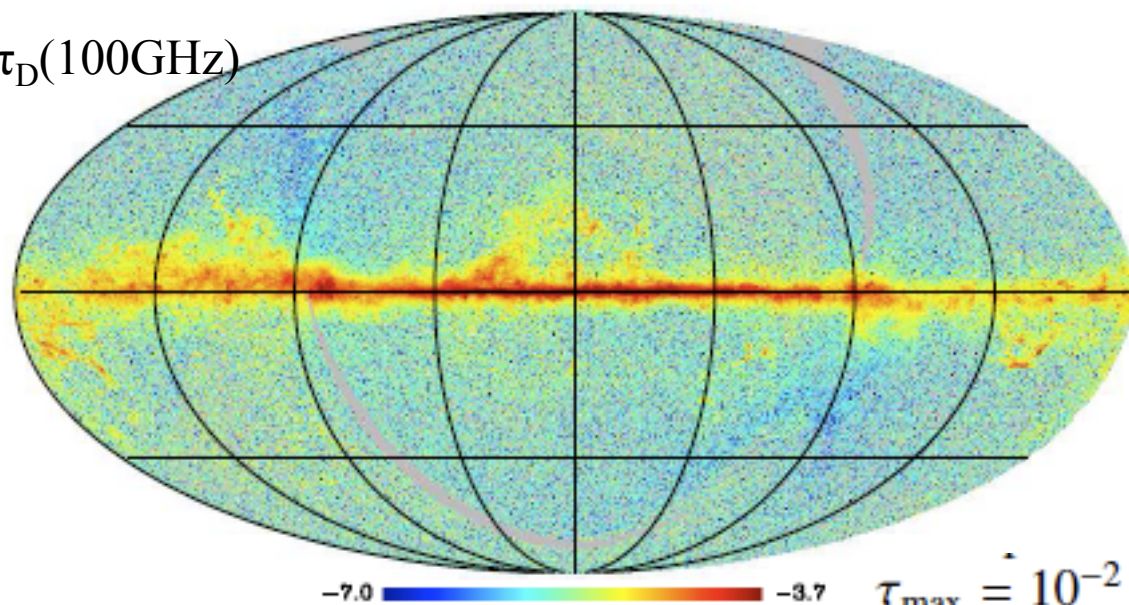
$\tau_D(857\text{GHz})$



Once the dust temperature is obtained, **dust optical depth maps** can be obtained at each frequency, as:

$$\tau_D(\lambda) = \frac{I_\nu(\lambda)}{B_\nu(T_D)}$$

$\tau_D(100\text{GHz})$



$$\Delta\tau_D(\nu) = \tau_D \left(\frac{\sigma_{II}^2}{I_\nu^2} + \left(\frac{\delta B_\nu(T_D)}{\delta T} \right)^2 \frac{\Delta T_D^2}{B_\nu^2(T_D)} \right)^{1/2}$$

(arXiv: 1101.2029)

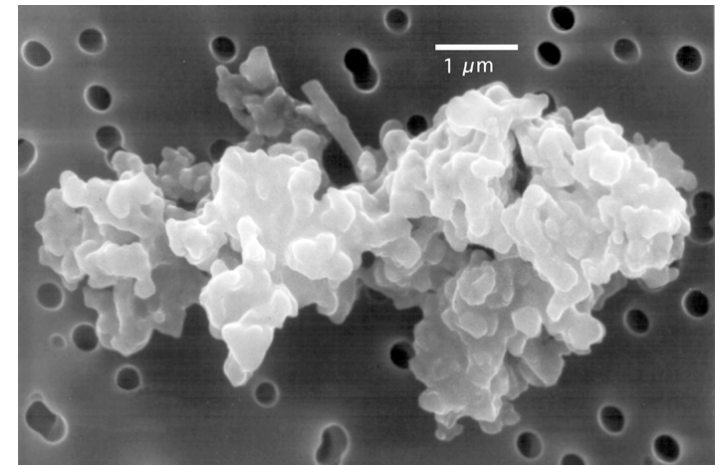
$$\tau_{\max} \hat{=} 10^{-2} \times (\lambda/100 \mu\text{m})^{-1.8}$$

Dust as a tracer of ISM

✧ Traces the **structure of the ISM** (from diffuse clouds to dense cores). The ISM is turbulent and therefore is full of structure on all spatial scales.

✧ Traces the **physical conditions in the ISM** (temperature, grain sizes and chemical composition).

✧ The ISM is **responsible for extinction and reddening**, the decreasing light intensity and shift in the dominant observable wavelengths of light from a star. These effects are caused by scattering and absorption of photons. Extinction in the optical bands is proportional to the amount of dust.



Thermal emission of a ionized gas

Due to [free-free emission](#) (bremsstrahlung). It appears in

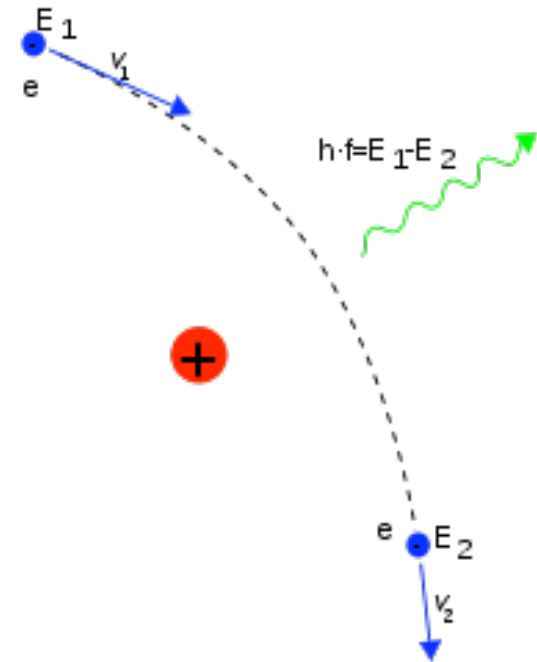
- HII regions.
- Planetary nebulae.
- Ionized stellar winds
- Solar atmosphere.

General properties:

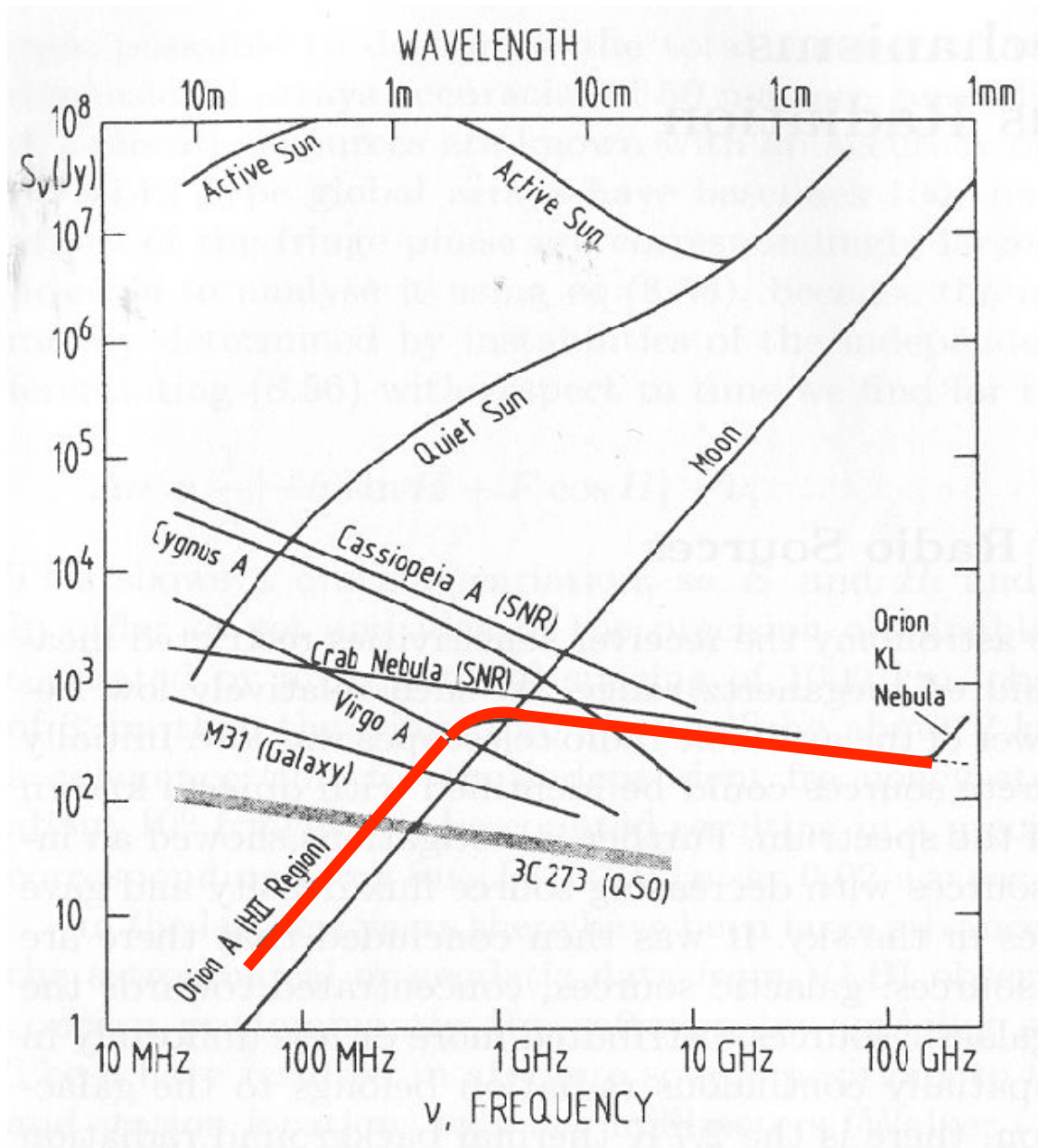
- At low frequencies, the SED follows a black-body spectrum
- At high frequencies, they show a frequency smooth dependence of $T \sim \nu^{-0.15}$
- Not polarized.
- In stellar winds, intermediate spectral index values are observed ($\nu^{0.6}$).

Examples of photo-ionized regions

- Emission nebulae: UV from type O stars. (E.g. Orion A).
- Planetary nebulae: white dwarf ionised the envelope. (E.g. NGC 7027).
- Hot and massive stars with intense stellar winds. (E.g. Wolf-Rayet stars).



Thermal emission of a ionized gas: Orion A



Thermal emission of a ionized gas

For $\nu < 30\text{GHz}$, we have

$$\tau_\nu \approx 0.082 (EM) T_e^{-1.35} \nu_{\text{GHz}}^{-2.1}$$

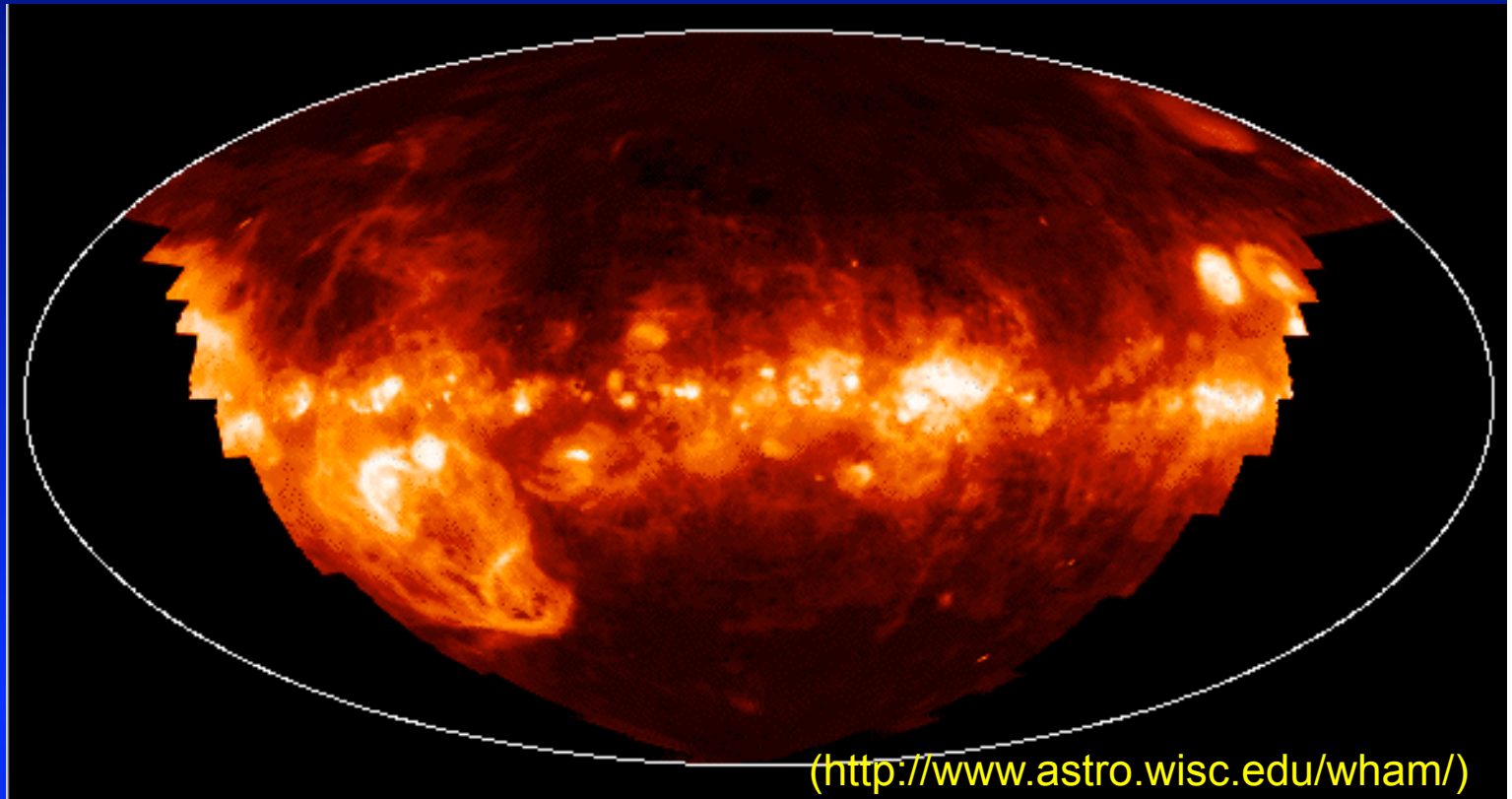
where we define the Emission Measure (EM) as

$$EM = \int n_e^2 dl$$

For a given physical conditions (density and temperature), the optical depth increases with decreasing frequency. For typical HII regions:

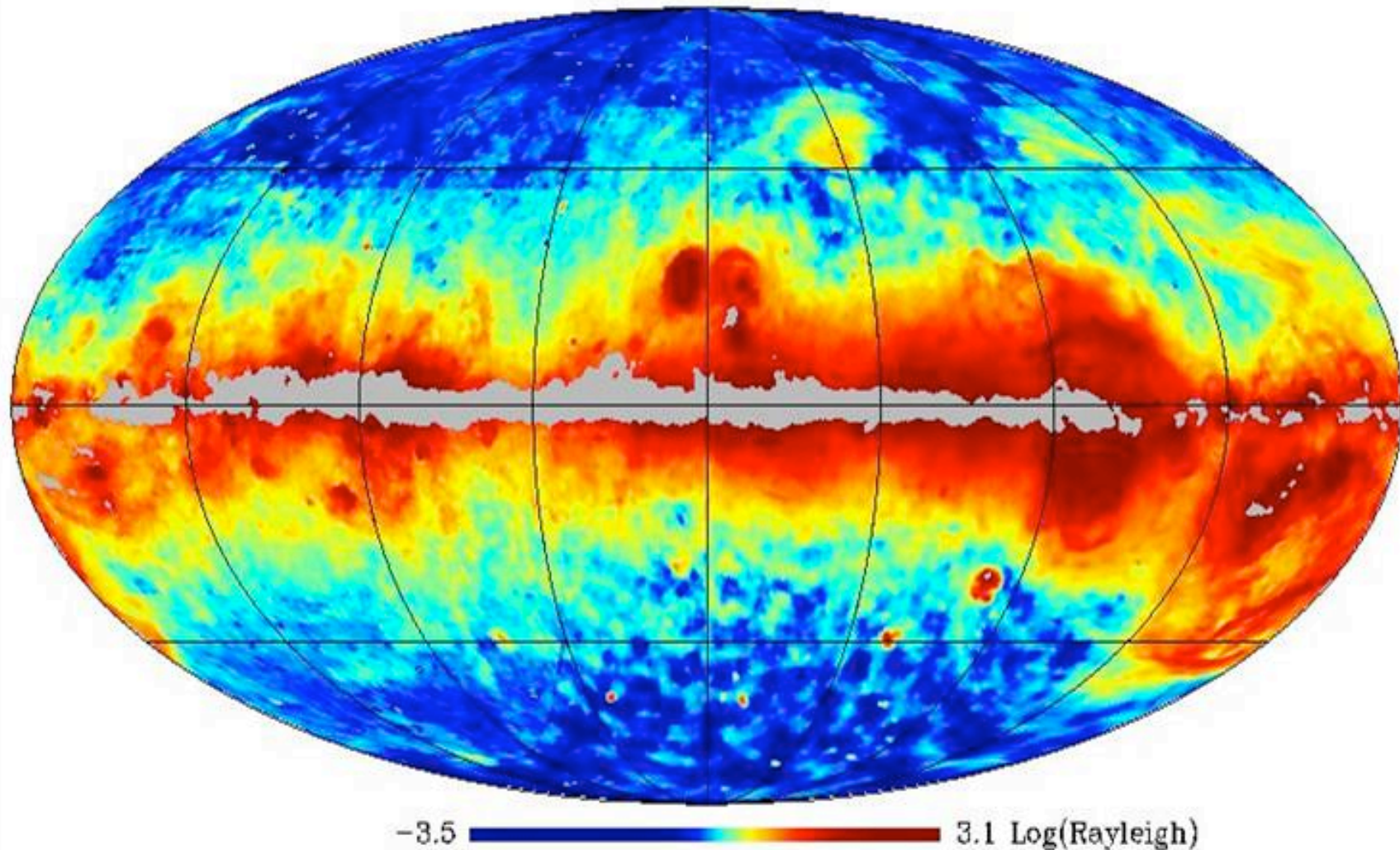
- $T_{\text{ex}} = T_e = 8000\text{K}$
- Knee frequency (ν_c): 0.1-1GHz.
- $\nu > \nu_c$: optically thick limit. $T_A = T_e$
- $\nu < \nu_c$: optically thin limit. $T_A = T_e \tau_\nu \sim \nu^{-2.1}$

*Free-free
emission*



- No direct template.
- Bennett et al. (1993):
could be traced using $H\alpha$
maps (warm ionised
medium). E.g. WHAM
- But $H\alpha$ affected by
absorption!

Full-sky dust corrected H α map



Dickinson et al. (2003)

$$I(\text{H}\alpha) \stackrel{\text{case B}}{=} 9.41 \times 10^{-8} T_4^{-1.017} 10^{-0.029/T_4} (\text{EM})_{\text{cm}^{-6} \text{pc}},$$

Non thermal emission

Due to [synchrotron emission](#) (relativistic electrons moving inside magnetic fields).

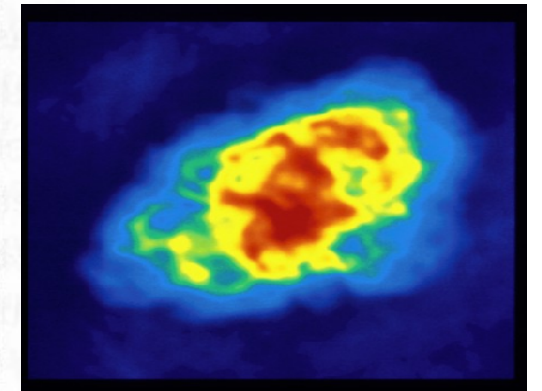
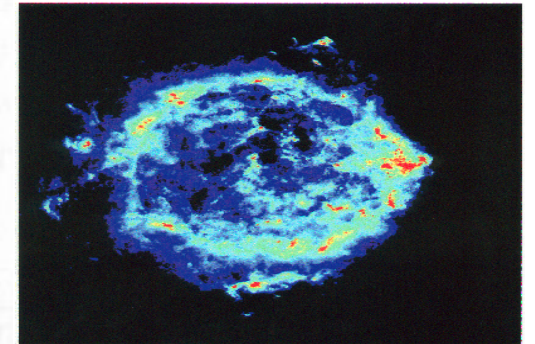
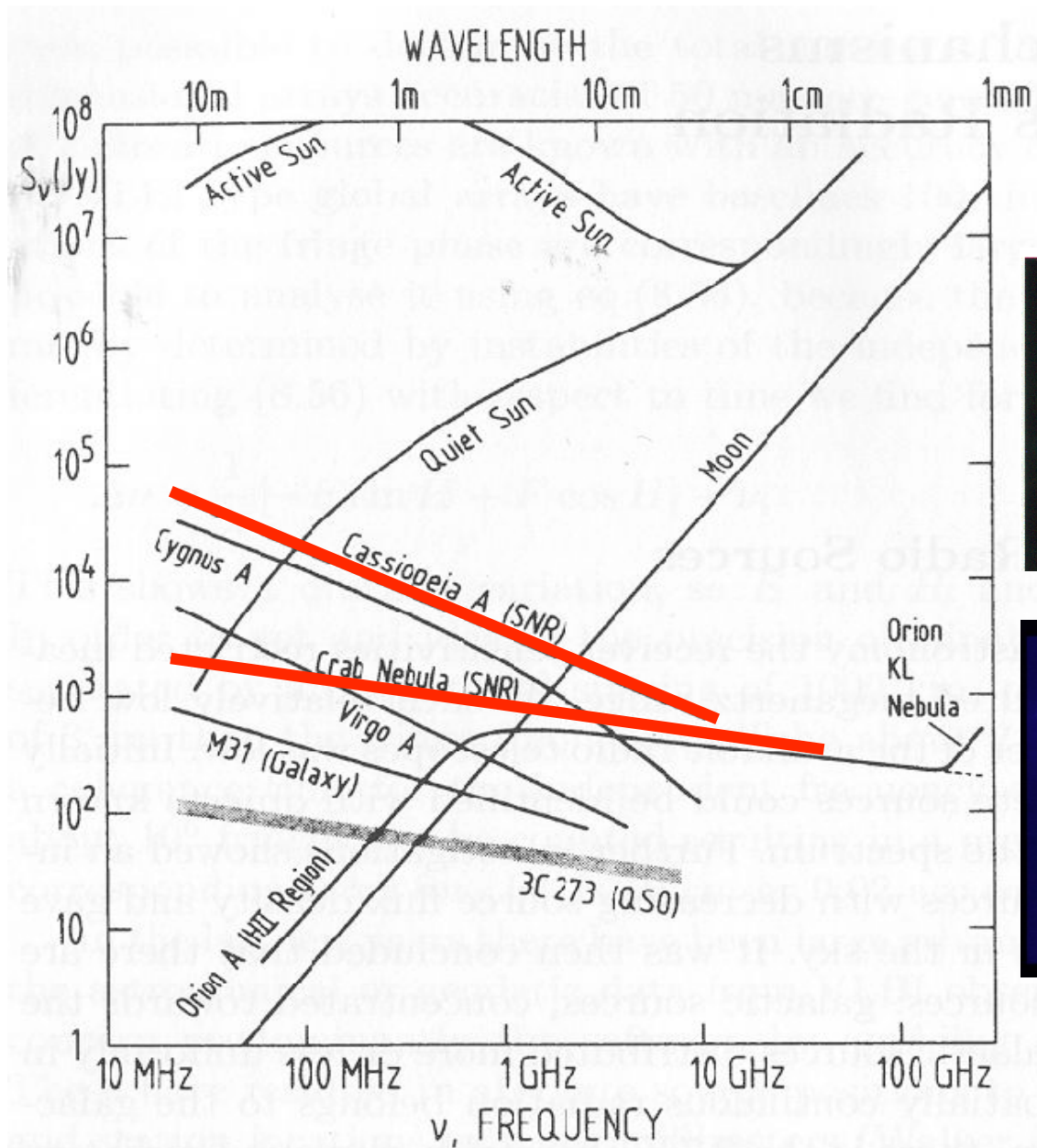
It can be found in:

- Solar fulgurations
- Low frequency radiation from Jupiter
- Pulsars
- Supernova remnants
- Continuum emission in our galaxy
- Radio-galaxies and quasars

General properties

- Dominates at low frequencies
- High degree of polarization
- Characteristic (non-thermal) frequency dependence $\nu^{-0.7}$.

Non-thermal emission. Supernova remnants



Synchrotron emission (I)

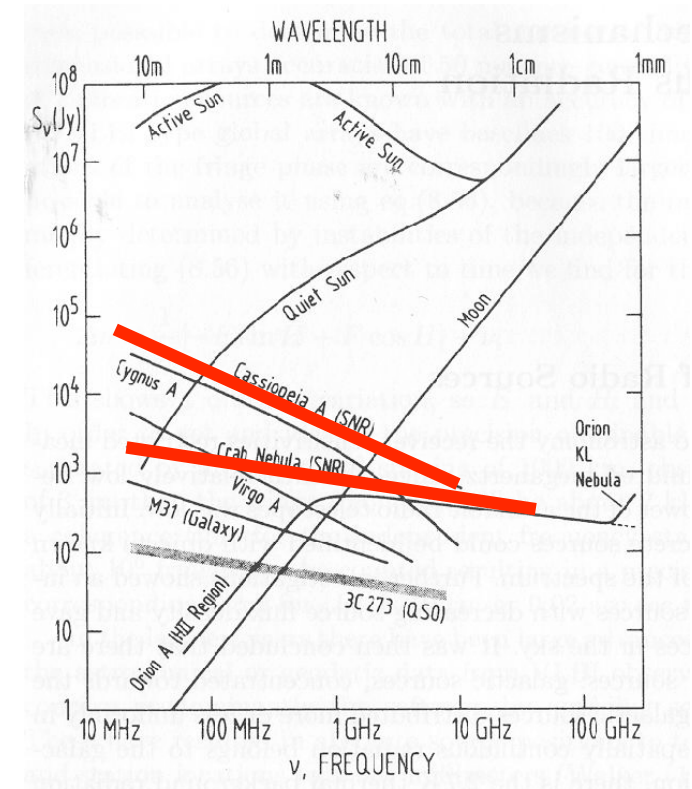
Electrons moving at **relativistic velocities** inside a **magnetic field**.

- At non-relativistic velocities, we have the classical cyclotron emission, at the Larmor frequency:

$$\nu_L = 2.8 \left(\frac{B}{1 \text{ Gauss}} \right) \text{ MHz}$$

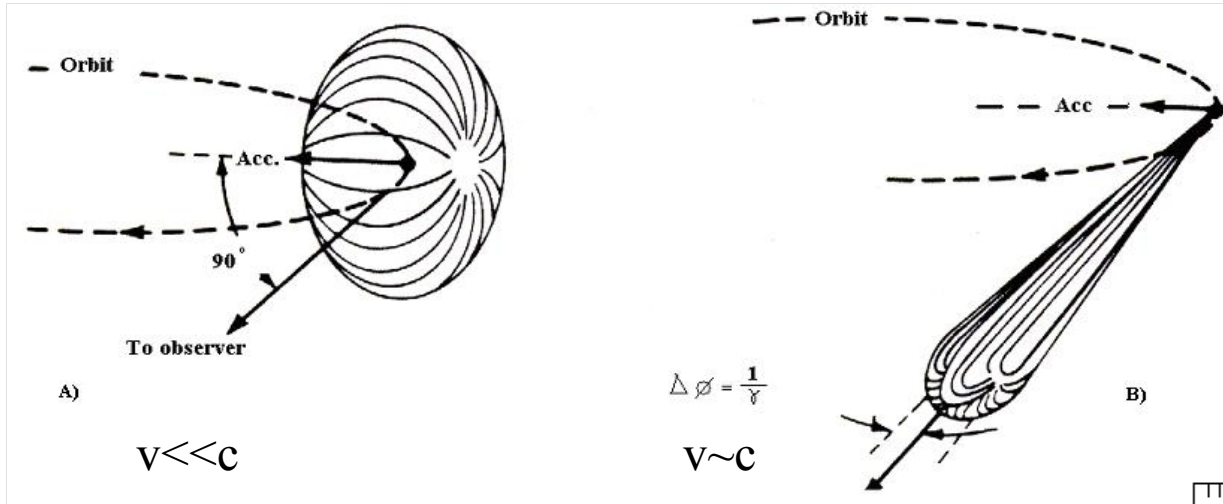
- For typical values of the magnetic field, this emission is at very low frequencies!
- **How to generate a continuum spectrum extending up to GHz frequencies??**
 - Relativistic beaming effect.
 - Relativistic Doppler shift.
- **Average synchrotron power:** (remember presentation by S. Colafrancesco yesterday).

$$\langle P \rangle = \frac{4}{3} \sigma_T \beta^2 \gamma^2 c U_B$$



Synchrotron emission (II)

Beaming effect:



Spectrum extends up to:

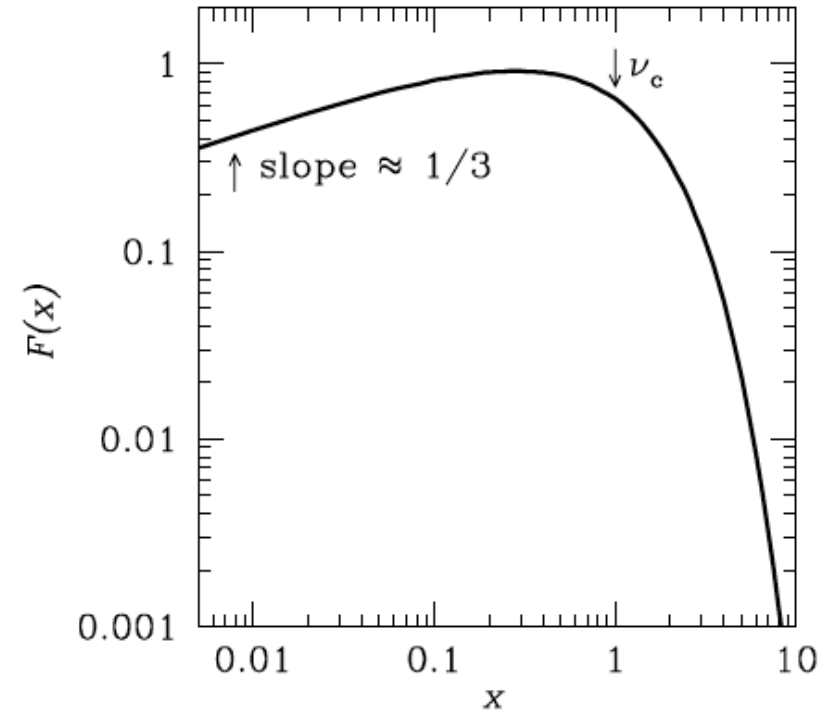
$$\nu_c = \frac{3}{4\pi} \gamma^2 \nu_L \sin \alpha$$

$$\gamma = \frac{1}{\sqrt{1 - \frac{v^2}{c^2}}}$$

Power radiated by a single electron:

$$P(\nu) = \frac{\sqrt{3}e^3 B \sin \alpha}{mc^2} \underbrace{\left(\frac{\nu}{\nu_c} \right) \int_{\nu/\nu_c}^{\infty} K_{5/3}(\eta) d\eta}_{F(x), x=\nu/\nu_c}$$

$B \leftarrow B_{perp}$



Synchrotron emission. Energy distribution of CR.

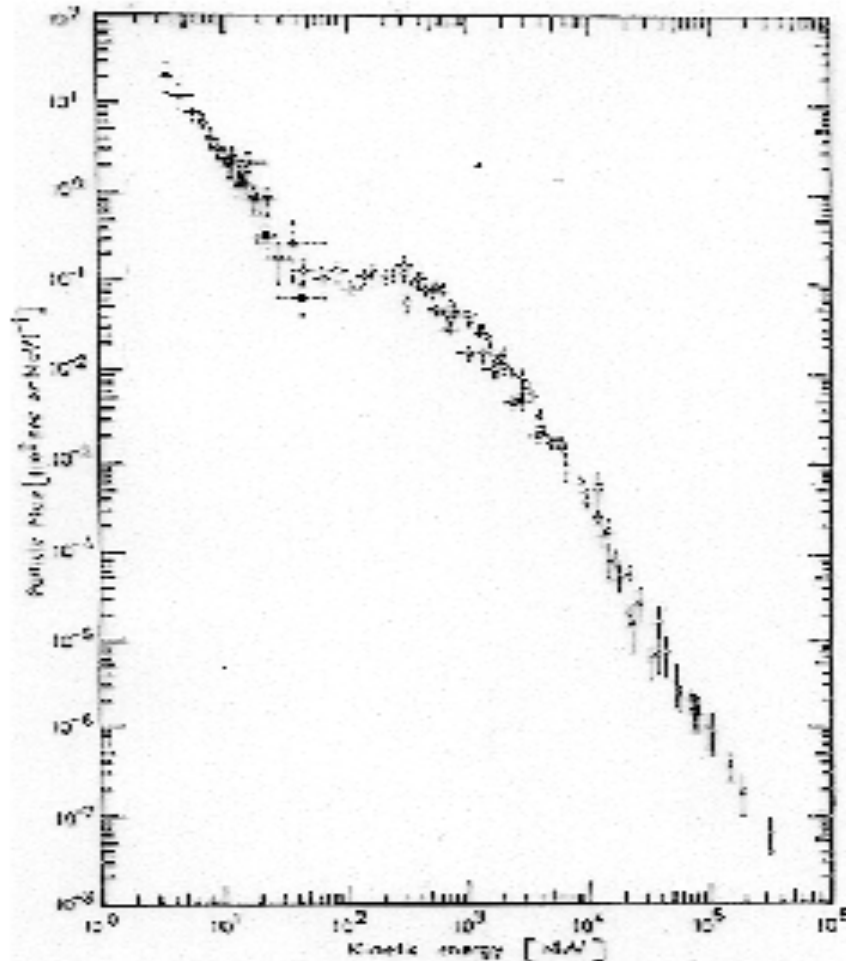


Fig. 24 Energy spectrum of the primary cosmic ray electrons after Fessenden et al., 1968, by permission of the American Astronomical Society and the University of Chicago Press. Each symbol denotes a different set of observations, and these are tabulated by Fessenden et al.

$$N(E) = k E^{-\delta}, \quad E_1 < E < E_2$$

$$\delta \approx 2.4 \quad (E < 0.3 \text{ TeV})$$

Integrating the power radiated by each electron multiplied by the number of electrons, we obtain the **total synchrotron emissivity**:

$$I_\nu \sim N_0 v^{-n} (B \sin \alpha)^{n+1}$$

$$n = (\delta - 1) / 2$$

1) $\delta \approx 2.4 \rightarrow n=0.7$

2) Spectral index is connected with the energy distribution of CR.

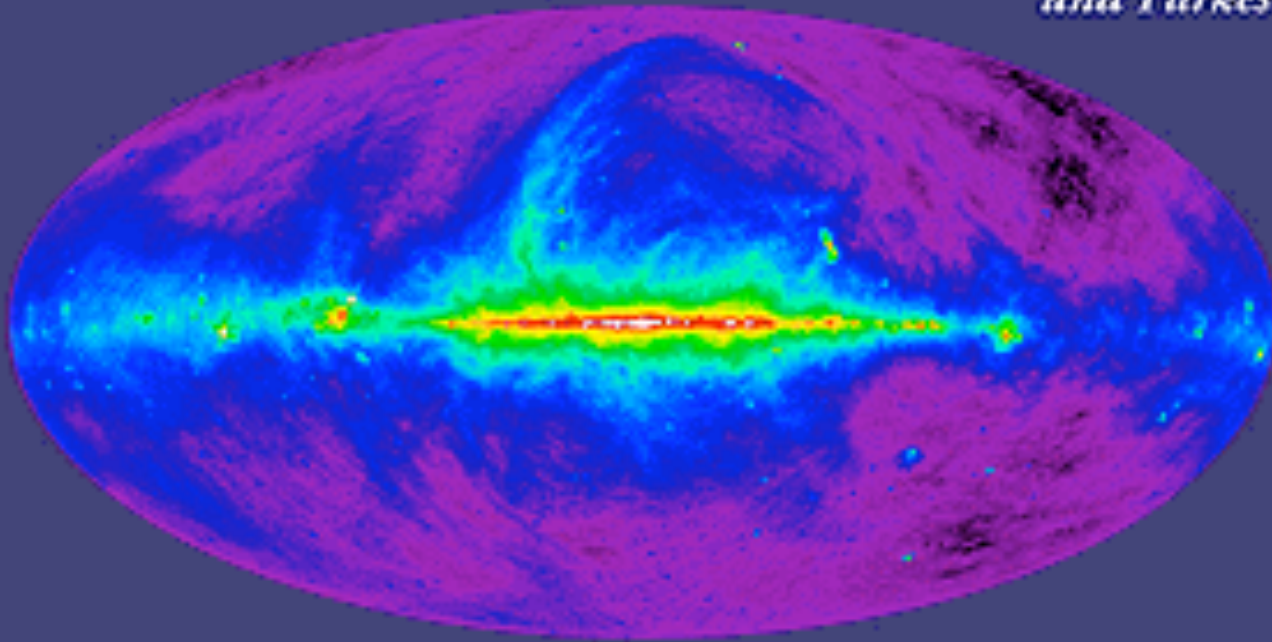
3) Probes magnetic field perpendicular to line of sight.

Synchrotron emission

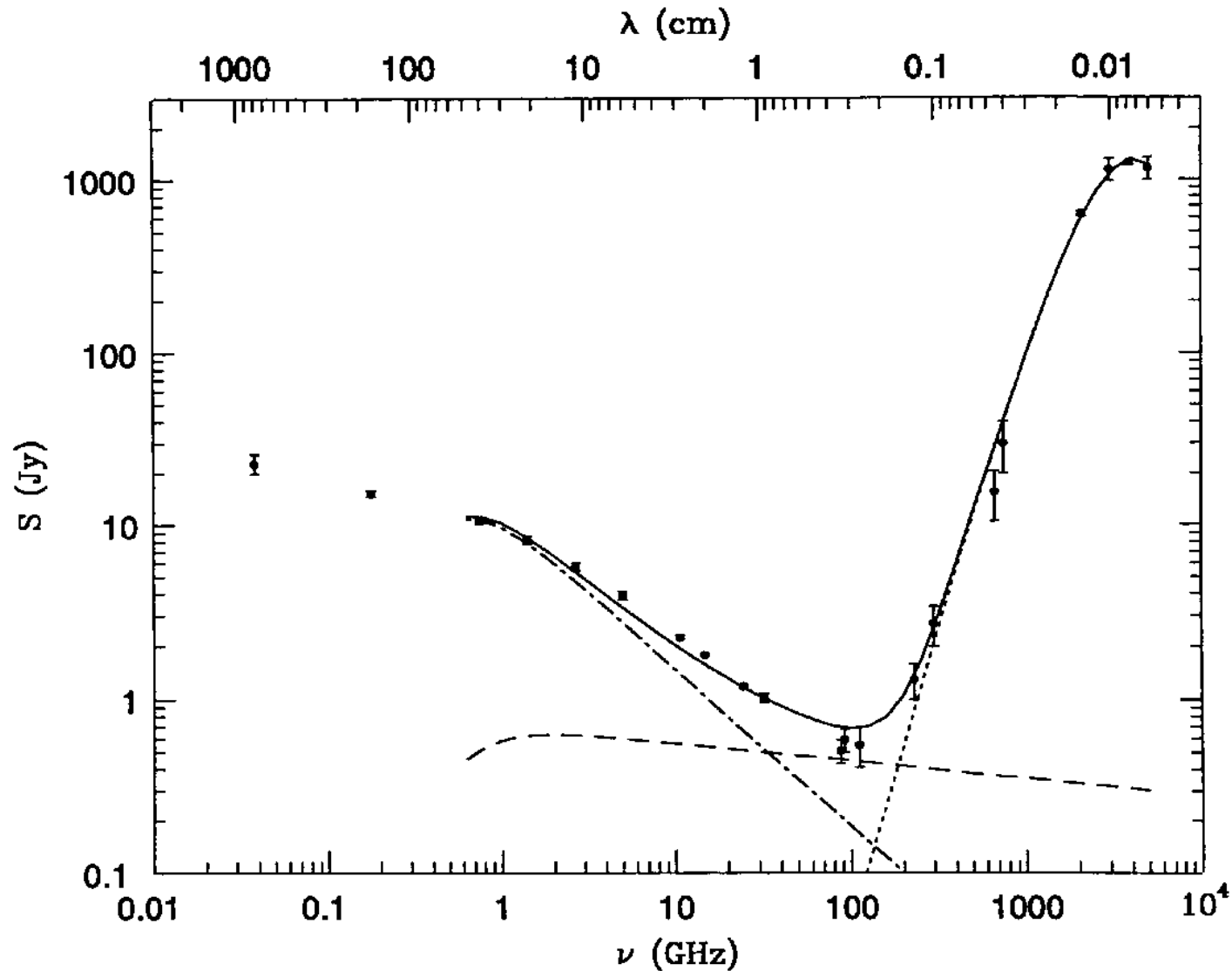
- Traced by low frequency maps. (Haslam 408MHz)

Radio Continuum (408 MHz)

*Bonn, Jodrell Bank,
and Parkes*



Radio and far-IR spectrum of M82



- The radio and far-infrared spectrum of the nearby starburst galaxy **M82**.
- Synchrotron (dot-dashed) and dust (dotted) emission dominate at low and high frequencies, respectively. Free-free absorption from HII regions distributed throughout the galaxy flattens the overall spectrum at the lowest frequencies.
- Free-free emission (dashed line) accounts for about 10% of the 1 GHz continuum luminosity in most spiral galaxies. It is the strongest component in the frequency range from 30 GHz to 200 GHz, above which thermal emission from cool dust grains dominates.

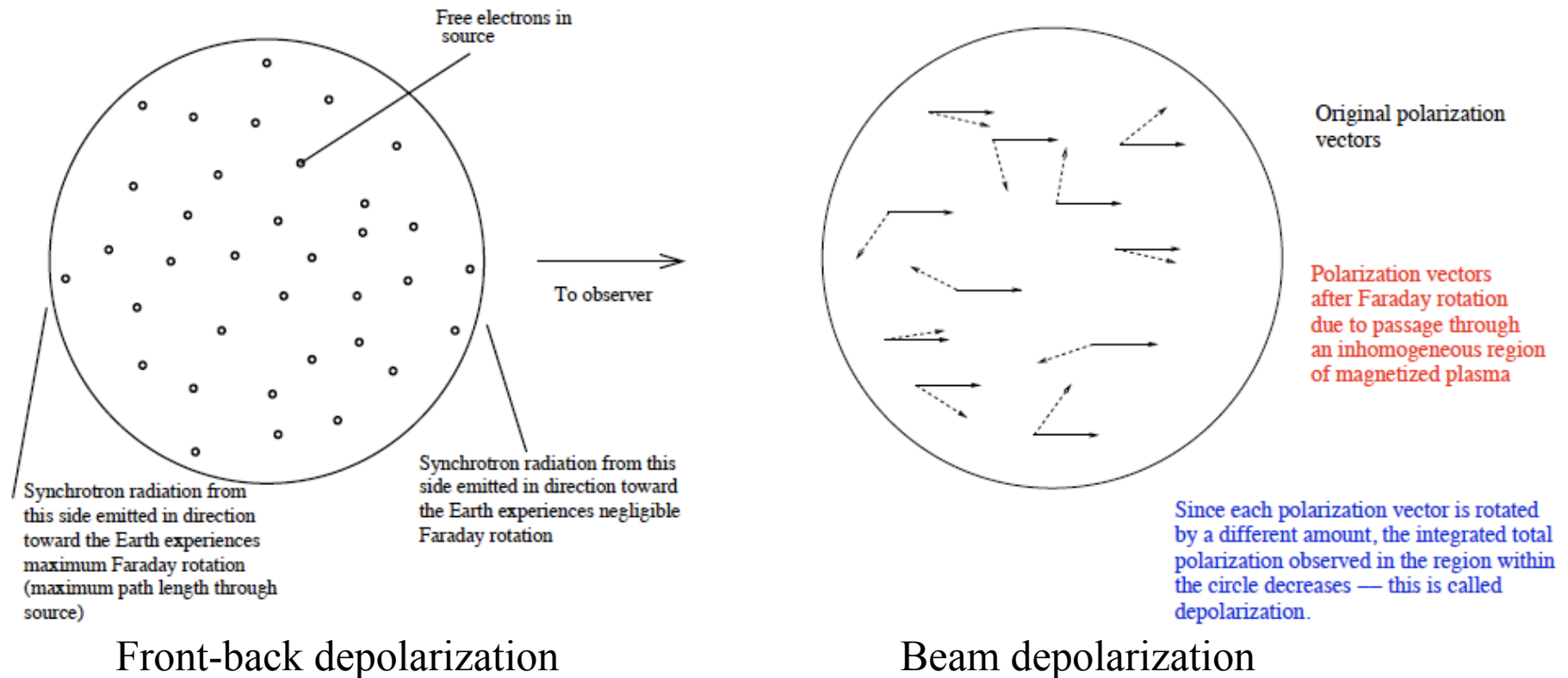
Synchrotron radiation. Propagation effects

A) **Faraday Rotation.** A rotation of the plane of polarization of an EMwave that occurs if it passes through a region with free electrons and magnetic field.

$$\Delta\theta = (RM)\lambda^2$$

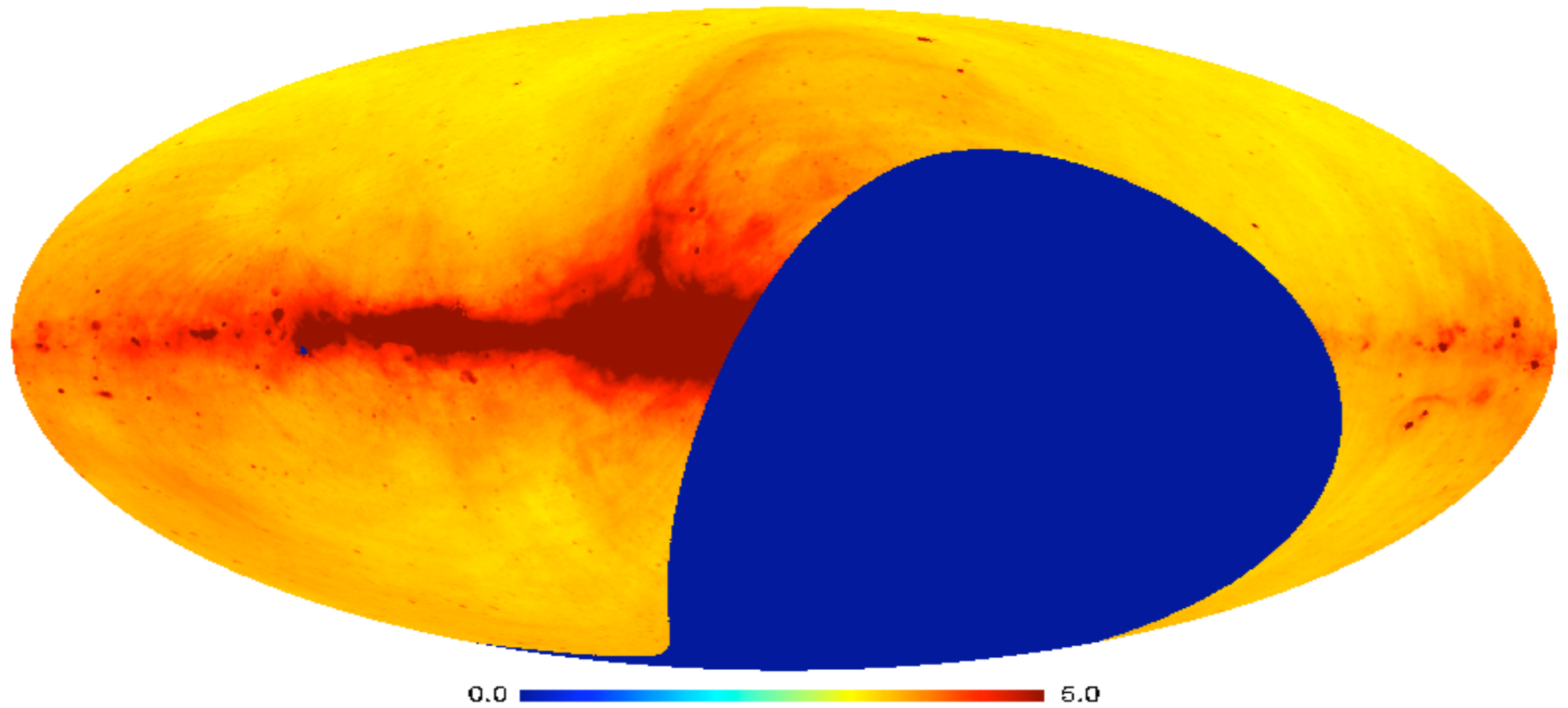
$$RM \propto \int B_{\parallel} n_e dl$$

B) **Depolarization.** Faraday Rotation can “depolarize” due to two effects.



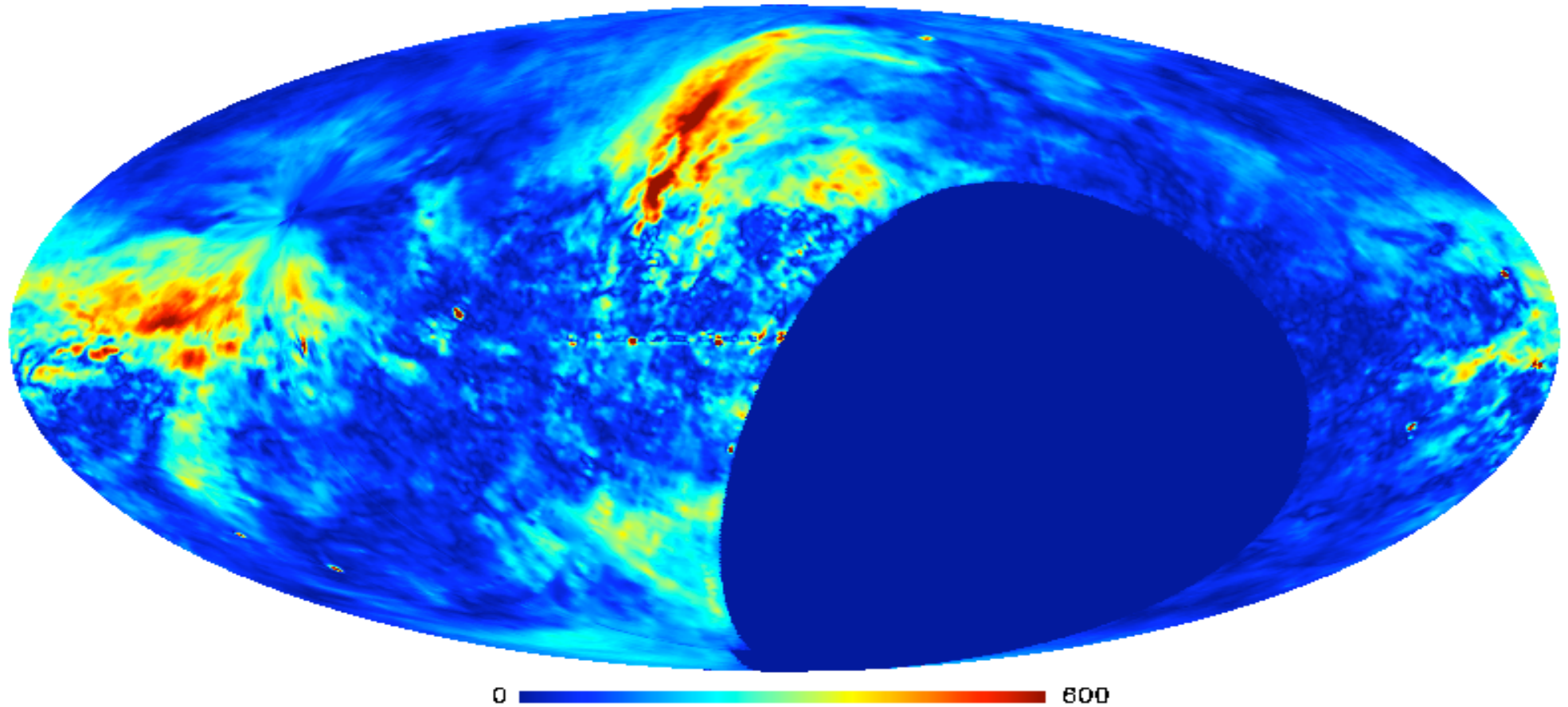
Continuum radio emission. 21 cm.

Reich & Reich (1420 MHz)



Continuum radio emission. 21 cm.

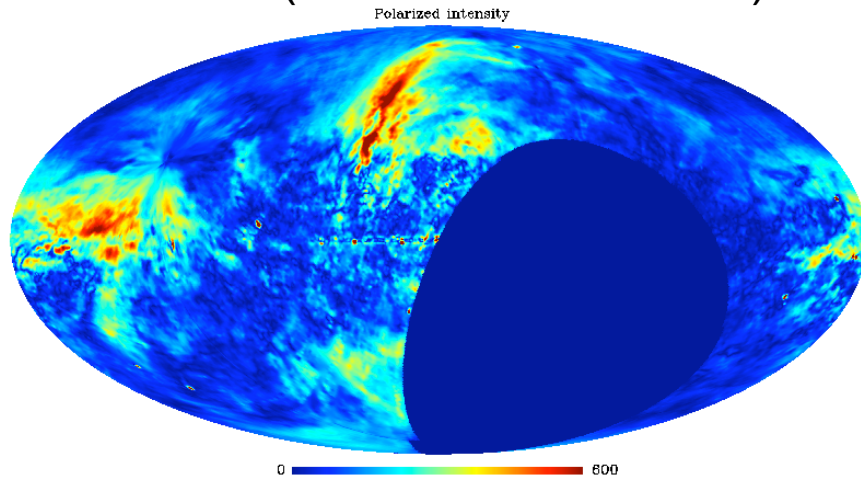
1.4GHz (Wolleben et al. 2005)
Polarized intensity



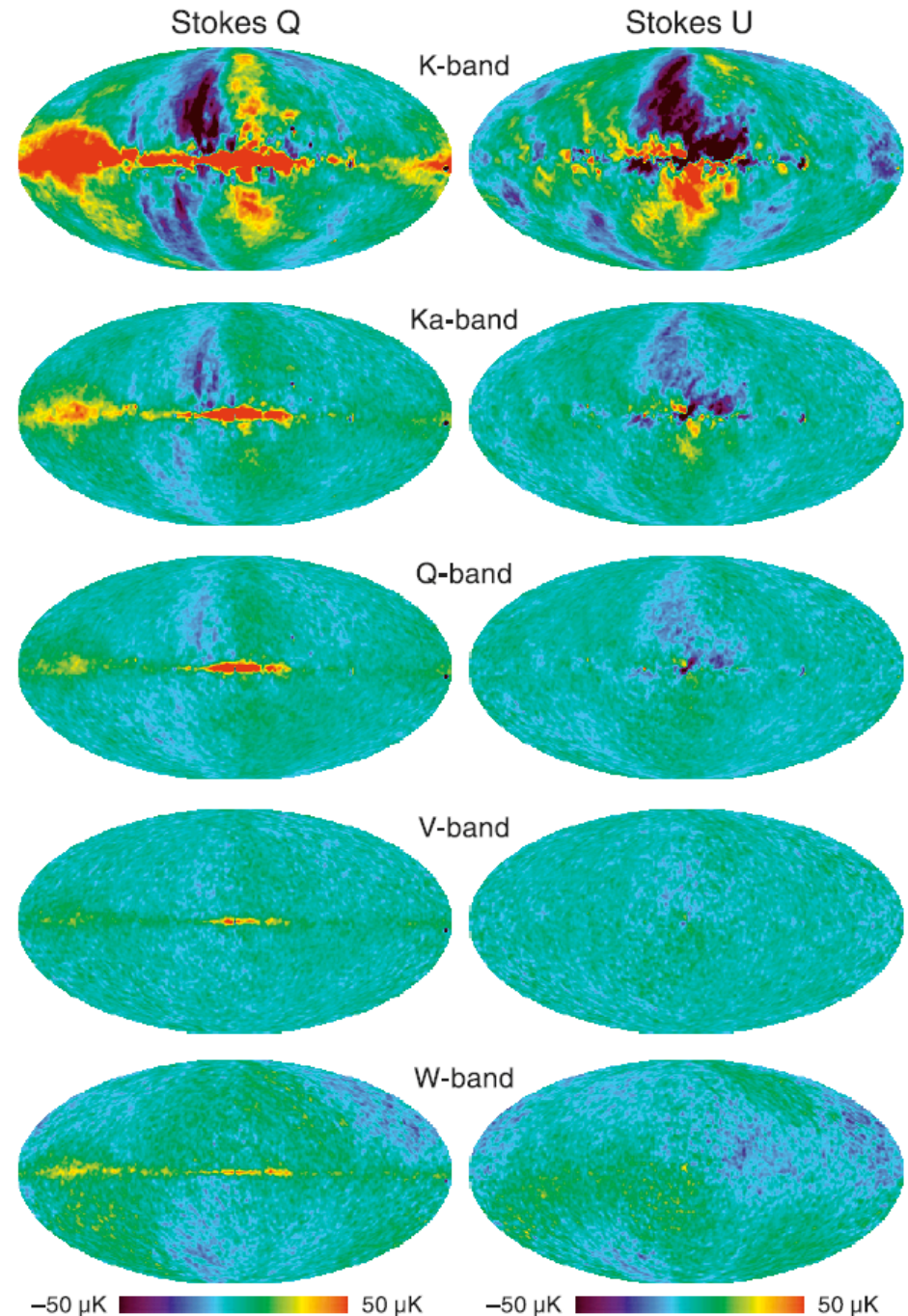
Polarization of the synchrotron emission at cm wavelengths: a window to the galactic magnetic field

- Free-free emission not polarized.
- Synchrotron emission highly polarized. Traces coherent MF.
- Spectral index depends on the CR energy distribution.
- At cm wavelengths, Faraday depolarization is negligible.

1.4GHz (Wolleben et al. 2005)



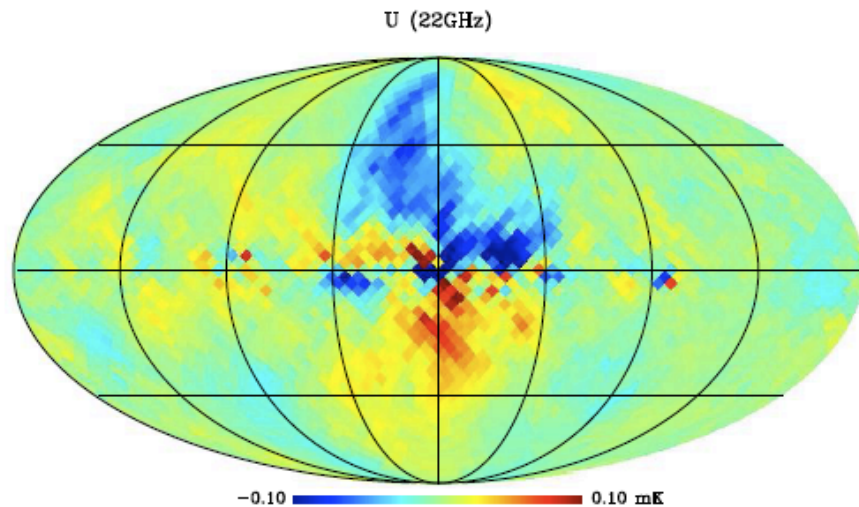
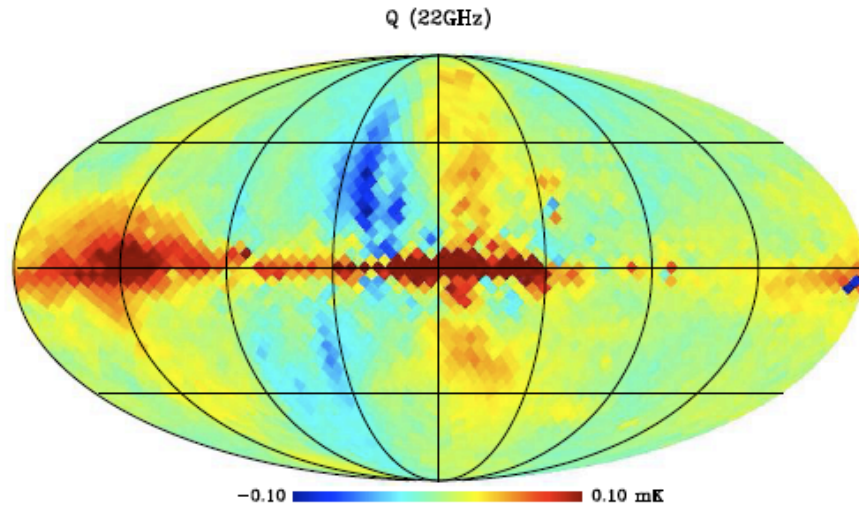
WMAP 7yr results



Jarosik et al. 2010

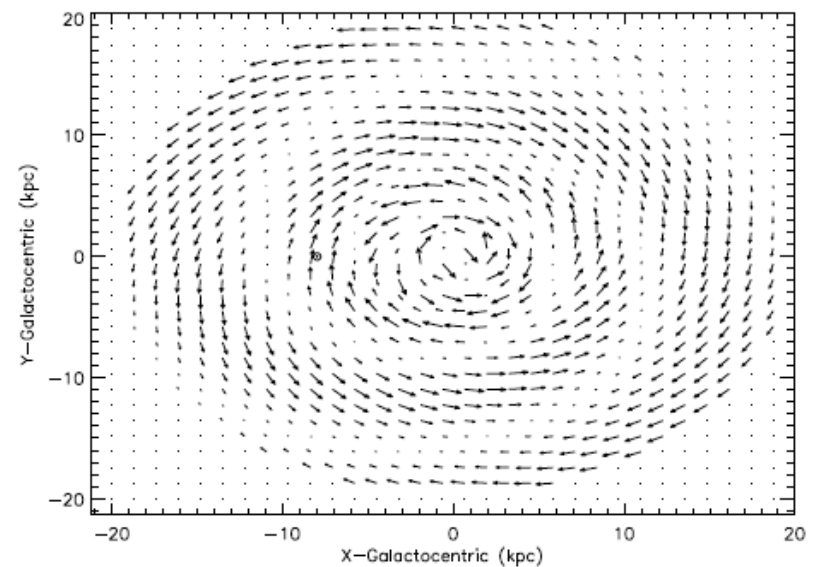
Regular pattern of the magnetic field in the Milky Way

- ❖ Ruiz-Granados, Rubiño-Martin & Battaner (2010). Polarized synchrotron emission at 22GHz (WMAP).
- ❖ Description of **magnetic field in the disc** is fully compatible with pulsars and EGRS measurements.
- ❖ **Direct constraints to the shape of the MF in the halo** (axi-simmetry, $p \approx 24^\circ$, $1 \mu\text{G}$ vertical at 1kpc, high r_1).



$$\epsilon_{\perp}(v) = N(r, z) \frac{\sqrt{3}e^3}{8\pi mc^2} \left(\frac{4\pi mc}{3e} \right)^{\frac{1-p}{2}} v^{\frac{1-p}{2}} (B \sin \alpha)^{\frac{p+1}{2}} \Gamma\left(\frac{p}{4} - \frac{1}{12}\right) \left[\frac{2^{\frac{p+1}{2}}}{p+1} \Gamma\left(\frac{p}{4} + \frac{19}{12}\right) + 2^{\frac{p-3}{2}} \Gamma\left(\frac{p}{4} + \frac{7}{12}\right) \right]$$

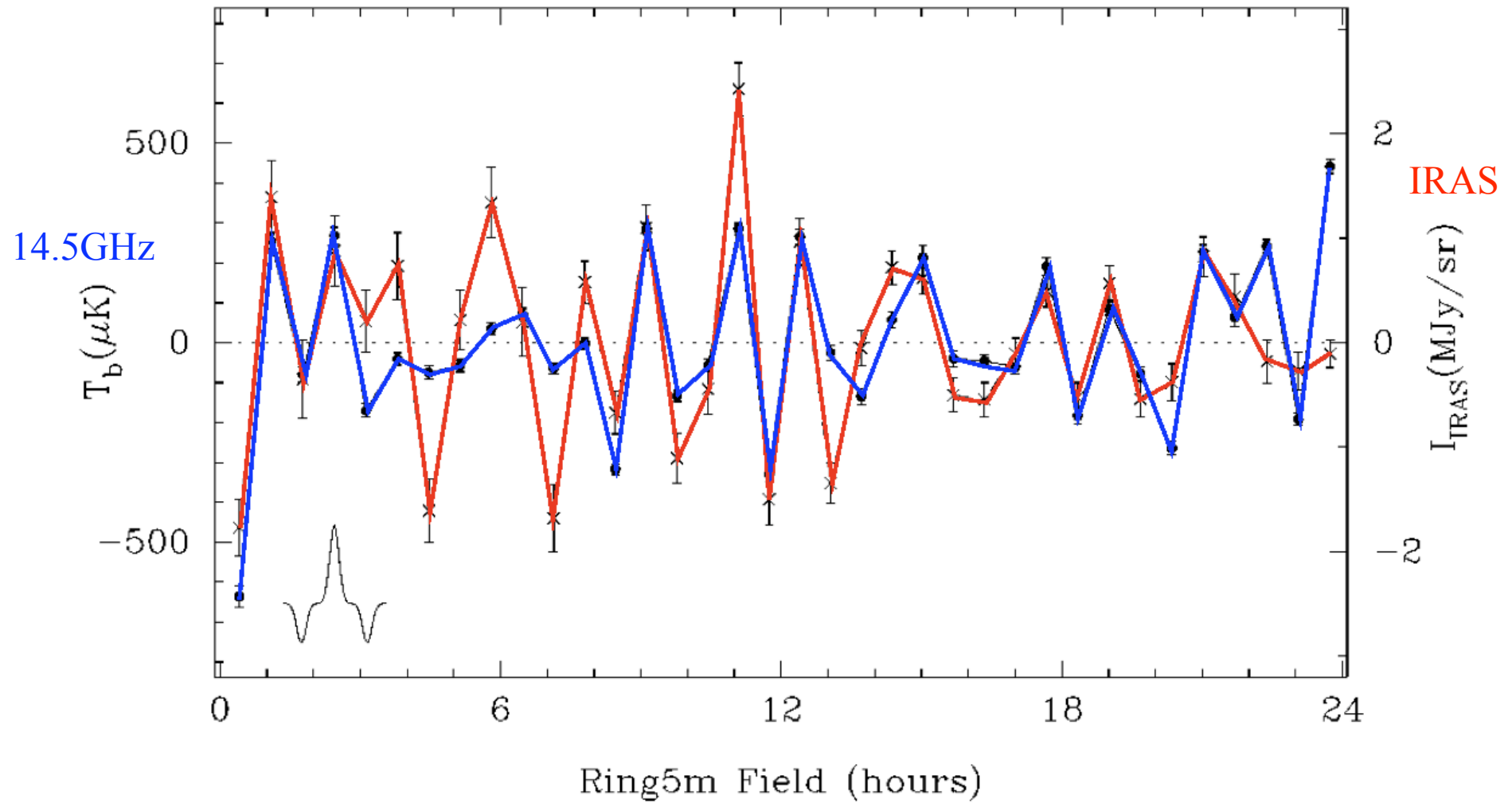
$$\epsilon_{\parallel}(v) = N(r, z) \frac{\sqrt{3}e^3}{8\pi mc^2} \left(\frac{4\pi mc}{3e} \right)^{\frac{1-p}{2}} v^{\frac{1-p}{2}} (B \sin \alpha)^{\frac{p+1}{2}} \Gamma\left(\frac{p}{4} - \frac{1}{12}\right) \left[\frac{2^{\frac{p+1}{2}}}{p+1} \Gamma\left(\frac{p}{4} + \frac{19}{12}\right) - 2^{\frac{p-3}{2}} \Gamma\left(\frac{p}{4} + \frac{7}{12}\right) \right]$$



New physics in the Galaxy

Discovery of the Anomalous Microwave Emission (AME)

14.5/32 GHz OVRO data (Leitch et al. 1997)



Evidence for anomalous microwave emission

Evidence for our Galaxy:

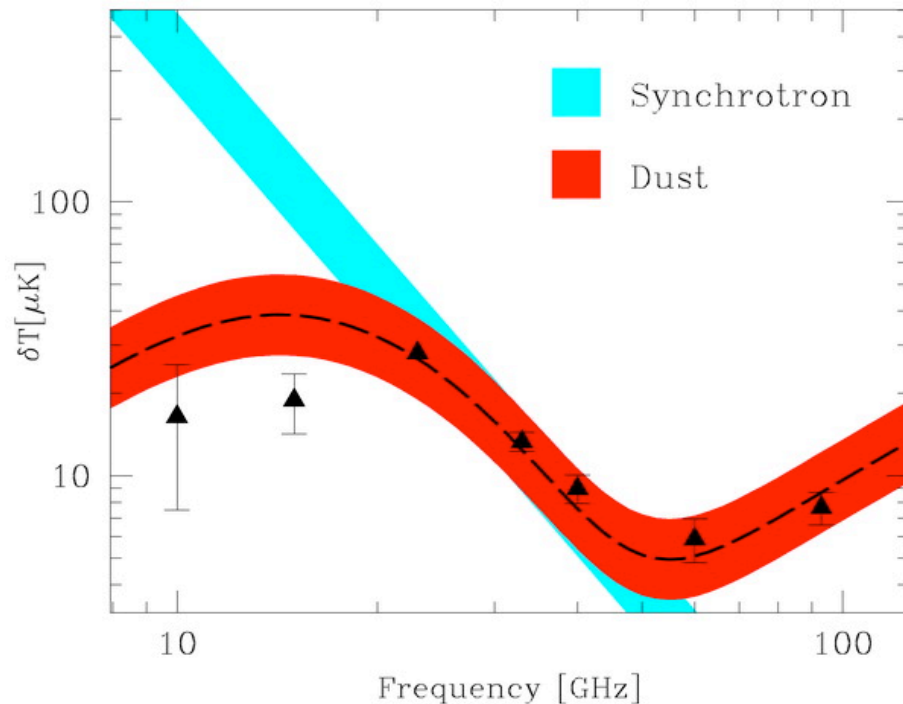
- **OVRO**: Leitch et al. (1997)
- **COBE-DMR**: Kogut et al. (1996), Banday et al. (2003).
- **Saskatoon**: de Oliveira-Costa (1997)
- **Tenerife**: Mukherjee et al. (2001), de Oliveira-Costa et al. (2002, 2004)
- **Python V**: Mukherjee et al. (2003)
- **Green Bank**: Finkbeiner (2002), Finkbeiner et al. (2004)
- **Cosmosomas**: Watson et al. (2005), Battistelli et al. (2006), Fernández-Cerezo et al. (2006), Hildebrandt et al. (2007)
- **VSA**: Scaife et al. (2007), Tibbs et al. (2009), Todorovic et al. (2010)
- **CBI**: Casassus et al. (2004,2006,2007,2008), Dickinson et al. (2006,2007,2009a,2010), Castellanos et al. (2011), Vidal et al. (2011)
- **AMI**: Scaife et al. (2008), Scaife et al. (2009a,b), Scaife et al. (2010)
- **WMAP**: Bennett et al. (2003), Lagache et al. (2003), Davies et al. (2006), Bonaldi et al. (2007), Miville-Deschenes et al. (2008), Gold et al. (2009), Dobler & Finkbeiner (2009), Ysard et al. (2009), Dickinson et al. (2009a), Lopez-Caraballo et al. (2011).
- **PLANCK**: The Planck Collaboration XX (2011).

Evidence for external galaxies:

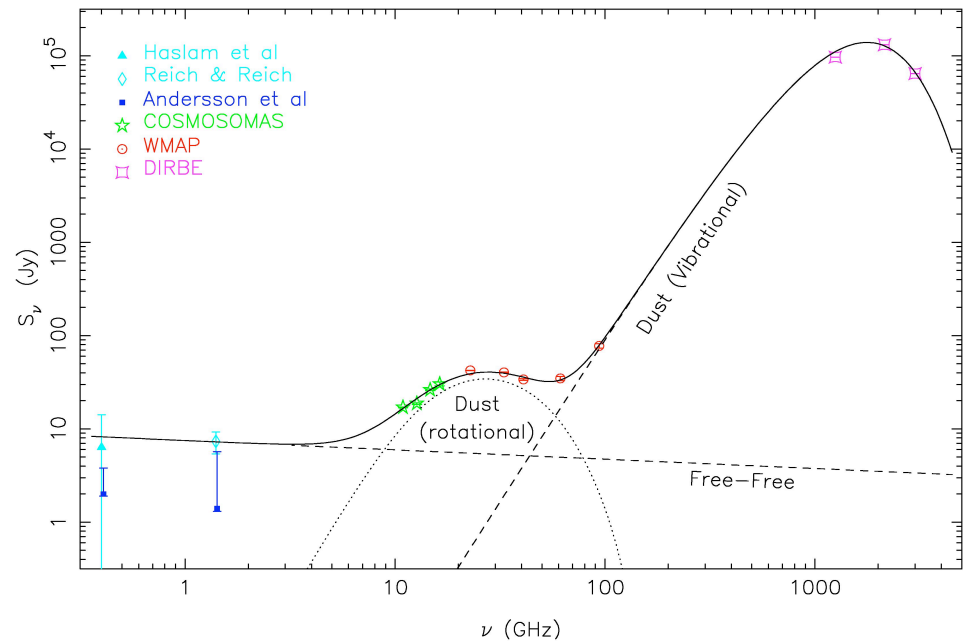
- **NGC 6946**: Murphy et al. 2010; Scaife et al. 2010.

Frequency dependence of the AME

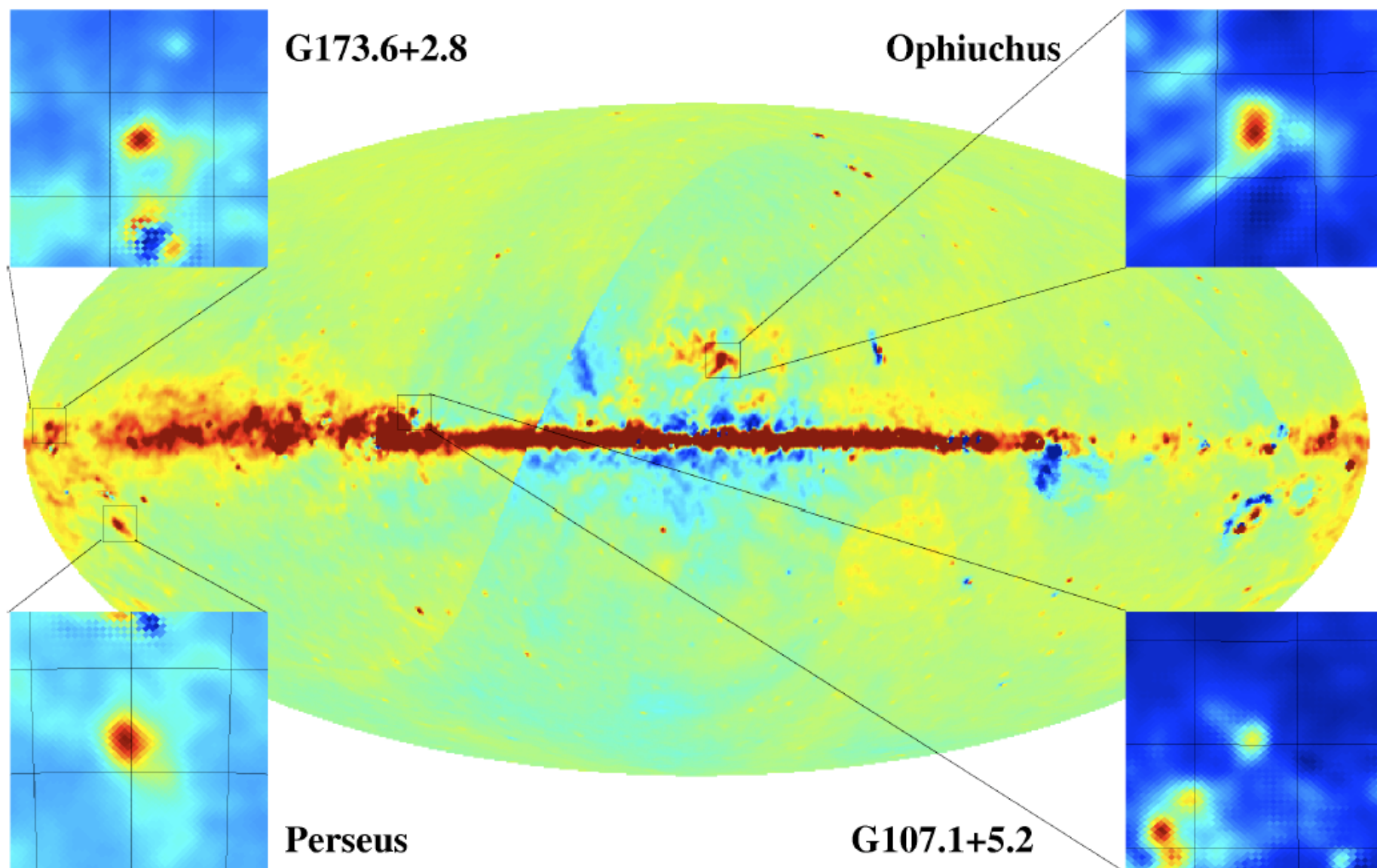
- High frequency data constrain the emission of thermal dust grains.
- Peak emission around 20-30GHz.
- Turn-over in the emission at low frequencies, which is not consistent with synchrotron emission.



Tenerife Experiment (de Oliveira-Costa et al. 2004)



COSMOSOMAS Experiment (Watson et al. 2005)



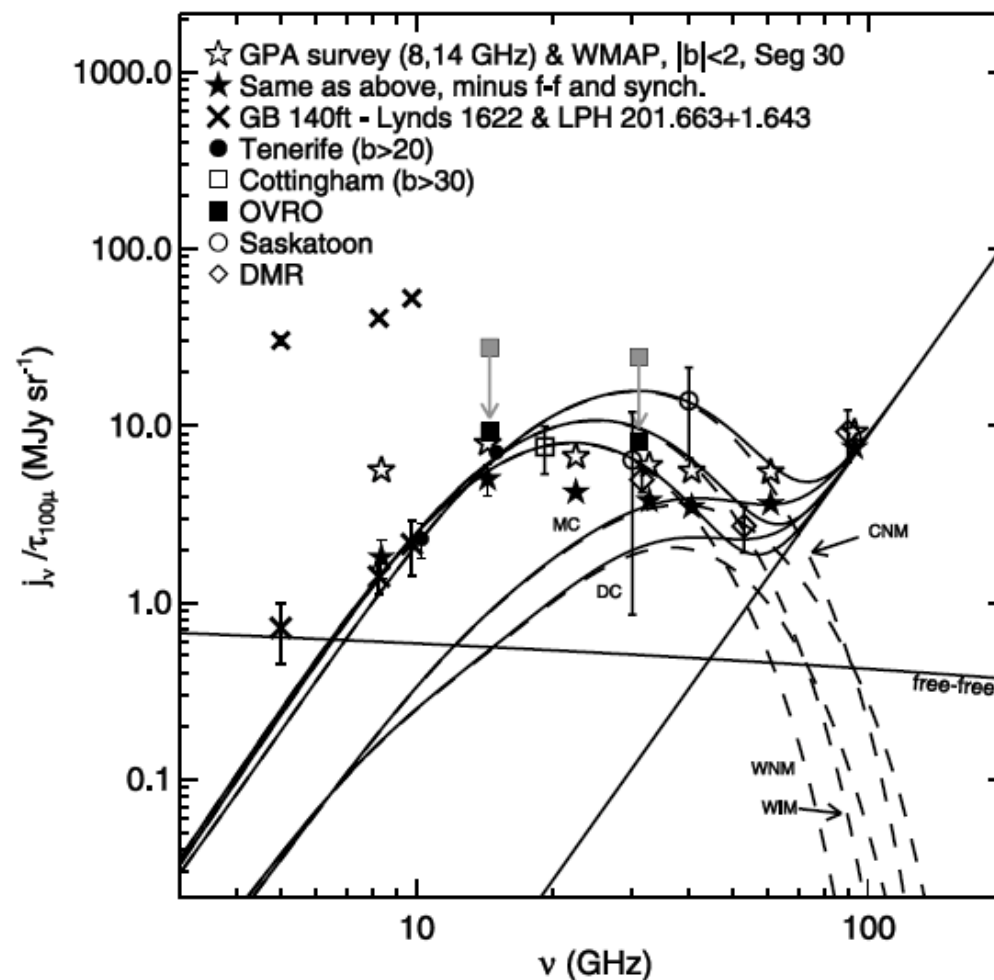
What is the Anomalous Microwave Emission?

Lots of possibilities considered:

- Warm ($T \sim 10000$ K) free-free
- Hot ($T \sim 10^6$ K) free-free
- Absorbed free-free from UCHII regions
- Flat spectrum ($\beta \sim -2.5$) synchrotron emission
- Magneto-dipole radiation
- Cold dust / emissivity variations
- ...

The best explanation is electro-dipole radiation from small spinning dust grains (“spinning dust”).

Models could be confirmed/refined by measuring the polarization of the emission.



Draine & Lazarian 1998

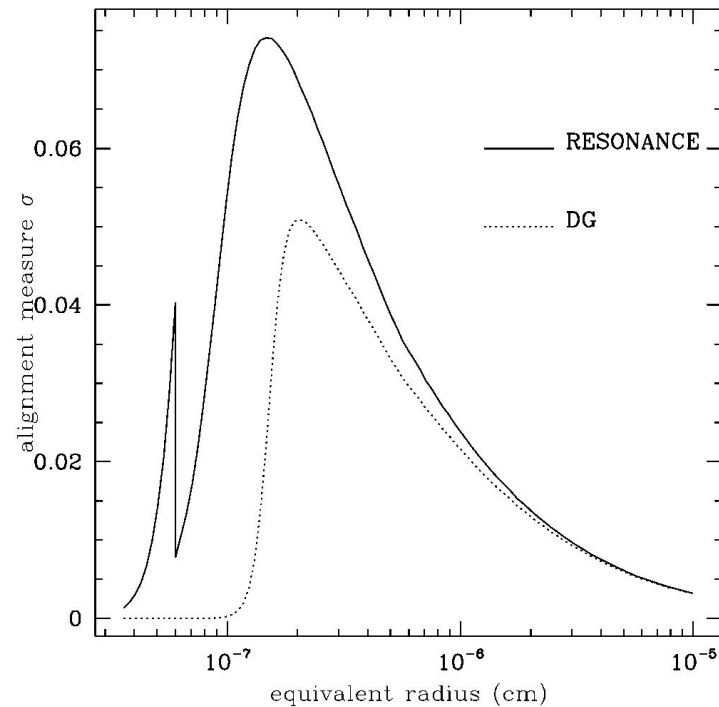
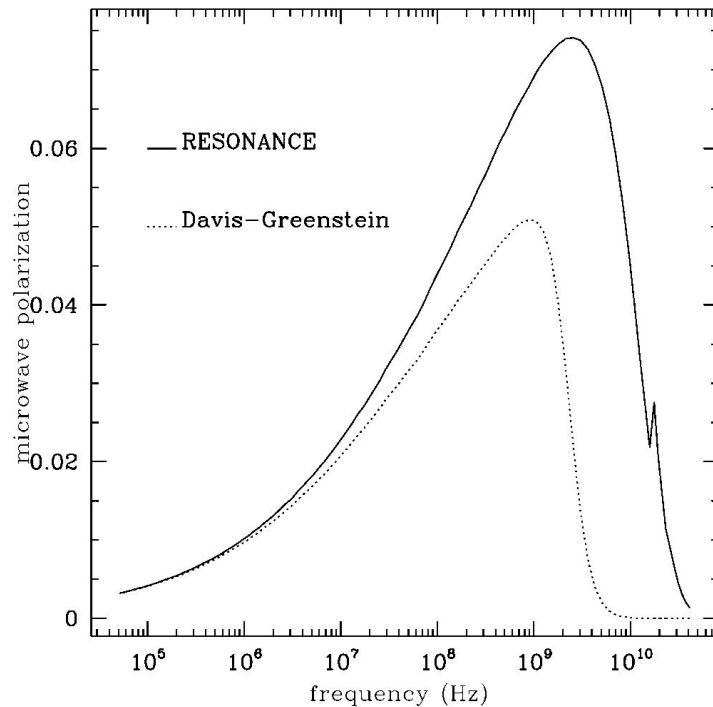
Finkbeiner 2004

Polarization of rotational electric dipole radiation

(Lazarian and Draine 2000 ApJ)

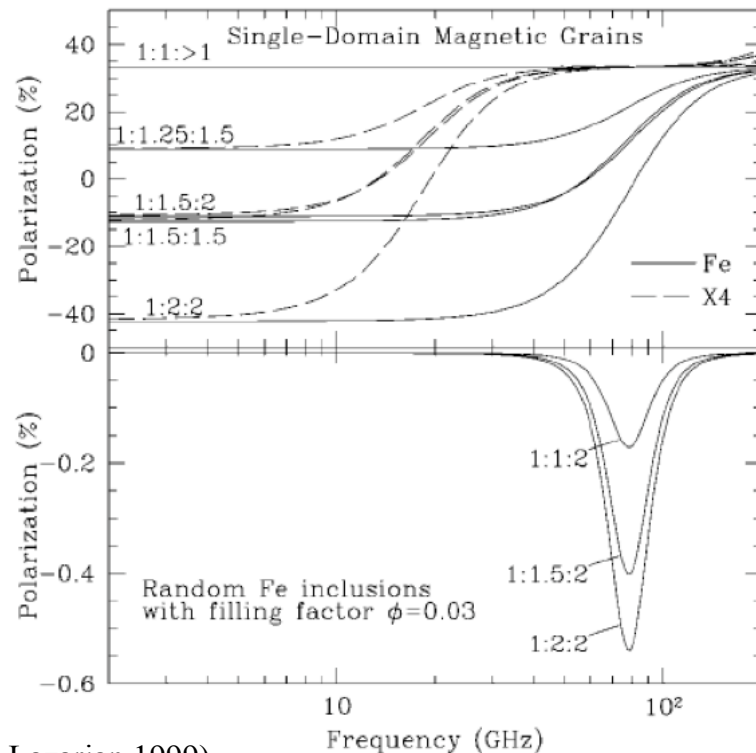
Are the molecules aligned and their emission polarized?

The energy level splitting arising from grain rotation ensures maximum efficiency of paramagnetic dissipation : time dependent magnetization, energy dissipation and torque causing the molecule to rotate with the axis parallel to the magnetic field

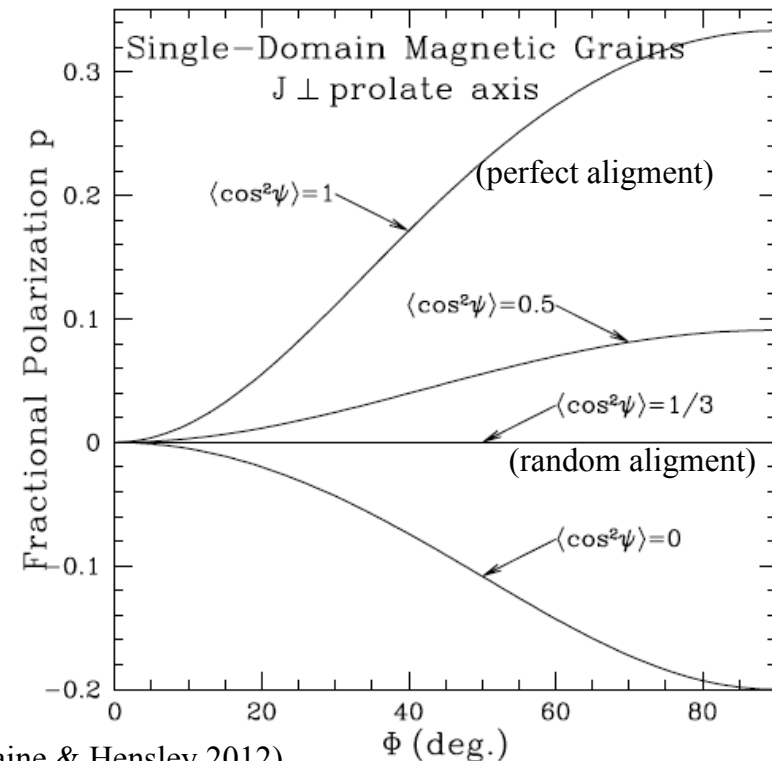


Polarization of magnetic dipole radiation

- Requires the presence of ferromagnetic material (Fe) in the dust grains (Draine & Lazarian, 1999). Spectrum peaking at $\nu \sim 10\text{-}80$ GHz.
- In the case of single-domain magnetic grains, and perfect alignment between their angular momenta and the magnetic field, this emission becomes strongly polarized. But strongly depends on alignment (Draine & Hensley 2012).
- Polarization can reach $\sim 30\%$ for $\nu > 40$ GHz. This may help to discriminate between this model and the spinning dust, which is weakly polarized, $< 2\%$ for $\nu > 20$ GHz (Lazarian & Draine, 2000).



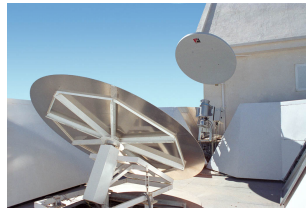
(Draine & Lazarian 1999)



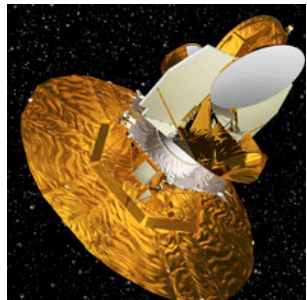
(Draine & Hensley 2012)

Anomalous microwave emission: polarization of the Perseus molecular complex

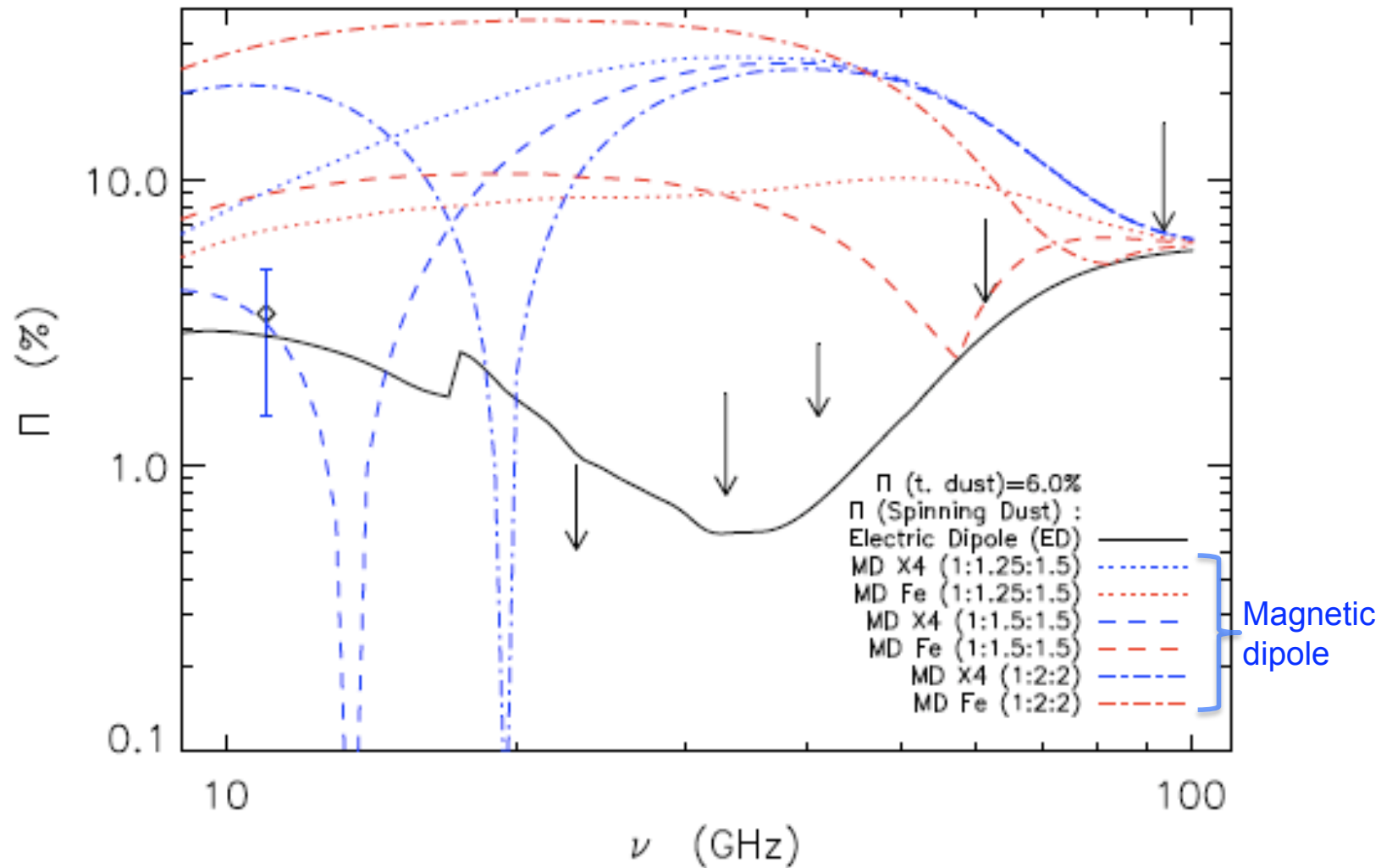
❖ **COSMOSOMAS** at 11GHz (Battistelli et al. 2006); **WMAP7** at 23-41GHz (López-Caraballo et al. 2010).



11GHz

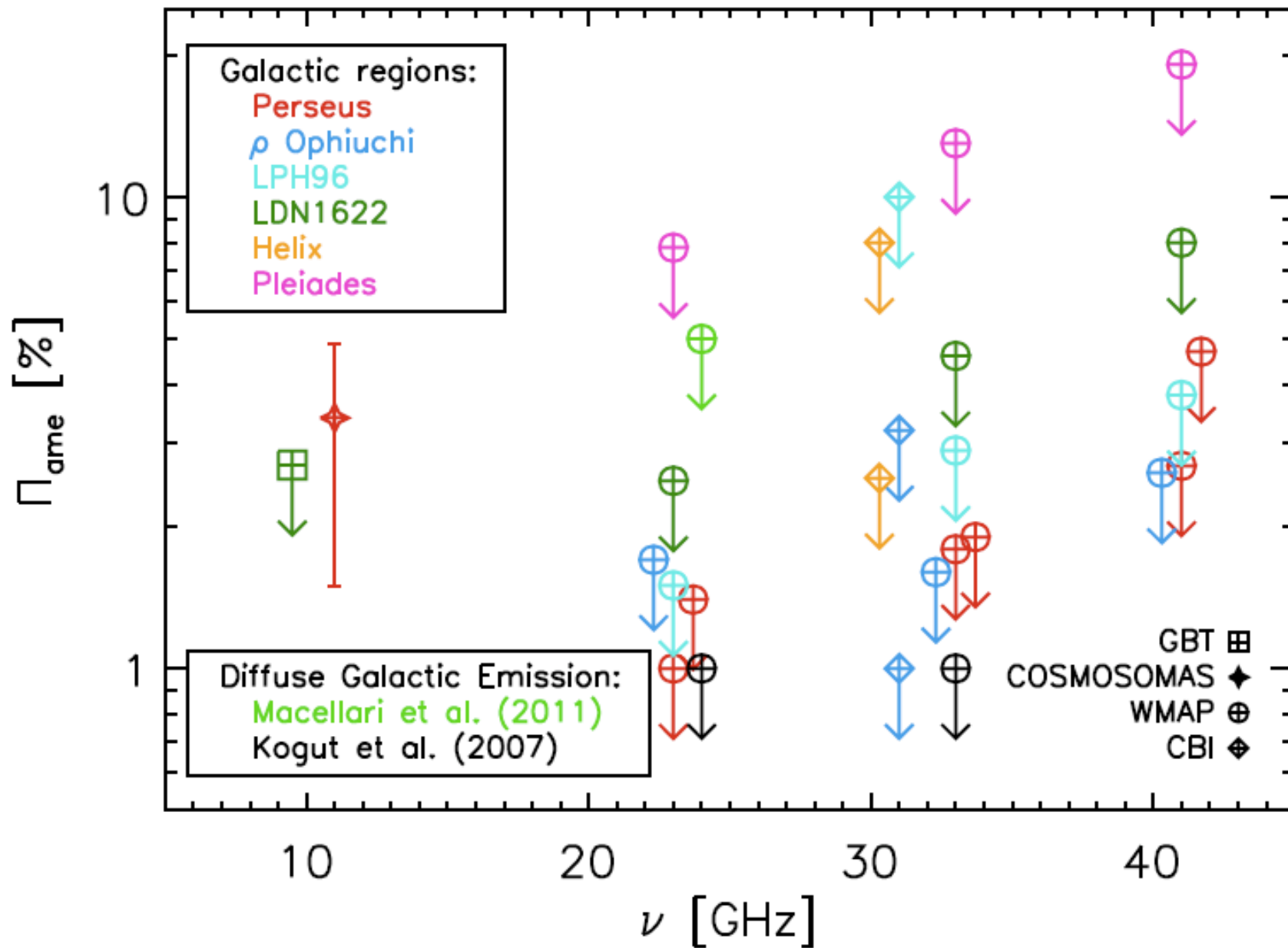


33GHz

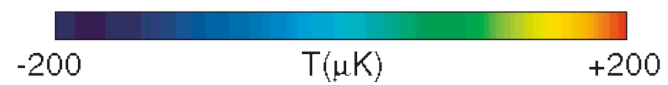
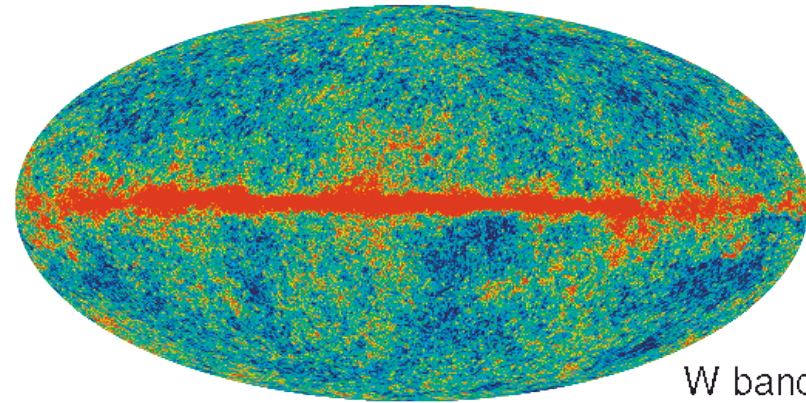
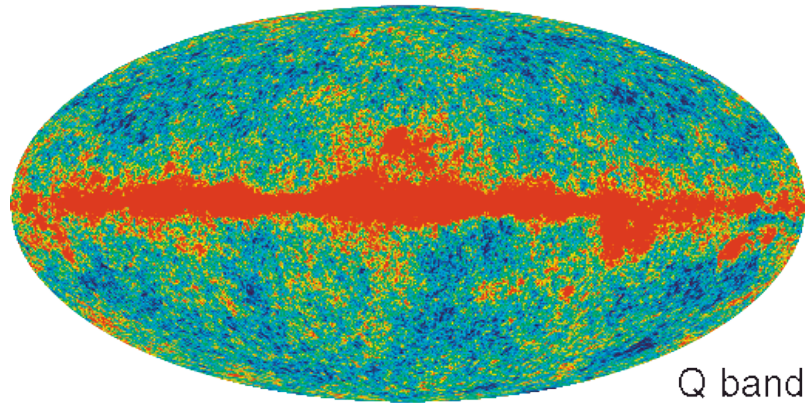
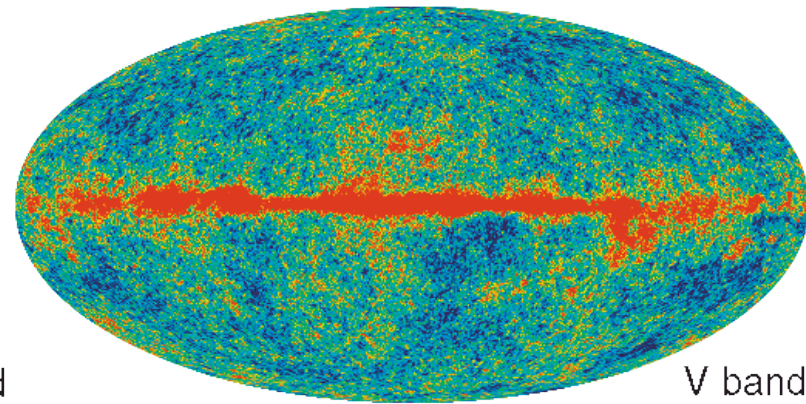
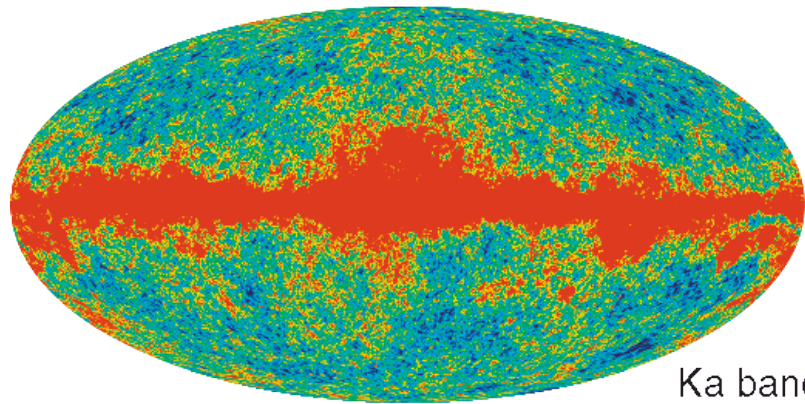
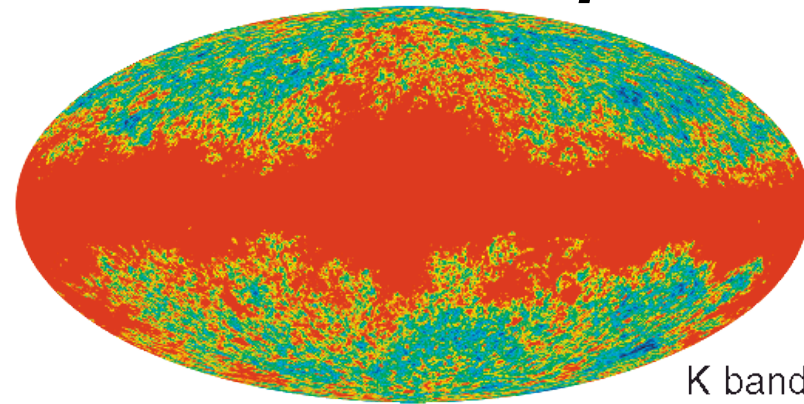


(for details, see poster by López-Caraballo)

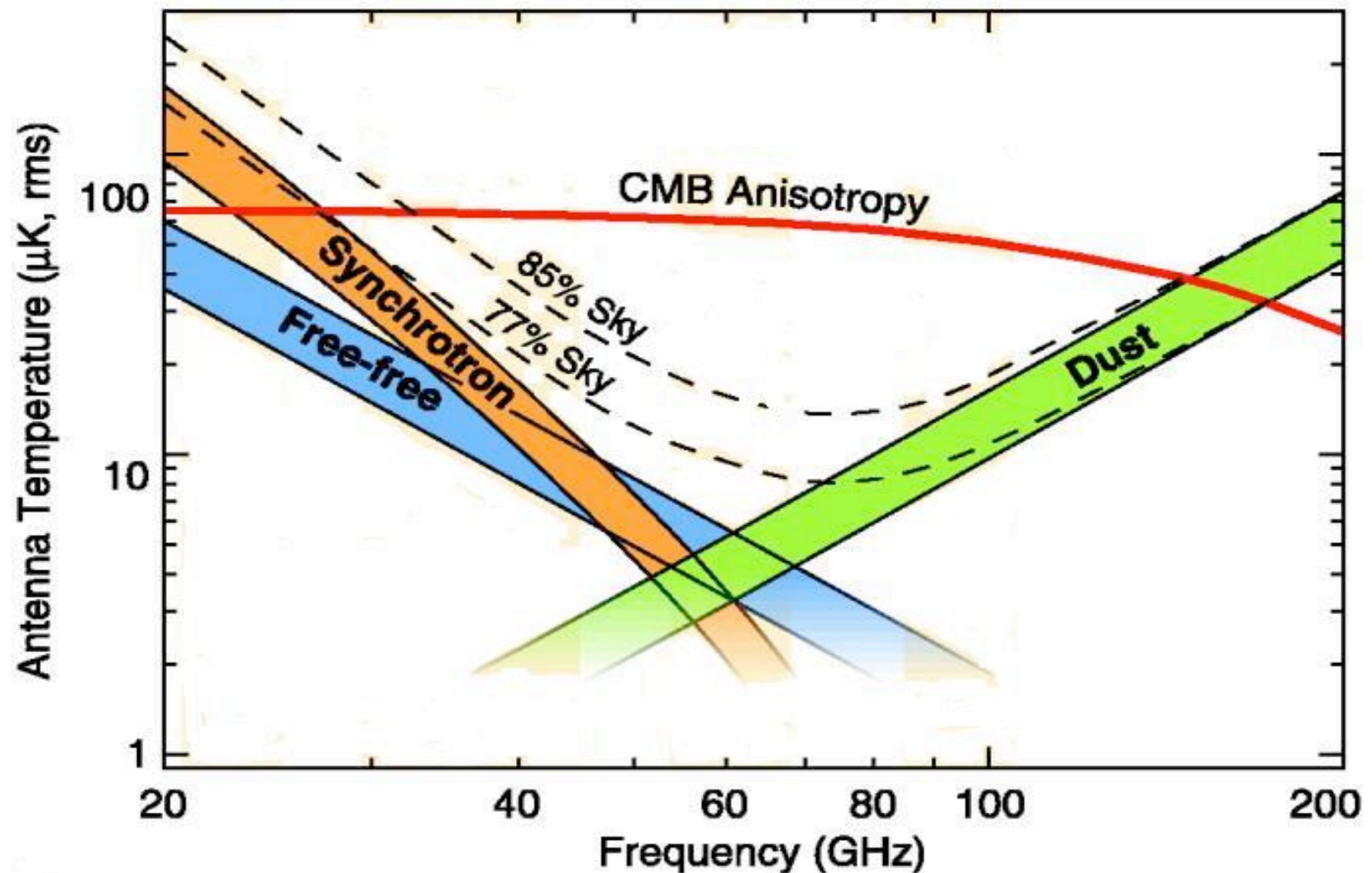
Current status of AME polarization measurements



WMAP7 maps

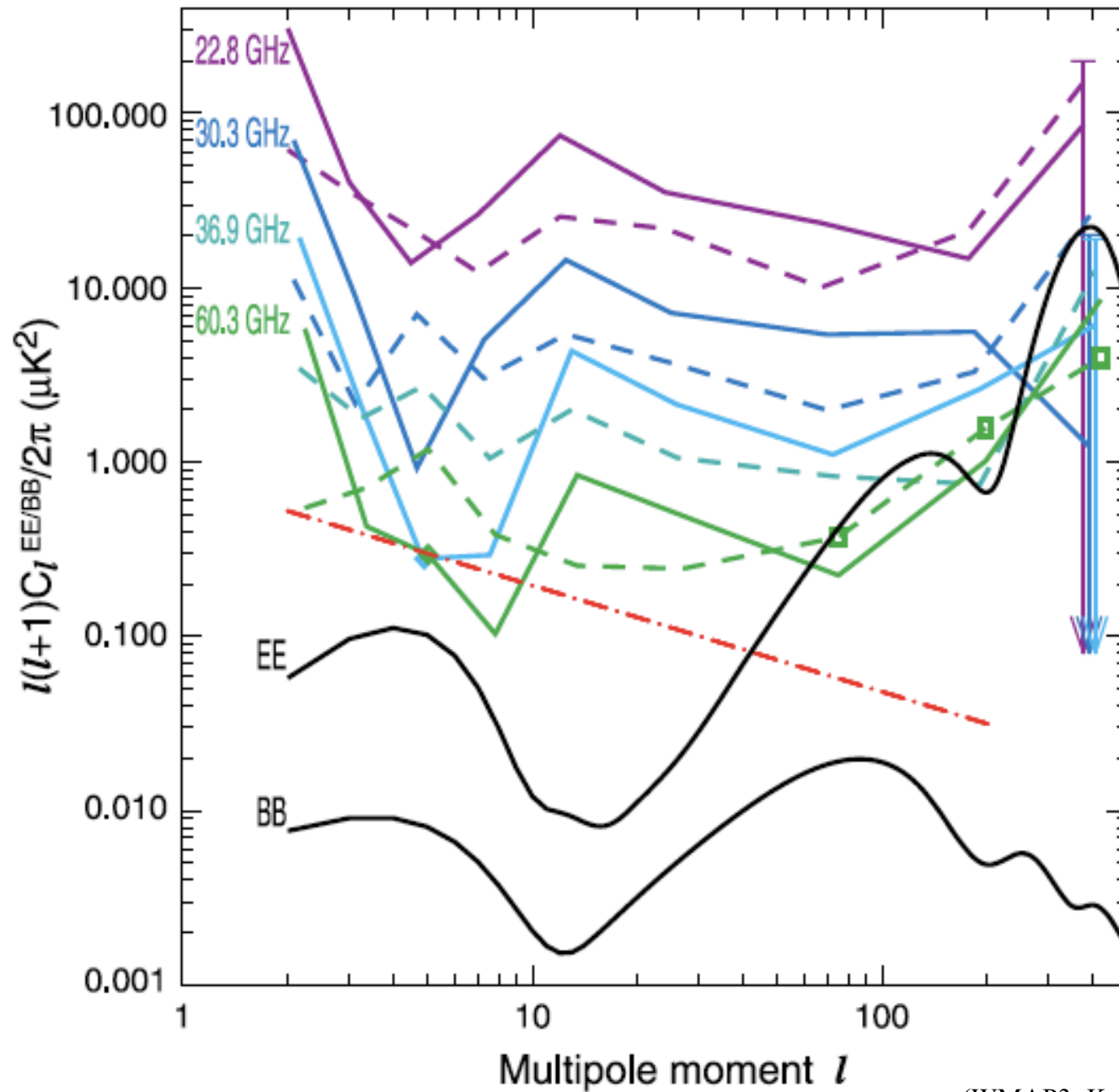


Galactic Components seen by WMAP

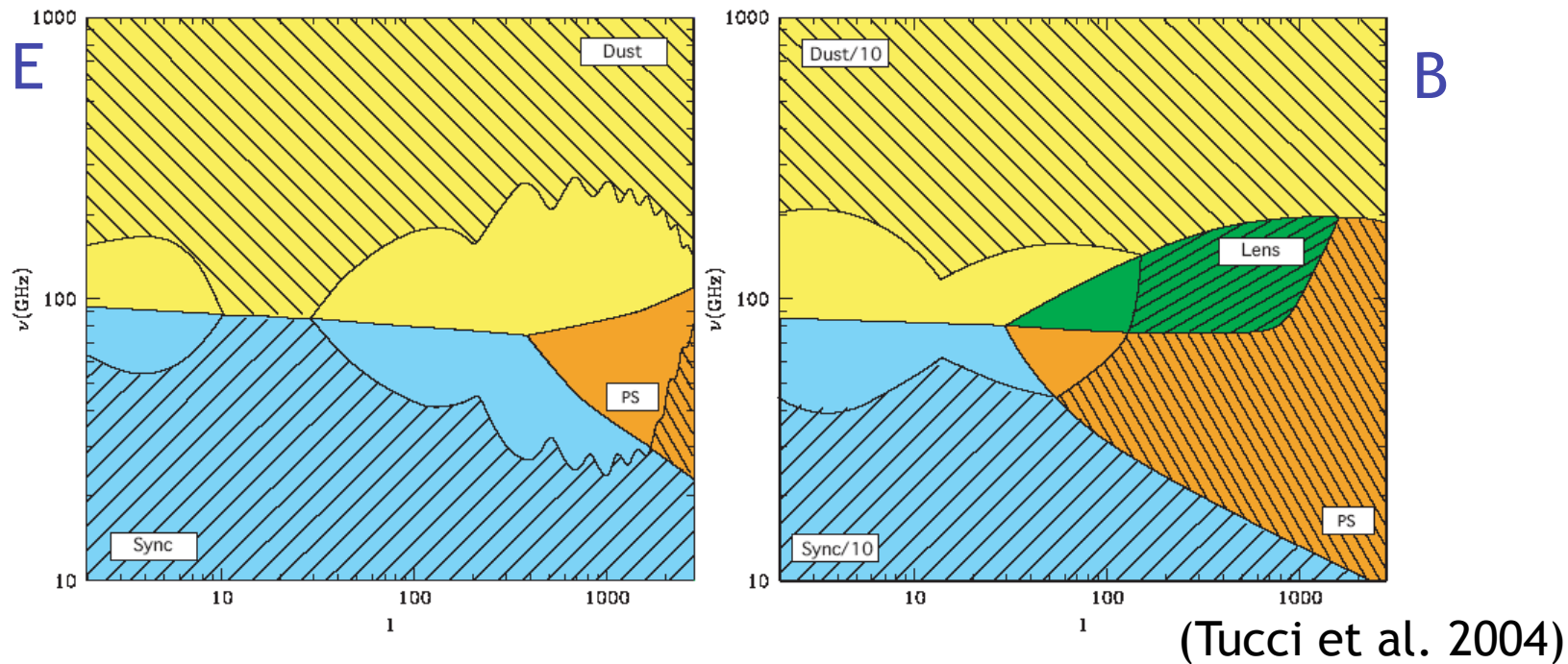


RMS fluctuation spectrum of all foregrounds at 1 deg resolution

CMB polarization: foregrounds



CMB polarization: foregrounds



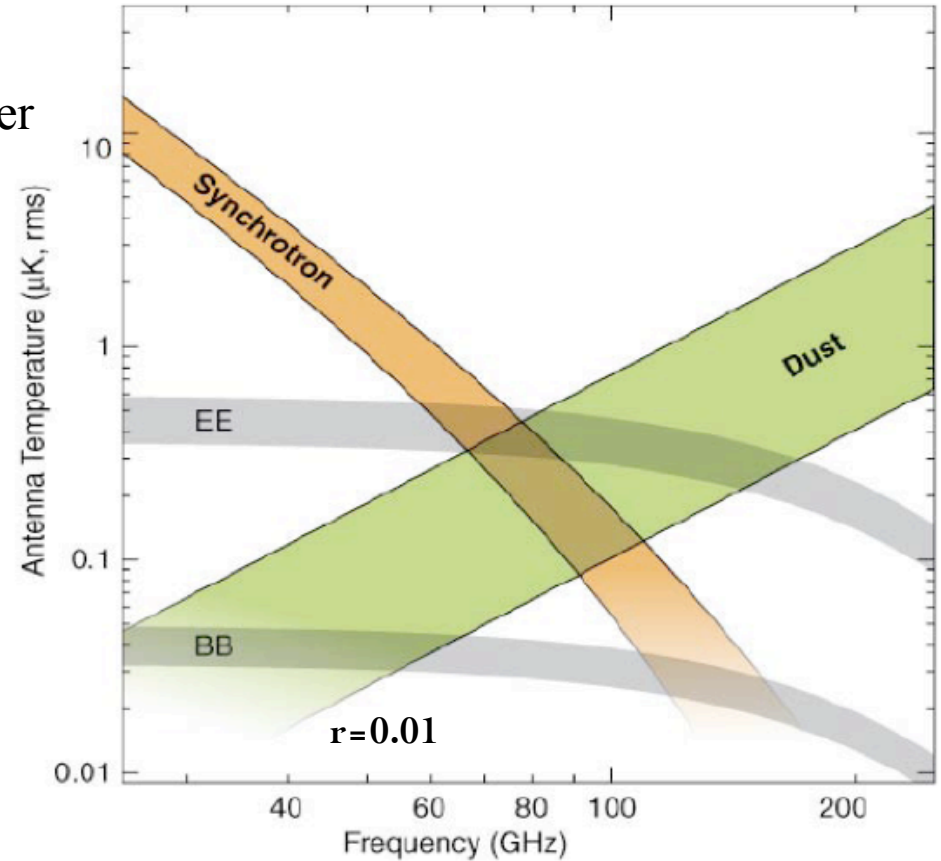
Left) Without any Galactic removal, only the CMB E-mode can dominate at $\nu \approx 100$ GHz and for $l \leq 2000$.

Right) With a Galactic subtraction of a factor 10 the CMB B-mode ($r=0.1$) can dominate at $\nu \approx 100$ GHz and for $l \leq 100$. The major limitation comes in this case from extragalactic sources ($S < 1$ Jy) and lensing.

“Component” separation is needed

❖ **Foregrounds.** B-mode signal is subdominant over Galactic foregrounds

- **Free-free**, low-freq, not polarized
- **Synchrotron**, low-freq, pol $\sim 10\%$
- **Thermal dust**, high-freq, pol $\sim 10\%$
- **Anomalous emission**, 20-60 GHz, pol $\sim 3\%$?
- **Point sources**, low-freq, pol $\sim 5\%$



Component separation

Statement of the problem:

- The signal that we observe is a superposition of signals arising from different physical processes.

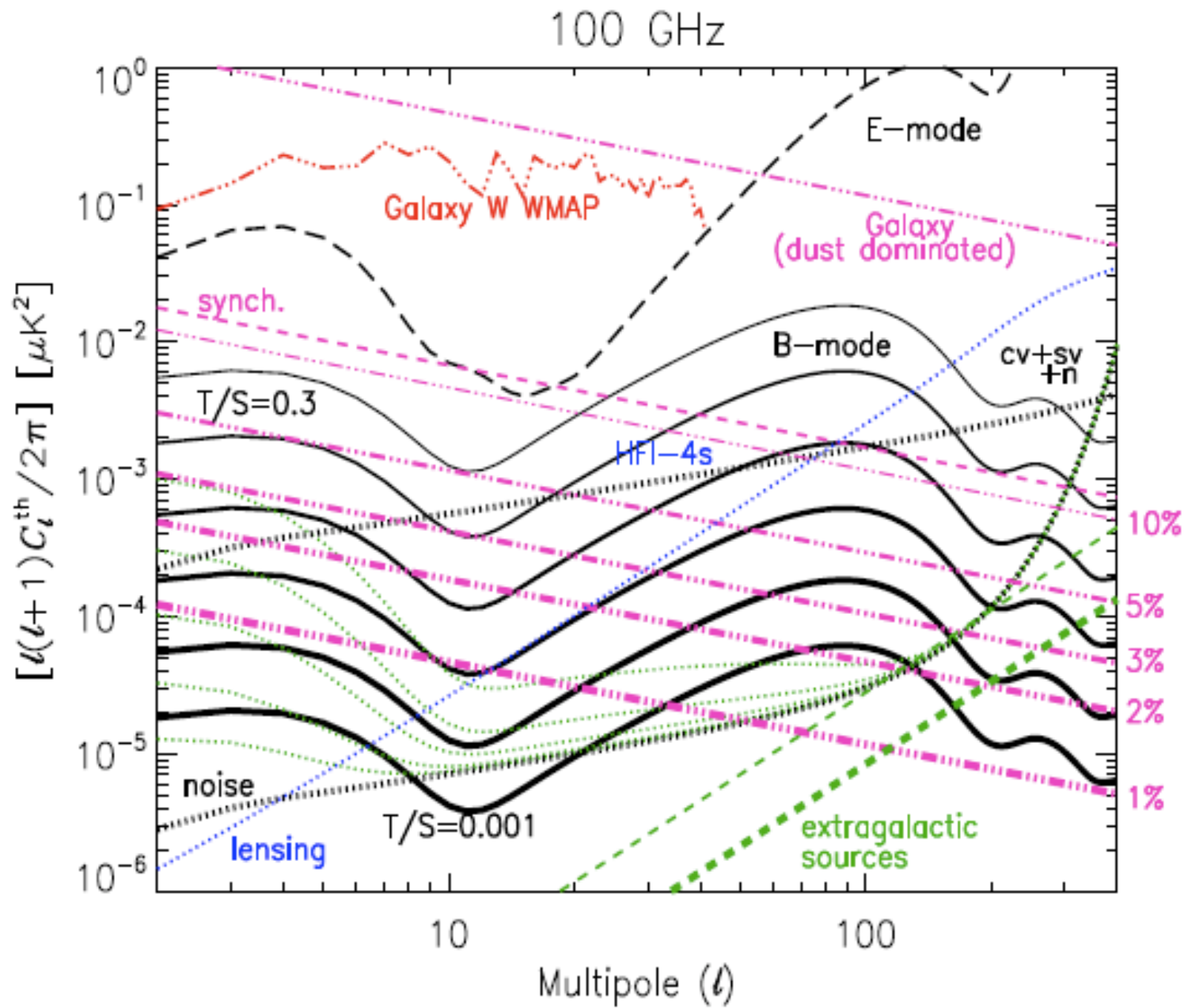
$$\tilde{x}(\hat{r}, \nu) = \sum_{j=1}^{N_c} \tilde{s}_j(\hat{r}, \nu).$$

- Our instrument integrates the signal over frequency, convolves with a certain kernel, and adds noise:

$$x_\nu(\hat{r}) = \int B(\hat{r} - \hat{r}', \nu') \sum_{j=1}^{N_c} t_\nu(\nu') \tilde{s}_j(\hat{r}', \nu') d\hat{r}' d\nu' + n_\nu(\hat{r}).$$

Conclusion:

- We need to define our experiment with appropriate sensitivity, frequency coverage (i.e. number of frequency bands) and spatial resolution to achieve the scientific goal.



Future CMB polarization experiments

Some Current/Future Polarization experiments

| Name | Platform | FWHM | Freq [GHz] | Detectors | r_{lim} | Starts |
|-----------|-----------|----------------|-------------|-------------|-----------|---------|
| BICEP | Ground | $\sim 1^\circ$ | 100,150 | PSB bolom. | 0.1 | 2007 |
| QUIET | Ground | 4'-30' | 40, 90 | MMIC HEMT | 0.05 | 2008 |
| QUIJOTE | Ground | $\sim 1^\circ$ | 10-40 | MMIC HEMT | 0.05 | 2012 |
| PolarBear | Ground | 3'-7' | 90,150, 220 | TES bolom | 0.025 | 2012 |
| QUBIC | Ground | $\sim 1^\circ$ | 90,150, 220 | Inter bolom | 0.01 | 2014-15 |
| EBEX | Balloon | 8' | 150,250,420 | TES bolom | 0.03 | 2011 |
| SPIDER | Balloon | 30'-70' | 90-270 | TES bolom | 0.03 | 2011 |
| Planck | Satellite | 5'-33' | 30-353 | MMIC/Bol | 0.05 | 2009 |
| Core | Satellite | 1.3' -23' | 45-795 | TES bolom. | 0.001 | ? |

1965



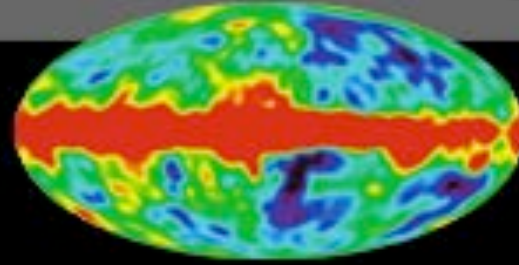
Penzias and
Wilson



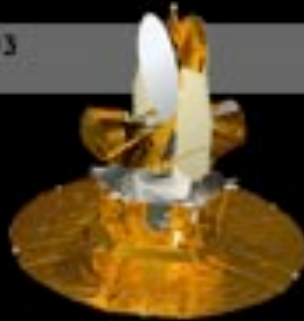
1992



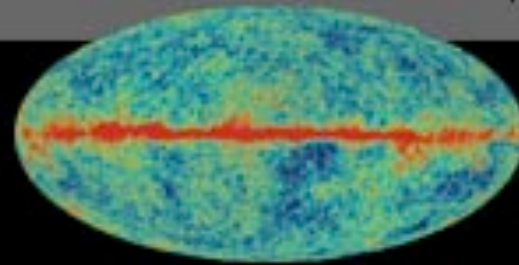
COBE



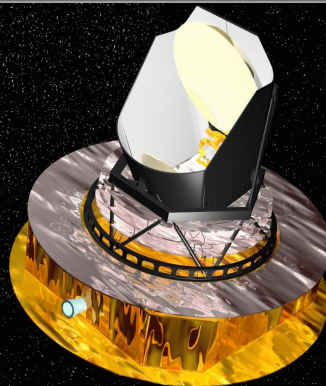
2003



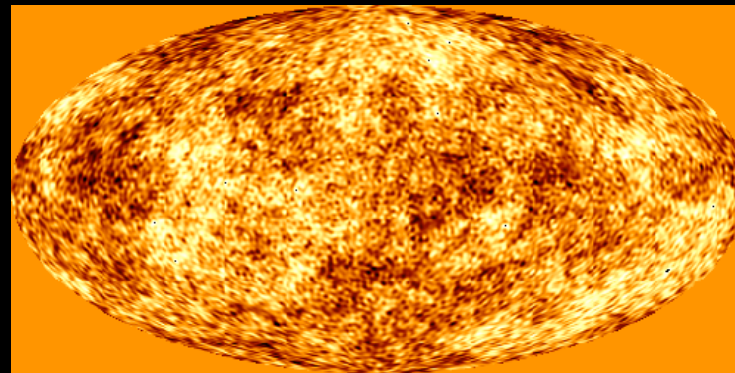
WMAP



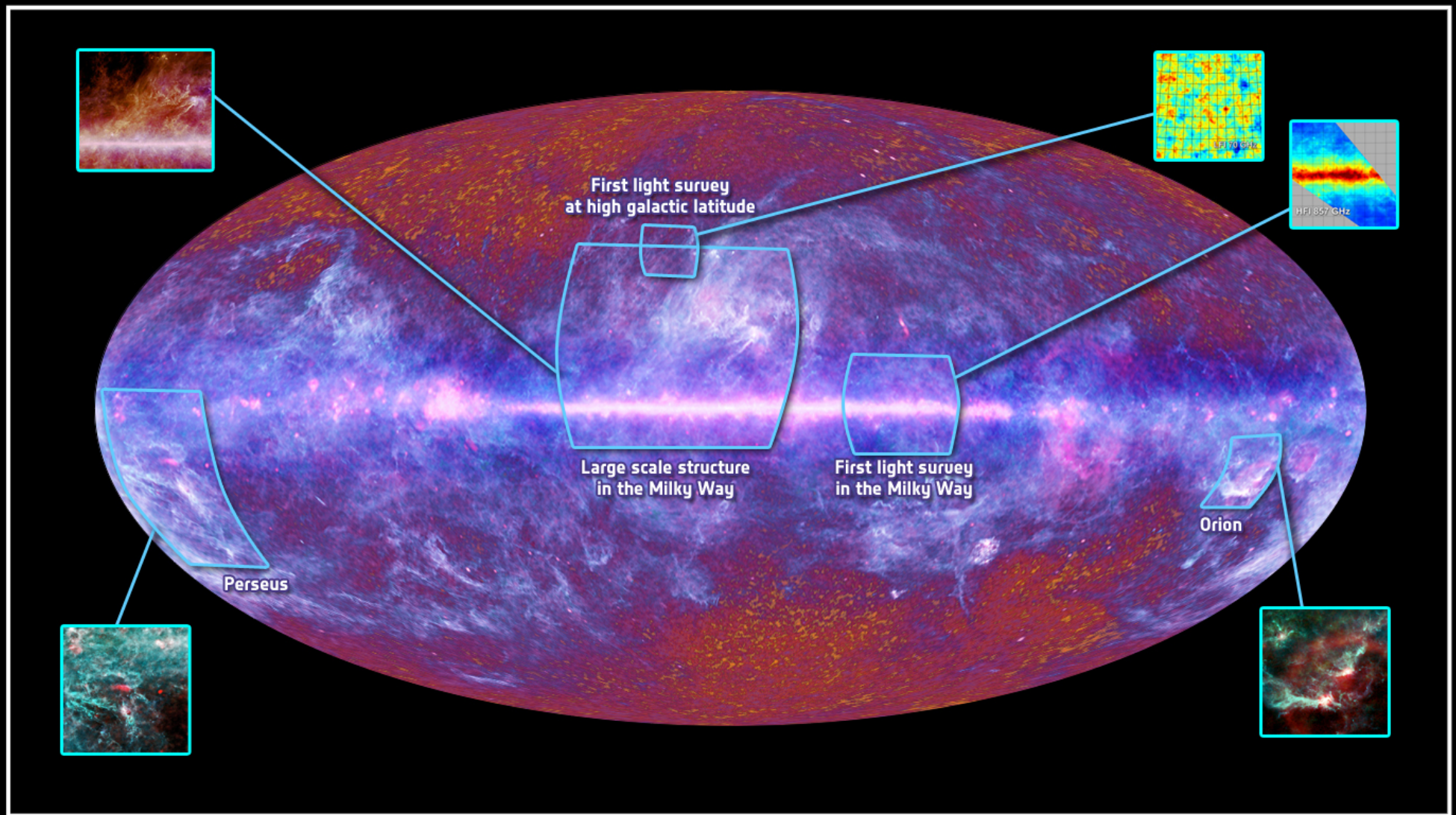
2011



Planck



Planck:
3rd Generation
CMB space
experiment

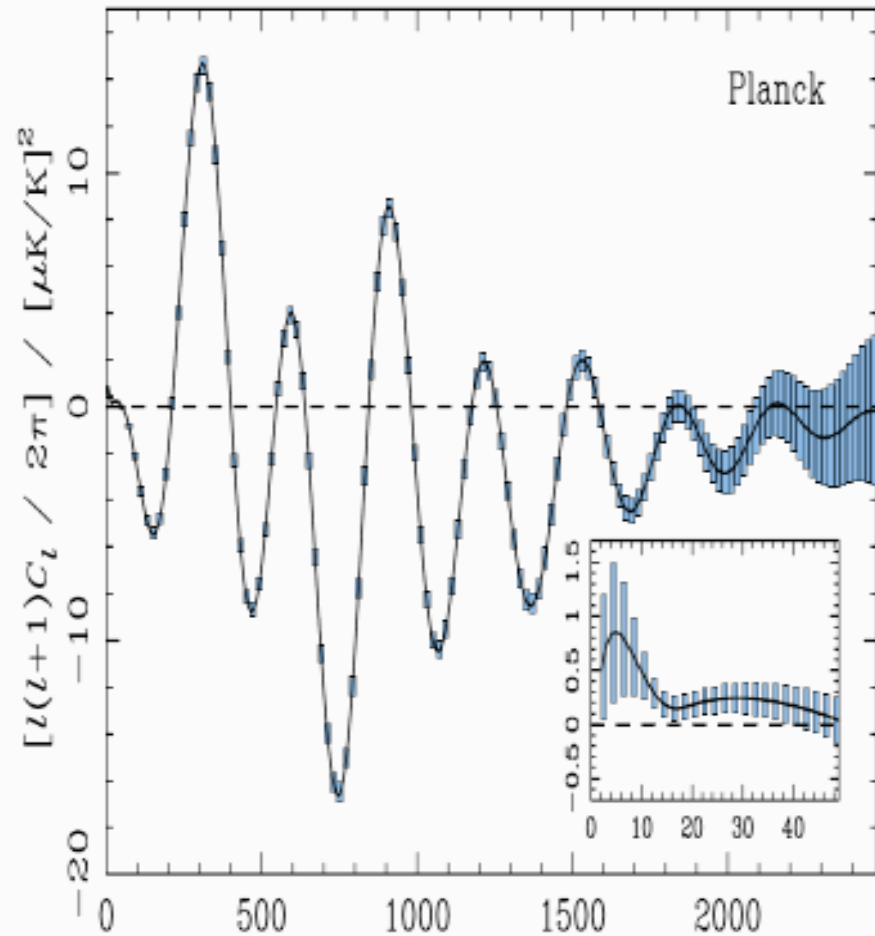


The Planck one-year all-sky survey

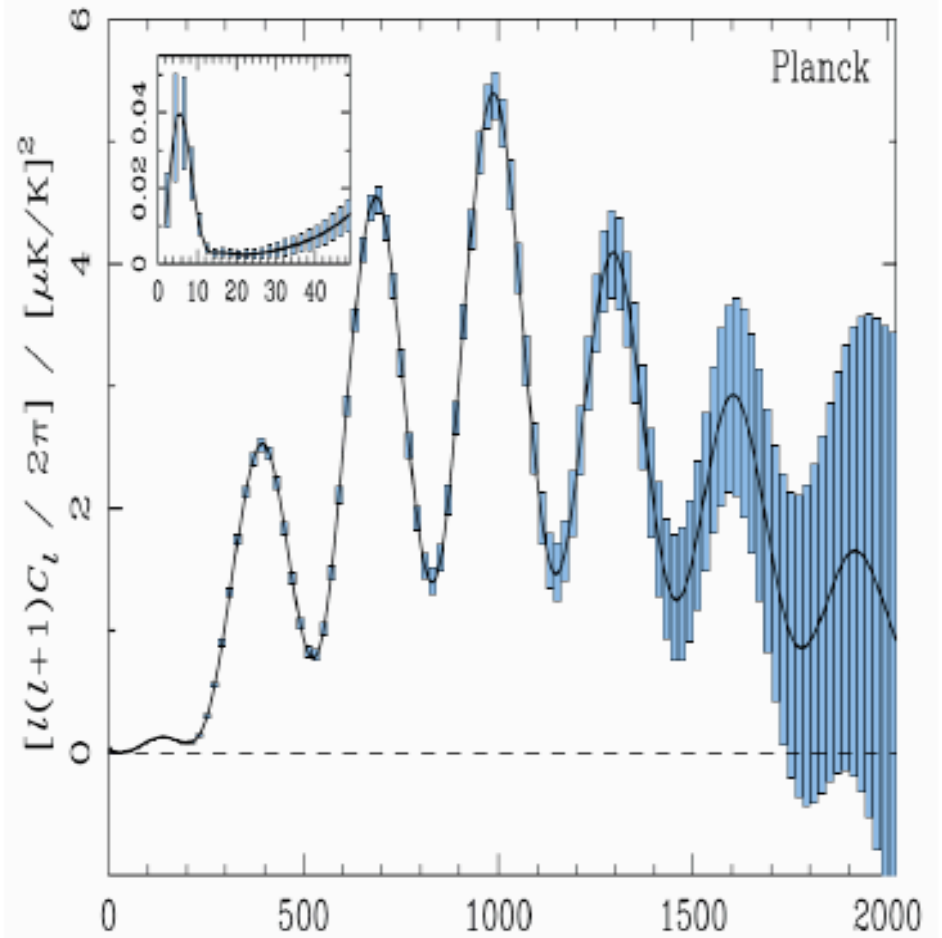


(c) ESA, HFI and LFI consortia, July 2010

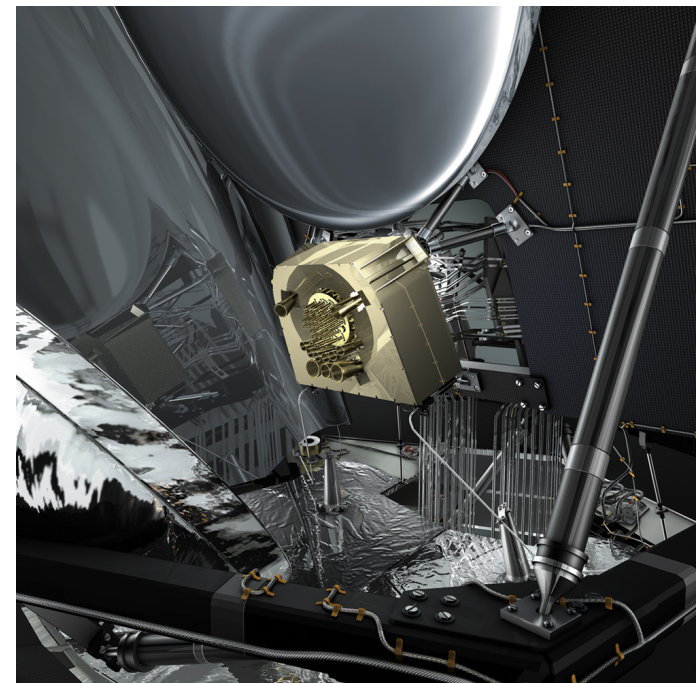
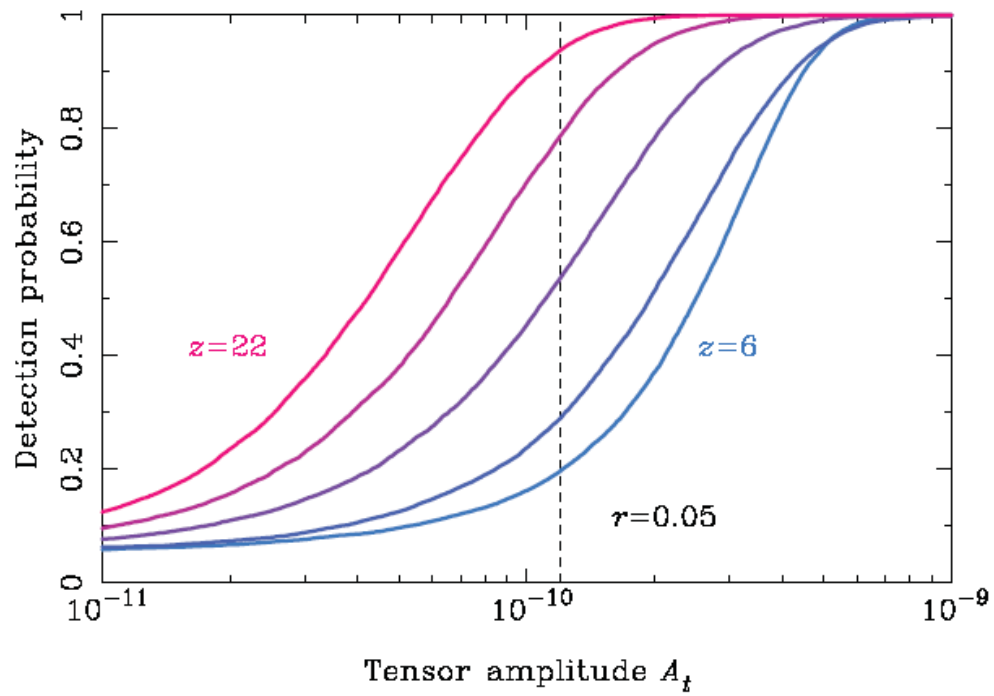
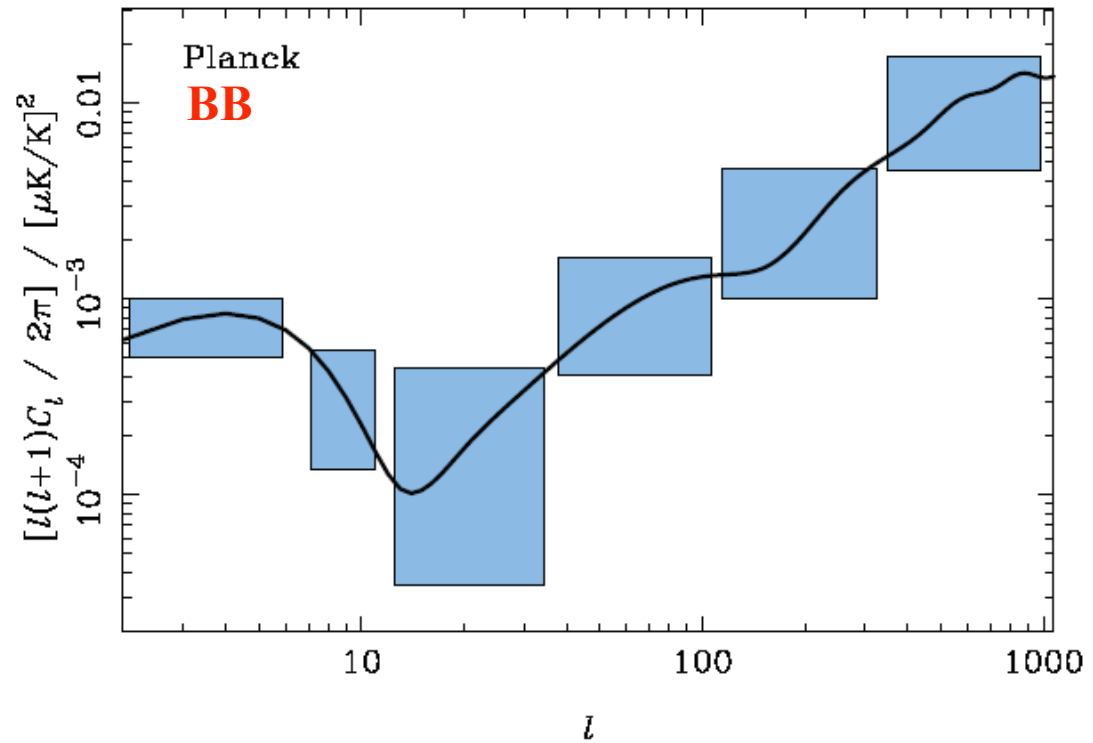
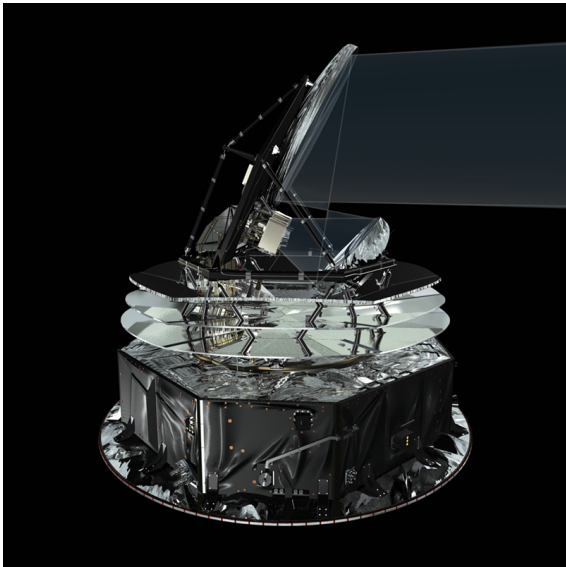
EE



TE



Planck



From Efstathiou & Gratton (2009)

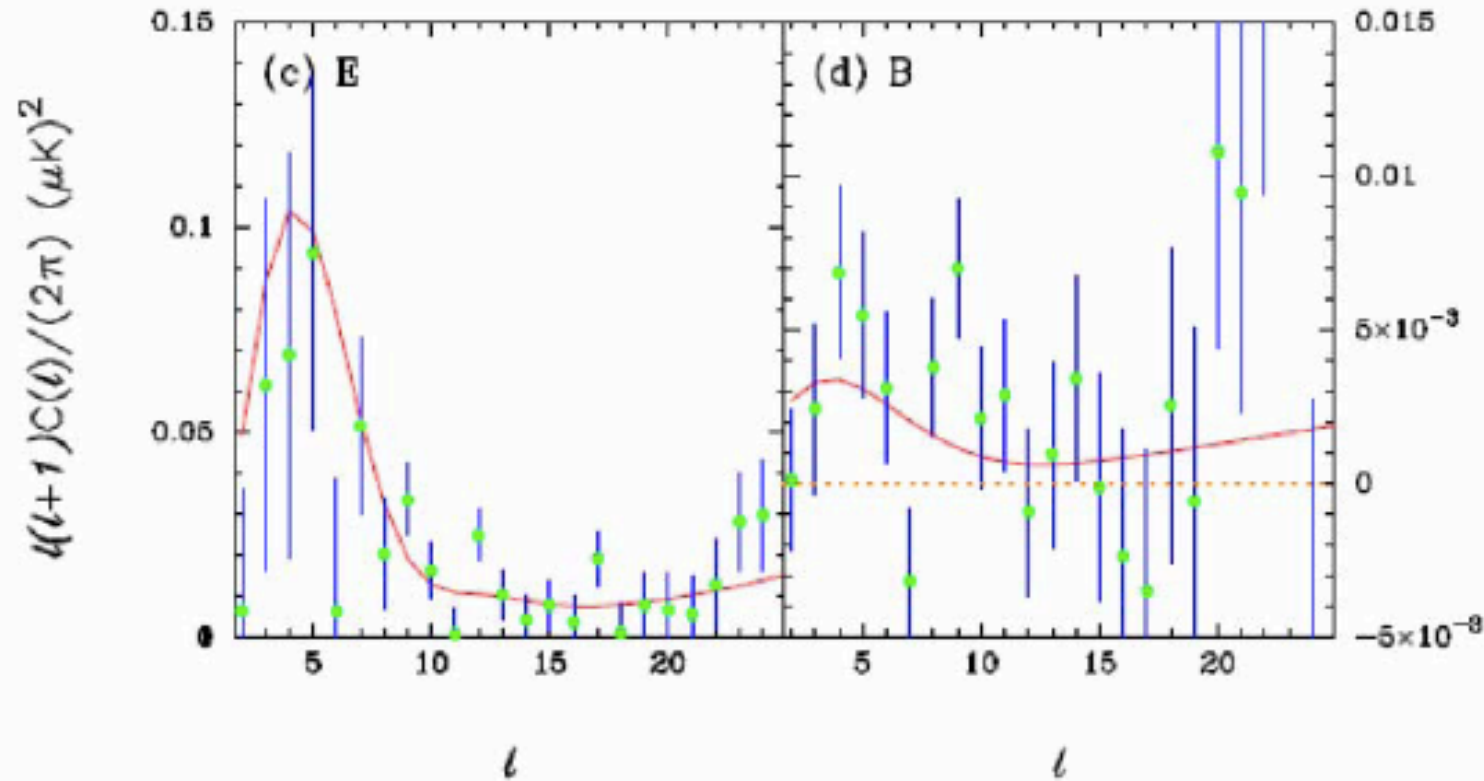


Figure 3. QML estimates of the E and B -mode polarization spectra for the simulations with $r = 0.05$. Figures 3a and 3b show power spectra for the nominal *Planck* mission. Figures 3c and 3d show power spectra for an extended *Planck* mission. The error bars are computed from the diagonal components of the inverse of the QML Fisher matrix using the theoretical input spectra for $r = 0.05$ (shown by the red lines).

The QUIJOTE CMB Experiment

(<http://www.iac.es/project/cmb/quijote>)



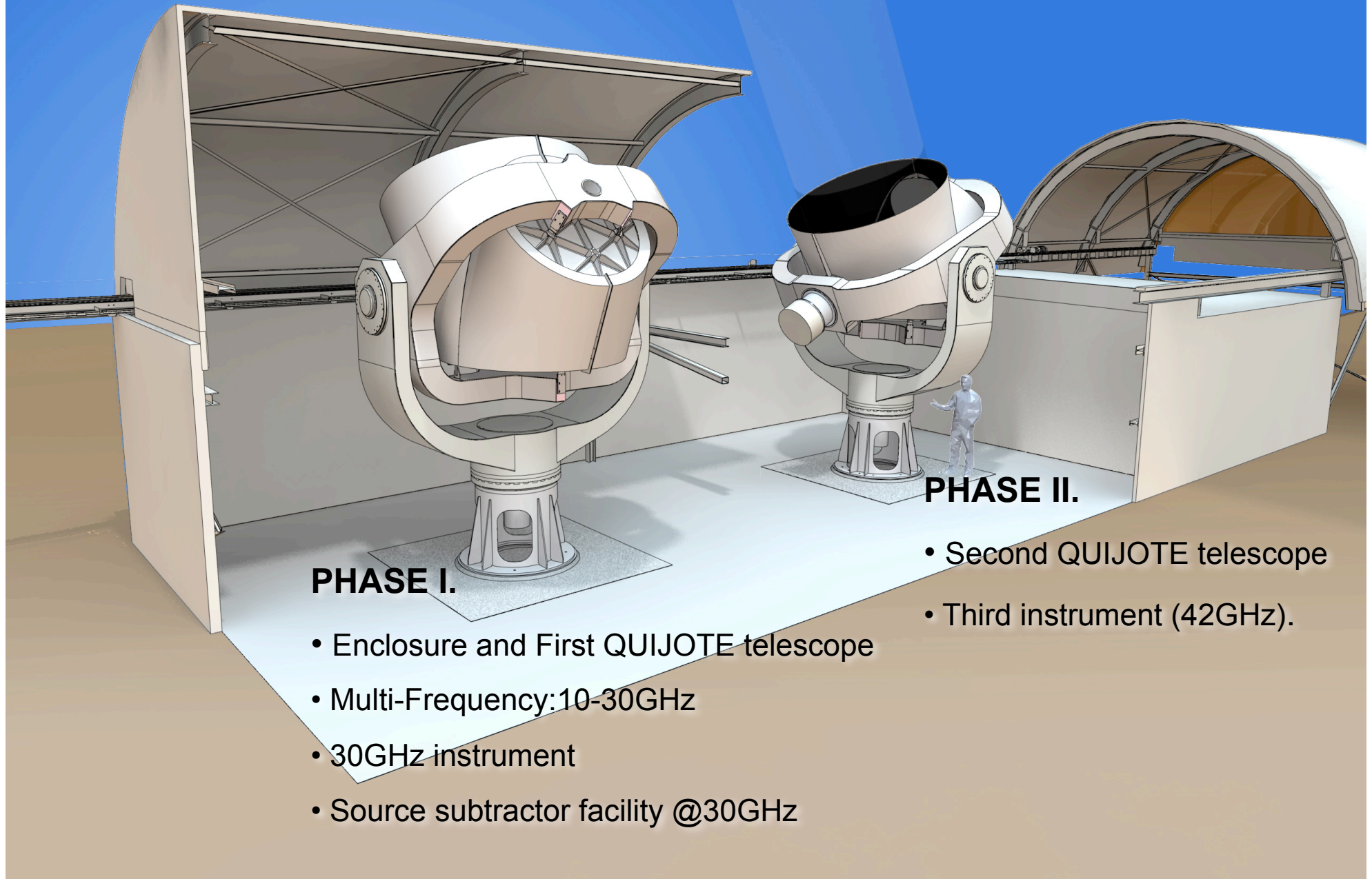
Jodrell Bank
Observatory



UNIVERSITY OF
CAMBRIDGE

- **Polarimeter at cm wavelengths.**
- **Aim:** To perform high sensitivity observations of the polarization of the sky emissions in the frequency range 10-40 GHz at large angular scales (one degree resolution).

QUIJOTE CMB Experiment



PHASE I.

- Enclosure and First QUIJOTE telescope
- Multi-Frequency: 10-30GHz
- 30GHz instrument
- Source subtractor facility @30GHz

PHASE II.

- Second QUIJOTE telescope
- Third instrument (42GHz).

The QUIJOTE-CMB Experiment: Goals

- Main science driver: to constrain (or to detect) gravitational B-modes if they have an amplitude of $r=0.05$.
- Complement Planck at low frequencies. In combination with Planck data, push the upper limits below that value.
- Measure polarized foregrounds (synchrotron) with high sensitivity to correct them in future space missions aiming to reach $r=0.001$.

QUIJOTE CMB Experiment - Phase I and II. Basic facts

| | MFI | | | | | TGI | FGI |
|-------------------------------------|------|------|------|------|------|------|------|
| Nominal Frequency [GHz] | 11 | 13 | 17 | 19 | 30 | 30 | 40 |
| Bandwidth [GHz] | 2 | 2 | 2 | 2 | 8 | 8 | 10 |
| Number of horns | 2 | 2 | 2 | 2 | 1 | 31 | 40 |
| Channels per horn | 4 | 4 | 4 | 4 | 2 | 4 | 4 |
| Beam FWHM [°] | 0.92 | 0.92 | 0.60 | 0.60 | 0.37 | 0.37 | 0.28 |
| T_{sys} [K] | 25 | 25 | 25 | 25 | 35 | 35 | 45 |
| NEP [$\mu\text{K s}^{1/2}$] | 280 | 280 | 280 | 280 | 390 | 50 | 50 |
| Sensitivity [$\text{Jy s}^{1/2}$] | 0.30 | 0.42 | 0.31 | 0.38 | 0.50 | 0.06 | 0.06 |

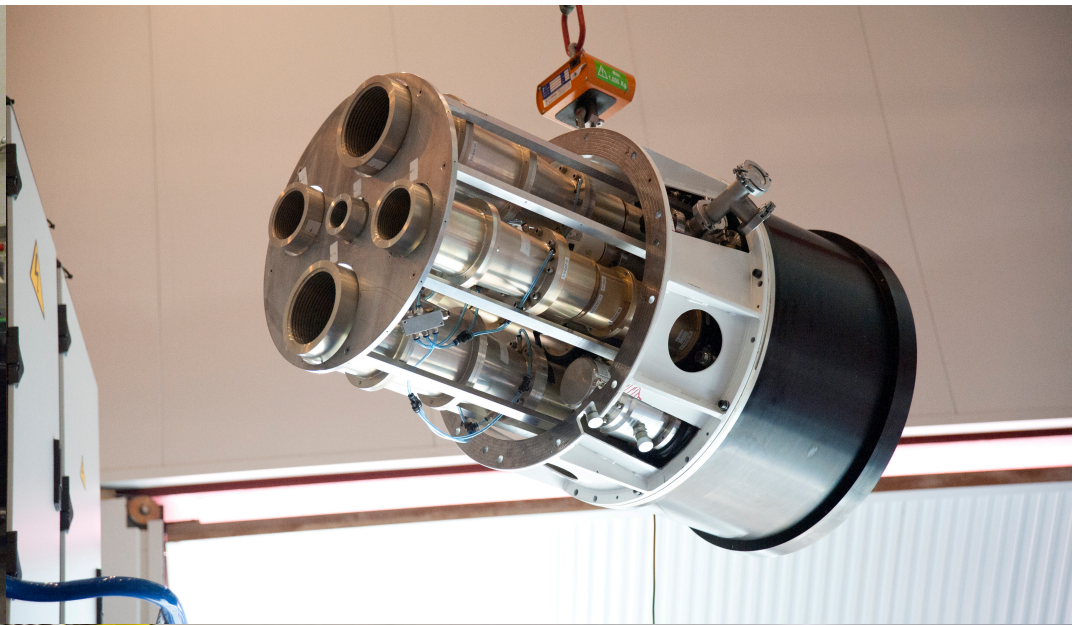
- Temperature sensitivity per beam, given by

$$\Delta Q = \Delta U = \sqrt{2} \frac{T_{\text{sys}}}{\sqrt{\Delta\nu \times t_{\text{int}} \times N_{\text{chan}}}}$$

First QUIJOTE Telescope (QT1)



Installed at the Teide Observatory
in May 3rd, 2012.

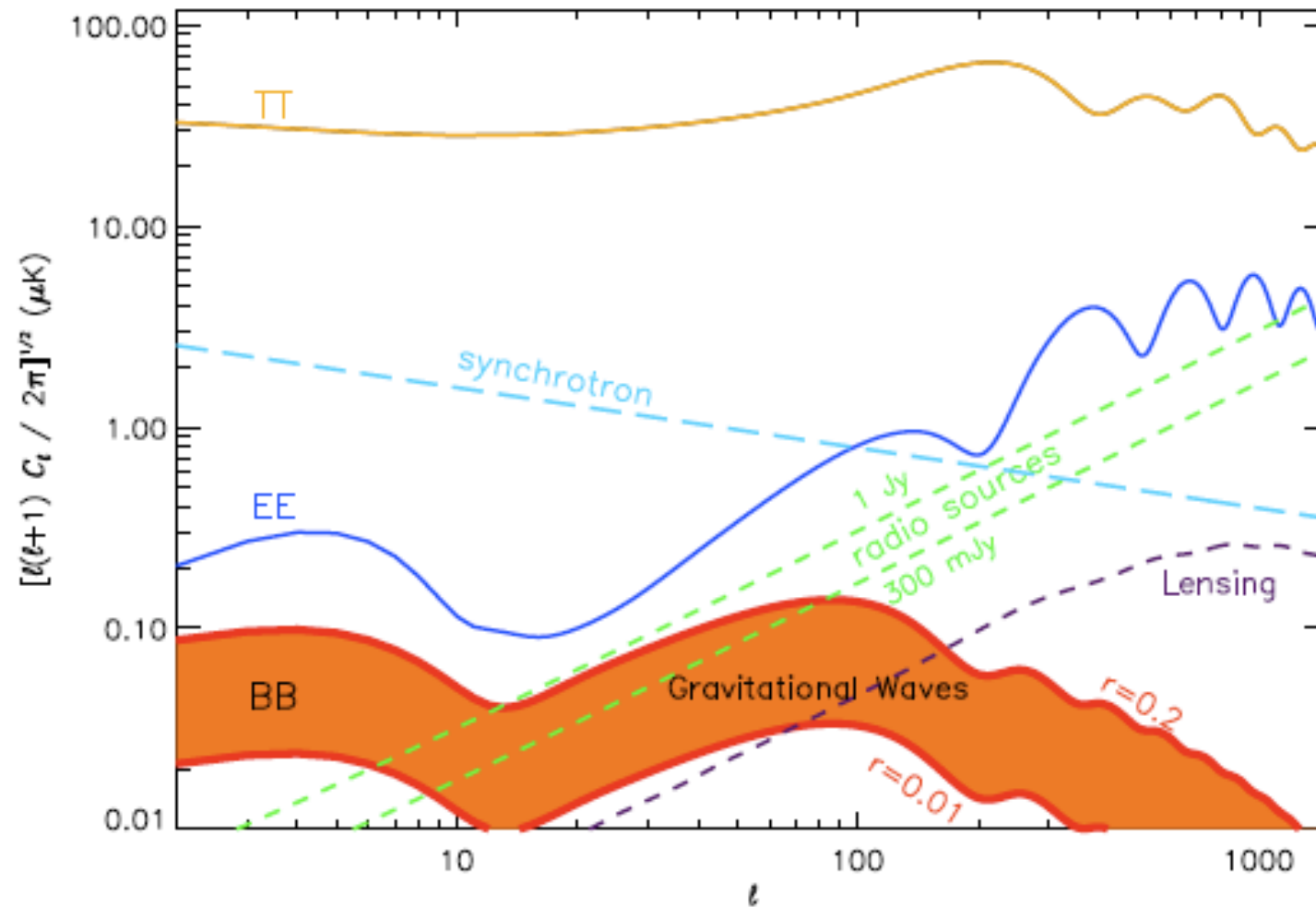


Integration tests of
the MFI and QT1 at
the AIV room
(February-March
2012)

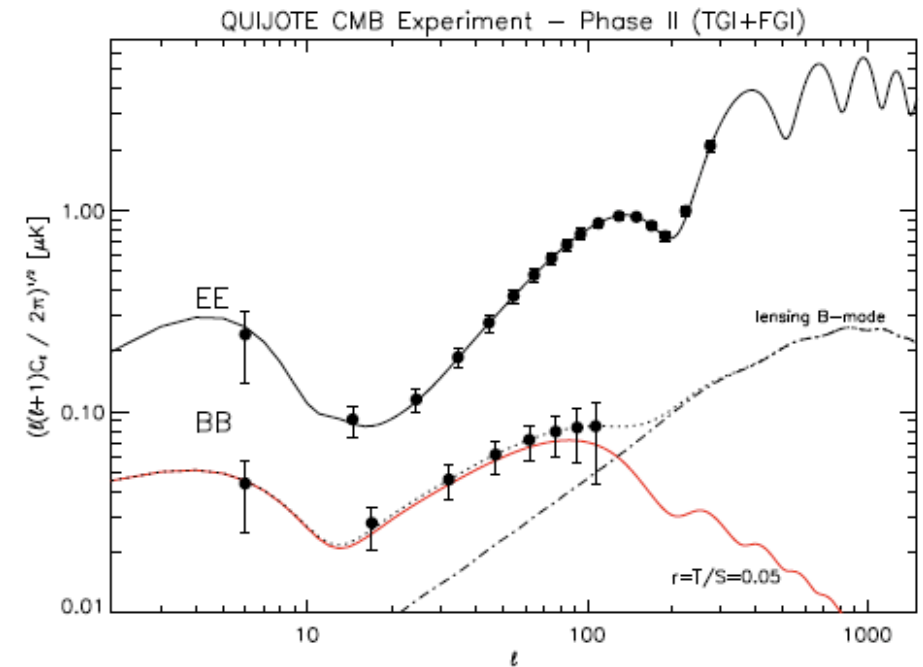
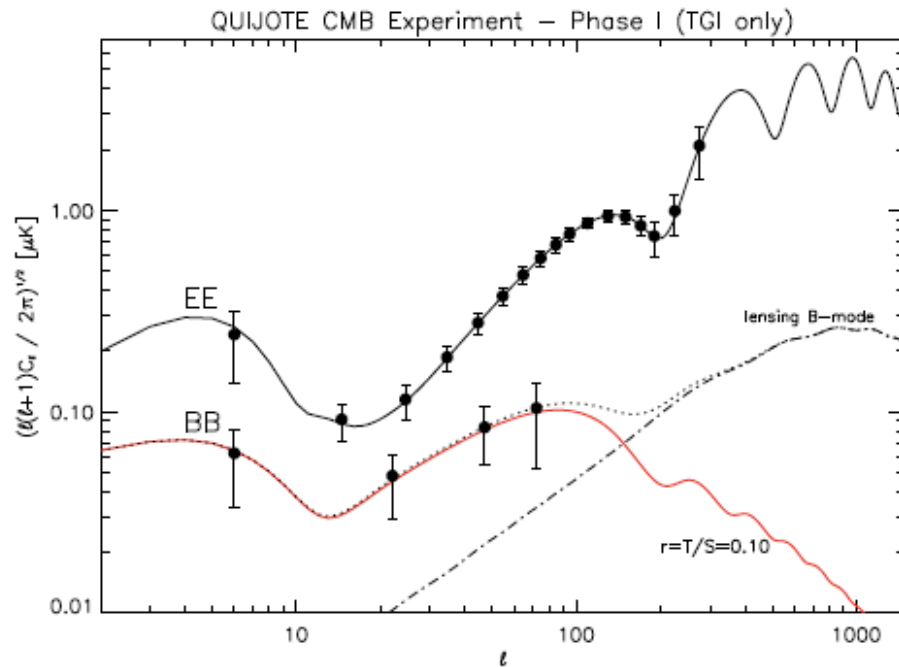
Science with QUIJOTE first instrument (MFI)

- ❖ After one year of operation, QUIJOTE will produce **five frequency maps (11, 13, 17, 19 and 30 GHz)** in Stokes Q, U and I, each one with a sensitivity around 2-3 μ K per one degree beam, and covering a sky area between 5000 to 10000 square degrees.
- ❖ These maps will provide valuable information about the **polarization** properties of:
 - Synchrotron emission: it should dominate the emission at our frequencies
 - Anomalous microwave emission (spinning dust? little known about its polarization).
 - Radio-sources: low contribution at degree scales, but relevant for B-modes science
- ❖ Maps used to clean the 30 GHz maps of the 2nd and 3rd QUIJOTE instruments (TGI and FGI).
- ❖ **Excellent complement to Planck at low frequencies.**

Expected foreground contamination at 30GHz



Science with QUIJOTE second (TGI) and third (FGI) instruments



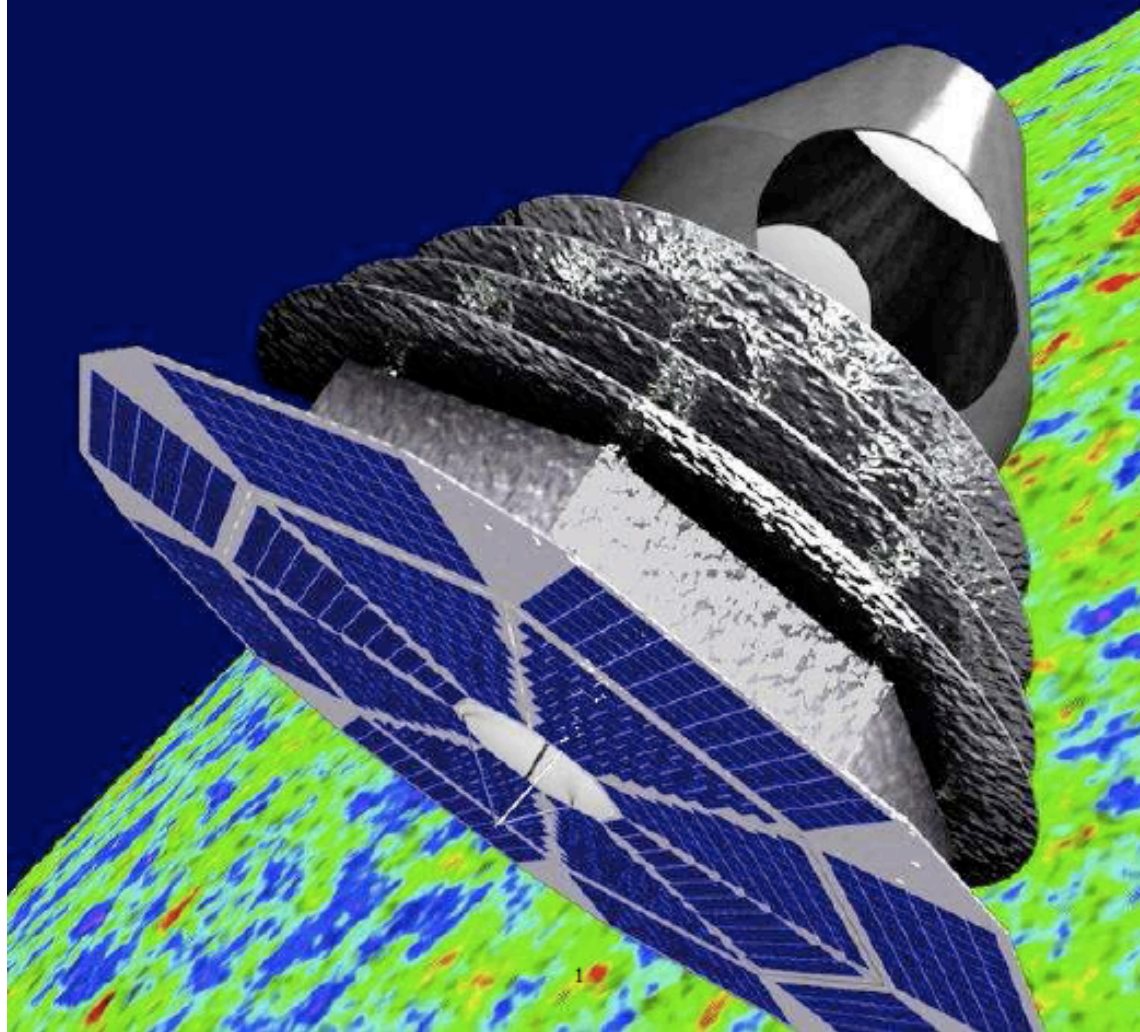
Left: Example of the QUIJOTE-CMB scientific goal after the Phase I. It is shown the case for 1 year (effective) observing time, and a sky coverage of 3,000 deg². The red line corresponds to the primordial B-mode contribution in the case of $r = 0.1$.

Right: QUIJOTE-CMB Phase II. Here we consider 3 years of effective operations with the TGI, and that during the last 2 years, the FGI will be also operative. The red line now corresponds to $r = 0.05$.

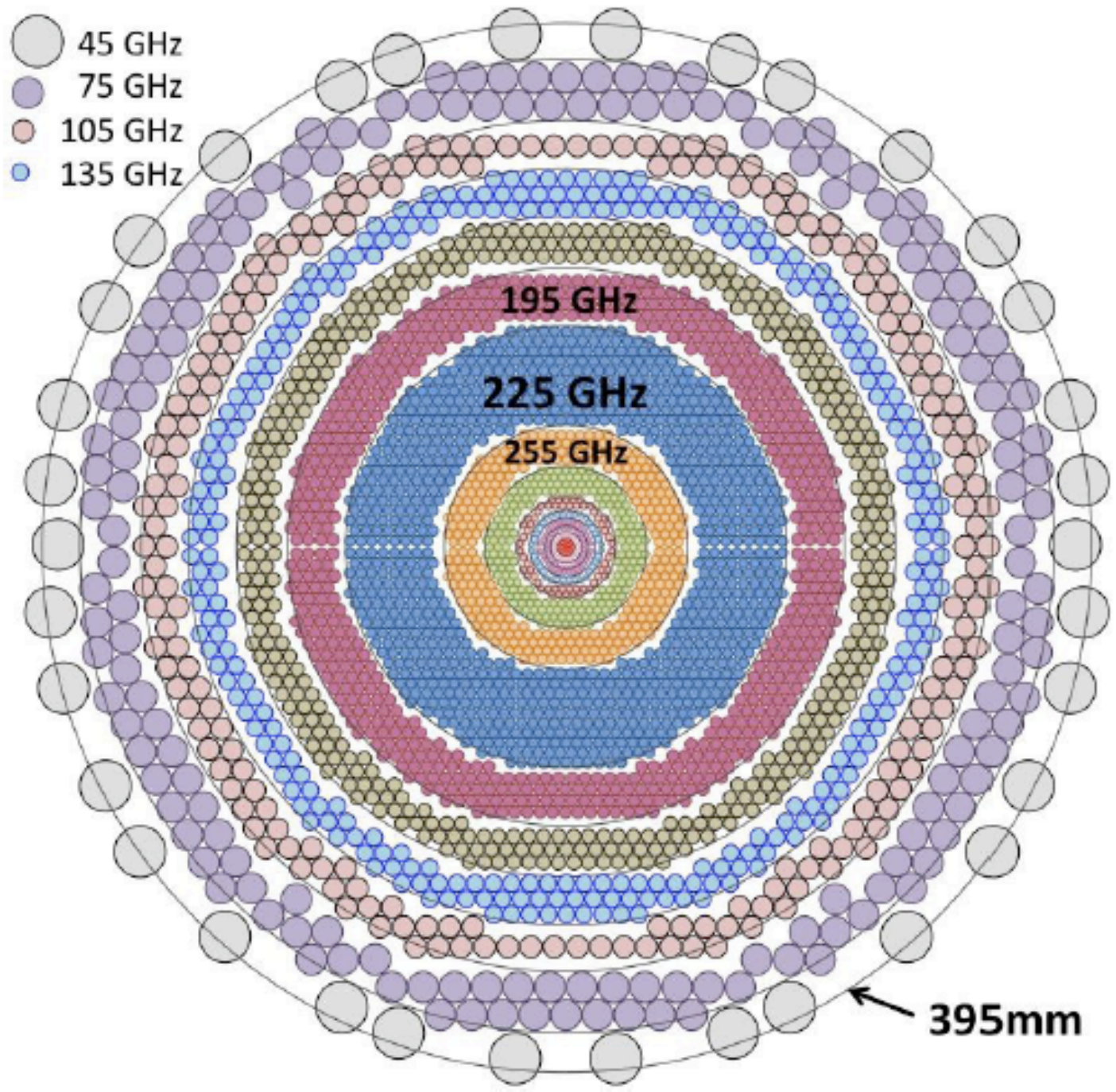
COrE

Cosmic Origins Explorer

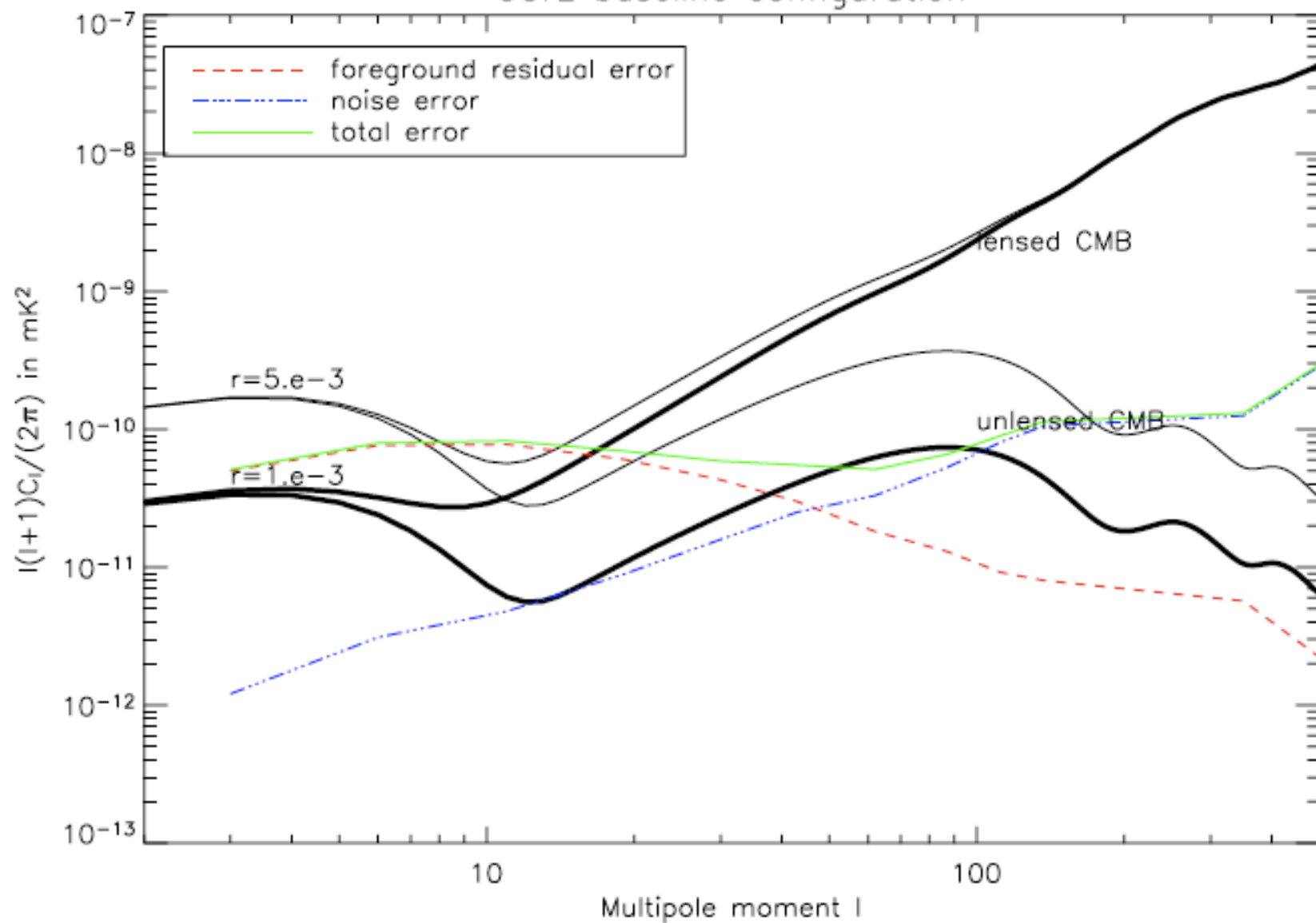
A White Paper

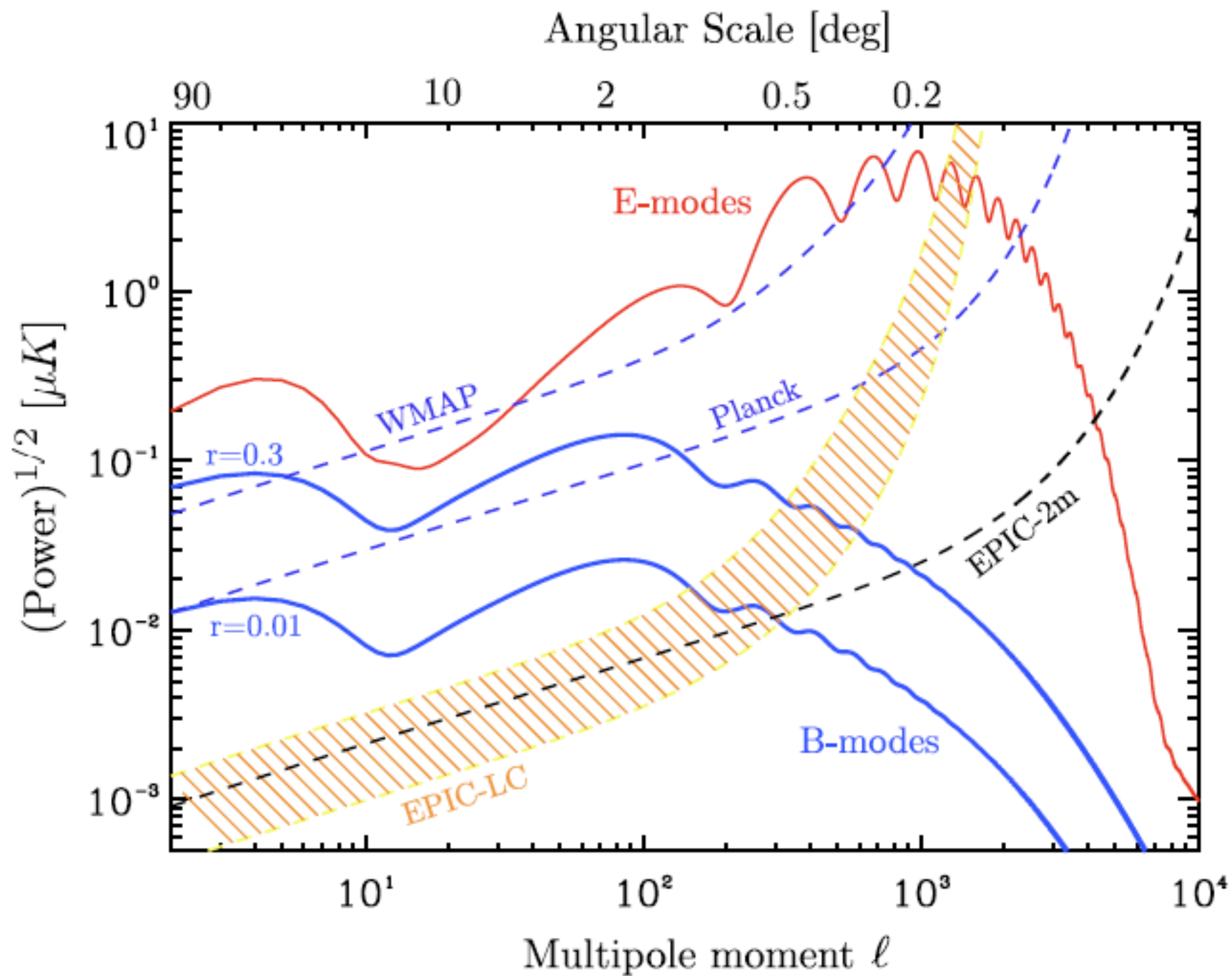


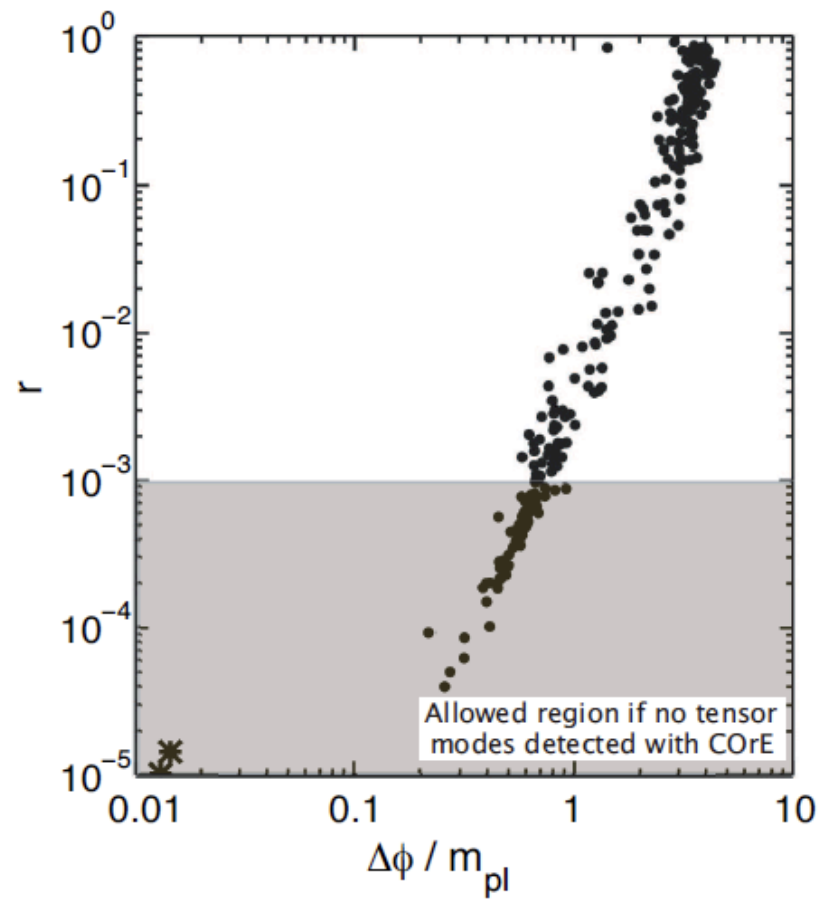
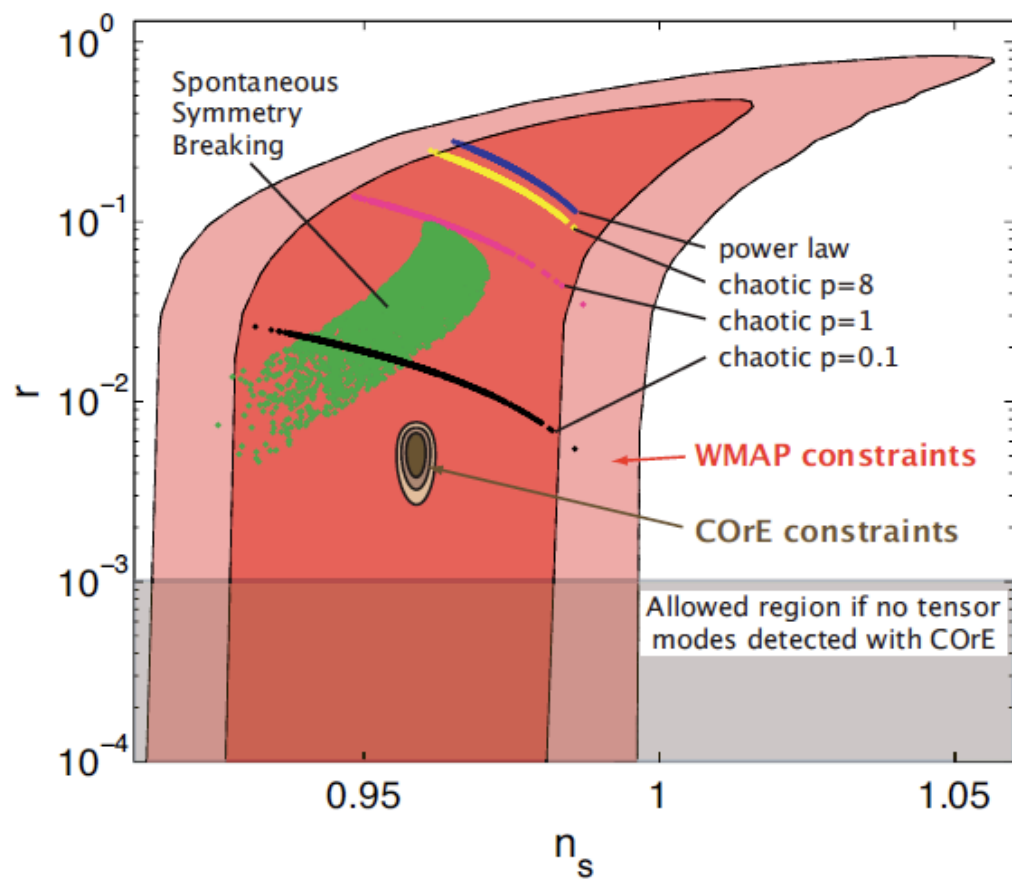
(arXiv1102.2181)



COrE baseline configuration







Conclusions:

Future Milestones on CMB research

- ❖ Determination of the **polarization power spectra (TE and EE)** down to cosmic variance level.
- ❖ Test the standard model down to percent accuracy. Testing extensions of the model.
- ❖ Determine the Gaussian properties of the CMB maps with great accuracy ($f_{\text{NL}} \sim \text{few}$). Implications for inflation.
- ❖ **Gravitational wave B-modes.**
- ❖ B-modes induced by primordial magnetic fields.
- ❖ Polarization tests of large-scale temperature anomalies.
- ❖ Sunyaev-Zel'dovich clusters & secondaries surveys
- ❖ Lensing B-modes
- ❖ Lensing mass reconstruction
- ❖ Reionization history & inhomogeneity
- ❖ Spectral distortions from the recombination or reionization epochs

The future is very bright and polarized!